# INTERMITTENCY AND LONG-RANGE STRUCTURIZATION OF HEART RATE

MAKSIM SÄKKI

The thesis'y cs accepted for the defense of the degree of Doctor of Philosophy in Natural Sciences at Tallinn University of Technology in the 27th of September, 2005.

Supervisor:

Dr. Jaan Kalda, *PhD*

Institute of Cybernetics at Tallinn University of Technology, Estonia

Opponents:

Dr. Jan Zebrowski, *PhD*

Warsaw University of Technology, Poland

Dr. Oleksiy Chechkin, *PhD*

Kharkov Institute of Physics and Technology, Ukraine

Defense:

The presentation of this thesis will take place on November 28th, 2005 at the Institute of Cybernetics at TUT, Akadeemia tee 21, Tallinn, Estonia.

Declaration:

Hereby I declare that this doctoral thesis, my original investigation and achievement, submitted for the doctoral degree at Tallinn University of Technology has not been submitted for any degree or examination.

Maksim Säkki

# SÜDAMERÜTMI PIKAMASTAABILINE KORD JA JUHUMUUTLIKKUS

MAKSIM SÄKKI

TTÜ Küberneetika Instituut, Matemaatika–loodusteaduskond,
TALLINNA TEHNIKAÜLIKOOL

Väitekiri on lubatud doktorikraadi kaitsmisele Tallinna Tehnikaülikoolis, 27. septembril 2005 aastal.

Juhendaja:

Jaan Kalda, *füüs.-mat. kand.*

Tallinna Tehnikaülikooli Küberneetika Instituut, Eesti

Ametlikud oponendid:

Dr. Jan Zebrowski, *PhD*

Varssavi Tehnoloogia Ülikool, Poola

Dr. Oleksiy Chechkin, *PhD*

Harkovi Füüsika ja Tehnoloogia Instituut, Ukraina

Kaitsmine:

Doktoritöö kaitsmine toimub 28. novembril 2005 aastal Tallinnas, Tallinna Tehnikaülikooli Küberneetika Instituudis, Akadeemia tee 21.

Deklaratsioon:

Deklareerin, et käesolev doktoritöö, mis on minu iseseisva töö tulemus, on esitatud Tallinna Tehnikaülikooli doktorikraadi taotlemiseks ja selle alusel ei ole varem taotletud akadeemilist kraadi.

Maksim Säkki

# Contents

# List of Publications

**Publication I**     M. Säkki, J. Kalda, M. Vainu, M. Laan. On the Zipf's law in human heartbeat dynamics. *Simplicity behind Complexity. Proceedings of the 3rd European Interdisciplinary School on Nonlinear Dynamics for System and Signal Analysis Euroattractor 2002.*, W. Klonowski (Ed.), Warsaw, 211–219, (2004).

**Publication II**     M. Vainu, J. Kalda, M. Laan, M. Säkki. Nonlinear methods of heart rate variability in patients with heart disease using ambulatory ECG monitoring. *Eesti Arst* (in Estonian) **82**, 8, 543–549, (2003).

**Publication III**     M. Säkki, J. Kalda, M. Vainu, M. Laan. What does measure the scaling exponent of the correlation sum in the case of human heart rate? *Chaos*, **14**, 138–144, (2004).

**Publication IV**     J. Kalda, M. Säkki, M. Vainu, M. Laan. Non-linear and scale-invariant analysis of the heart rate variability. *Proc. Est. Acad. Sci. Phys. Math.* **53**, 1, 26–44, (2004).

**Publication V**     M. Säkki, J. Kalda, M. Vainu, M. Laan. The distribution of low-variability periods in human heartbeat dynamics. *Physica A* **338**, 255–260, (2004).

**Publication VI**     M. Bachmann, J. Kalda, J. Lass, V. Tuulik, M. Säkki, H. Hinrikus. Non-linear analysis of the electroencephalogram for detecting effects of low-level electromagnetic fields. *Med. Biol. Eng. Comput.* **43**, 1, 142–149, (2005).

**Publication VII**     M. Bachmann, M. Säkki, J. Kalda, J. Lass, V. Tuulik, H. Hinrikus. Effect of 450 MHz microwave modulated with 217 Hz on human EEG in rest. *The Environmentalist*, **25**, 165–171, (2005).

# Introduction

In the past, heart rate was a measure of regularity and people often used their pulse to time the duration of some events. Galileo Galilei did so in 1582 observing the swinging lamps in the cathedral of Pisa. In those observations, Galileo found that the periods of large and small swings were exactly the same. This discovery led Galileo to the famous design of a clock regulated by a pendulum. Ironically, later, the clock was used to detect intrinsic irregularities in the heart rate. Whereas the normal activity of the heart is traditionally described as *regular sinus rhythm*, the heart rate constantly fluctuates in a complex manner. These nonstationary and nonlinear fluctuations on a beat-to-beat basis are associated mainly with the autonomic neural regulation of the heart. It is known that parasympathetic input decreases and sympathetic stimulation increases the heart rate. Moreover, the parasympathetic activity, which is synchronous with the respiratory cycle, causes the well-known effect of *respiratory sinus arrhythmia*. The oscillations in the blood pressure cause so called *Mayer waves* or *baroreflex* regulation [1]. Age, medication, as well as physical and mental stress also affect the heart rate variability (HRV) [2]. Meanwhile, cardiovascular and neurologic diseases may decrease the responsiveness of the heart and lead to a failure to respond to the external stimuli. Evidently, such pathologies lead to an overall reduction of HRV.

Apparently, the clinical importance of HRV was first noted in 1965 by Hon and Lee [3]. Since then, the statistical properties of the interbeat interval sequences have attracted the attention of a wide scientific community. In 1978, Wolf *et al.* [4] associated the increased risk of post-infarction mortality with reduced HRV. Wider attention to the problem has been attained in the early 1980s, when Akselrod *et al.* introduced the spectral methods for HRV analysis [5]. In the late 1980s, the clinical importance of HRV became generally recognized. Several studies confirmed that HRV was a strong and independent predictor of mortality following an acute myocardial infarction [6, 7, 8]. In particular, Goldberger *et al.* [9] showed that a loss of complex physiological HRV can be seen in patients minutes to months prior to sudden cardiac death. Understanding the diagnostic and prognostic significance of the various measures of HRV has a great importance for cardiology as a whole, because unlike the invasive methods of diagnostics, the required measurements are low-cost and harmless for the patients. A particularly important application is the prognostics of the increased risk of sudden cardiac death.

The autonomic regulation of the heart rate has been investigated widely during the last decades, but no uniform concept exists regarding the function of neural mechanisms. Moreover, there is still a lack of standardization of the parameters and their meaning in HRV analysis. In 1996, the *Task Force* of the European Society of Cardiology *et al.* [10] touched on the need of developing appropriate standards for clinical applications of HRV measures. The *Task Force* gave a comprehensive overview of HRV analysis methods widely used in clinical prac-

tice and identified areas for future research. It should be noted that this paper mainly focused on "linear" measures of HRV (see **Appendix 1** for list of selected standard measures in clinical use), mentioning nonlinear measures only as "potentially promising tools for HRV assessment", and clearly stating that "advances in technology and the interpretation of the results of nonlinear methods are needed before these methods are ready for physiological and clinical studies" [10]. Indeed, while the "linear" measures of HRV are nowadays widely used in clinical practice, the importance of more complicated measures have been hotly disputed in scientific literature during the recent decades: there is no consensus on which methods are the most efficient from the point of view of clinical applications. On the one hand, this is caused by the high nonstationarity and irreproducibility of heart rate time series: the complex measures of HRV depend not only on the healthiness of the heart, but also on the daily habits of the subject [11], and on the random events of the recording day. On the other hand, dialogue between physicists and doctors seems to be inefficient: physicists publish research results based on relatively small test groups; doctors expect follow-up studies using extended and homogeneous test groups.

Recent attempts to bring together cardiologists and physicists in order to evaluate and compare the performance of different nonlinear analysis techniques resulted in the creation of *PhysioNet*, a cooperative project of Harvard Medical School, Boston University, McGill University, and MIT [12, 13]. This project provides a common database of biomedical signals (including ECG and heart interbeat intervals time series) and methods of their treatment. Such a deep cooperation allows us to believe that the *stylised* nonlinear measures of HRV, applicable for clinical diagnostics, will be finally worked out.

The aim of this thesis is to give an overview of the main research results in the field of heart rate analysis and present the original results of the author. Thus, the publications are an inseparable part of this thesis. The thesis is divided into Sections as follows. The first Section discusses early studies of the nonlinear aspects of HRV by methods based on the reconstructed phase space analysis. The author provides the modern view on the applicability of these methods. **Publication III** discusses the applicability of the notion of *correlation dimension* for describing the heart rate. In Section 2, the author gives an overview of the evolution of the entropy-based approach to the analysis of HRV. Section 3 summarizes the author's original results in the analysis of mode-locking between heart rhythm and respiration. The author provides a comparison of the developed technique with approaches used in other studies. Section 4 gives an overview of the methods of analysis, closely related to *(multi)fractal* formalism. Also, the author proposes a novel approach to the analysis of *intermittency* in biological signals, which reveals a new aspect of nonlinear time series: the scale-invariance of low-variability periods. The first results were reported at the *Euroattractor* conference in Warsaw (Poland) in 2002 (**Publication I**). The author presented further research on the low-variability periods of the heart rate at the *Frontier Science* conference in

Pavia (Italy) in 2003, and published his results in **Publication V**.

**Publication II** (in Estonian) and **Publication IV** both review the existing variety of nonlinear methods in HRV analysis. **Publication IV** discusses the intrinsic features of HRV signals, focusing on the *multifractal* formalism in HRV description, whereas **Publication II** focuses on the clinical perfomance of the novel approach and its possible application in medical practice. **Publication VI** and **Publication VII** study the applicability of the developed techniques for analysing the influence of electromagnetic fields on the EEG signal. In these publications, the author was mainly responsible for the multichannel EEG data analysis by a method derived on the basis of the technique of low-variability periods.

**Appendix 1** gives a list of the most important standard measures currently used in medical practice for describing HRV. An analogous list of the (non-standard) nonlinear parameters which have been considered in recent studies is summarized in **Appendix 2**. Also, the author found it useful to provide a short reference to the Bonferroni correction (**Appendix 3**), which was used in statistical tests of the significance of results in **Publication V**, **Publication VI**, and **Publication VII**.

To summarize, there are three main topics in this thesis:

- The thesis provides a detailed overview of recent studies of HRV time series, and discusses issues related to the nonlinear dynamics approach based on phase-space reconstruction. The discussion focuses on the intrinsic difficulties of estimating the correlation dimension and interpretation of obtained values.

- The author proposes a simple method for the detection of synchronization between the heart rhythm and respiration.

- The thesis presents a new aspect of the multifractality of intermittent nonlinear time series: the scale-invariance of low-variability periods. Published papers provide the results of this novel approach for the multifractal analysis of HRV and EEG signals.

# Acknowledgements

# 1 Phase-space analysis

## 1.1 Phase-space reconstruction

It has been found that heart rate generation can be reasonably well described by nonlinear dynamical models [14, 15, 16, 17, 18, 19]. Such nonlinear models have a strong physiological motivation: sinoatrial (SA) and atrioventricular (AV) nodes form a nonlinear system of coupled oscillators: the electrical signal controlling the heartbeat is generated by the SA node and conducted through the AV node. The activity of the heart is also affected by interactions of haemodynamic and humoral variables, as well as by the autonomic and central nervous systems. The electrophysiological model proposed by Engelbrecht *et al.* in 1995 (cf. [18]) has been proven to be viable and it predicts several experimentally observed phenomena, such as *a)* second-degree AV block (some dropped beats), including Mobitz Type I (Wenckebach) and Mobitz Type II arrhythmias, and *b)* bistable behaviour. A semi-empirical nonlinear model for electrical heart activity proposed by Mc-Sharry *et al.* in 2003 [20], and known as *synthetic electrocardiogram*, generates a realistic ECG signal, reproducing QT dispersion and R-peak amplitude modulation.

However, a fully adequate model of heart activity is still quite a difficult task; one can study the nature of heart rate generation by reconstructing the trajectories of the underlying signal (ECG or heart rate) in phase space. The question what might be the canonical variables in the case of physiological data (when one has few information about it), can be avoided by the method of *delays*: time series $x_n = x(n\Delta t)$ measured with fixed sampling period $\Delta t$ can be reconstructed to the vectors $\boldsymbol{\beta}_n$ in $m$-dimensional phase space:

$$\boldsymbol{\beta}_n = (x_{n-(m-1)\nu}, x_{n-(m-2)\nu}, \ldots, x_{n-\nu}, x_n). \tag{1}$$

The difference in the number of samples $\nu$ (in time units, $\nu\Delta t$) between adjacent components of the delay vectors is called the *lag* or *delay* time; the process of reconstruction is referred to as *embedding* and $m$ is called the *embedding dimension*. A number of embedding theorems exists [26, 27], and it is expected that the reconstructed phase trajectory can be transformed to the original trajectory by a "uniquely invertible smooth map" [28].

The deterministic nonlinear model predicts that the trajectories of heart rhythm in reconstructed phase space lie on an attractor of the system of coupled oscillators. Such a theoretical reasoning and belief that nonlinear phenomena are certainly involved in the generation of the heart rate have led to the idea that the characteristics from the theory of nonlinear dynamics might reveal valuable information for the physiological interpretation of HRV and could be used for diagnostic purposes, especially for assessing the risk of sudden death.

The experimental observations of intrinsic nonlinearity in HRV seemingly confirmed the theoretical expectations. Mansier *et al.* [30] applied a nonlinear

forecasting method of Sugihara *et al.* [31], and surrogate data sets to address the question whether the HRV series is the output of a deterministic dynamical system. They showed that prediction is better for the experimental series than for its surrogate data and suggested that these differences are an evidence of a nonlinear deterministic system generating HRV time series [30]. Chon *et al.* [32] proposed a method to test chaotic determinism based on fitting a nonlinear autoregressive model to the time series, followed by the analysis of the characteristic exponents of the model over the observed probability distribution of states for the system. They showed that relatively short HRV time series (4096 data points) contain a nonchaotic deterministic component [32].

Such a presumption of an underlying chaotic attractor gave rise to extensive studies of the heart rate in the 1990s by applying analysis methods from the theory of nonlinear systems (for example, cf. [21, 57, 23, 24, 25]).

## 1.2  Lyapunov exponents

The most useful characteristics that can be estimated from the time series are *invariants* in the sense that changes in the measurement procedures do not affect calculated values. One such invariant is the rate of divergence (or convergence) of nearby trajectories in phase space. In the case of a chaotic attractor, an infinitely small perturbation $\delta_0$ will grow exponentially in time ($\delta_t \propto \delta_0 \exp \lambda t$). The growth rate $\lambda$ is called the *Lyapunov exponent* (a measure was introduced by A. Lyapunov at the end of the 19th century) and is defined as:

$$\lambda(\delta_0) \equiv \lim_{t \to \infty} \frac{1}{t} \ln \frac{\delta_t}{\delta_0}, \tag{2}$$

where $\delta_0$ is the initial perturbation between two points, and $\delta_t$ is the distance between two trajectories emerging from these points after time $t$. For the ergodic system, $\lambda$ does not depend on the choice of $\delta_0$, which means that Lyapunov exponents are invariants. A positive but *finite* $\lambda$ is a clear criterion for the existence of deterministic chaos in the underlying system. In practice, the exponent equality to zero (usually, within the estimation error) shows that the system is deterministic. Also, for nonstationary data, one can calculate *local* Lyapunov exponents (cf. [33]), and thus describe the local behaviour of an attractor.

There are a number of robust algorithms to estimate $\lambda$ for finite and noisy experimental data that work well for very small noise levels. These algorithms can be divided roughly into two groups: in the *first* approach (introduced by Wolf *et al.* in 1985 (cf. [36]) and developed by Rosenstein *et al.* in 1993 (cf. [34])), only the largest $\lambda$ is evaluated by following two nearby points in phase space; in the *second* approach (proposed almost simultaneously by Eckmann *et al.* (cf. [38]) and by Sano *et al.* (cf. [37]) in 1986), the Jacobians of the return map are estimated.

Finite positive $\lambda$ were reported in several studies of the heart rate and ECG, cf. [21, 41, 25]. However, Lyapunov exponents are extremely difficult to estimate from experimental data with the presence of a stochastic component (cf. [35, 39, 40]). Therefore, finding a positive largest $\lambda$ in a finite time series is not sufficient for one to conclude that the dynamical process is chaotic (deterministic). As a result, the popularity of Lyapunov exponents for characterizing the dynamics of biological signals (especially those registered *in vivo*) constantly decreased.

## 1.3 Scaling of correlation sum

The notion of *correlation dimension* was introduced by Grassberger and Procaccia in 1983 [68]. The correlation dimension of an experimental data sequence is typically calculated according to the following algorithm. First, the correlation sum of second order for a set of points in some $m$-dimensional vector space is defined as a fraction of all possible pairs of those points, which are closer than a given (small) distance $r$ :

$$C_2(r, N) = \frac{2}{N(N-1)} \sum_{i<j} \theta(r - \mid \boldsymbol{\beta}_i - \boldsymbol{\beta}_j \mid), \tag{3}$$

where $\theta(r)$ is the Heaviside step function, and $\boldsymbol{\beta}_i$ is a point in the reconstructed phase space given by Eq. (1), and $i, j = 1, 2, \ldots, N$; $N$ is the length of the dataset. In practice, the sum $C_2$ is taken only for those pairs of $\boldsymbol{\beta}_i$ and $\boldsymbol{\beta}_j$ that are separated by more than $z$ sampling times to avoid artificial correlation among consecutively sampled points on the attractor [51]. For small enough $r$ and in the limit of an infinite amount of data, the correlation sum is expected to scale as $C_2(r) \propto r^{D_2}$, assuming that $D_2 < m$:

$$D_2 = \lim_{r \to 0} \lim_{N \to \infty} \frac{d \ln C(r, N)}{d \ln r}. \tag{4}$$

The scaling exponent $D_2$ is called the *correlation dimension* of the system. A nonlinear dynamical system may be chaotic and then the phase trajectory fills a certain subset of the phase space. In that case, the correlation dimension $D_2$ is expected to be equal to the number of degrees of freedom (the dimensionality of the phase space minus the number of conservation laws). This is why $D_2$ is often considered as a measure of the complexity of the system. Babloyantz and Destexhe [21] studied the correlation dimension of the sequence of NN-intervals (intervals between normal heartbeats) of the human heart rhythm. For healthy patients and data series consisting of 1000 intervals, they found $D_2 = 5.9 \pm 0.4$. It is widely recognized that life threatening heart pathologies lead to the reduction of the complexity of the HRV signal, c.f. [22]. Correspondingly, the correlation dimension of the heart rate has often been believed to measure the "healthiness" of the heart.

However, there are various arguments leading one to the conclusion that the formally calculated correlation dimension of a heart rhythm does not correspond to the dimensionality of an intrinsic attractor; similarly, the formally calculated Lyapunov exponents, entropies etc. do not describe the respective aspects of underlying nonlinear dynamics:

*First*, it has been pointed out that physiological time series are typically non-stationary and noisy, and therefore, the correlation dimension cannot be calculated reliably [42, 44, 45]; this fact is nowadays widely accepted, and it has been estimated that the maximum noise level for the credible calculation of the $D_2$ is 2-3% [28]. In the case of the human heart, the "noise" comes from the autonomous nervous system in the form of inputs regulating the heart rate (cf. [46, 47, 48]): from the viewpoint of an underlying nonlinear deterministic system, these effectively non-deterministic signals perform the role of high level noise [50]. It should also be noted that some inputs of the autonomous nervous system may lead to quasi-periodic signals, which are an easy source of false detection of low-dimensional chaos and apparent patterns in simple time delay maps. Thus, respiration gives rise to the signal of a typical period of 4 seconds; the effect is most pronounced when the patient is at rest, and is stronger for young persons.

*Second*, it has been emphasized that a reasonable fitting of a correlation sum to a power law does not necessarily mean that the obtained exponent is the correlation dimension of the underlying dynamical system; instead, one has to perform a thorough non-automatable verification procedure [28].

*Third*, the length of the data sequences is often inadequate for reliable calculation of high values of the correlation dimension $D_2 \gtrsim 6$ (cf. [25, 28]). Too short a record length can cause a saturation effect and lead to a false detection of the scaling exponent of the correlation sum. It has been suggested [42, 43] that the calculation of the correlation dimension $D_2$ is reliable, if the number $N$ of data points in the time series satisfies the criterion:

$$N \gtrsim 10^{D_2/2+1}. \tag{5}$$

Typically, values of $D_2$ have been found to be at the limit (or even beyond) of a credible analysis [42, 43]. The comparison of theoretically required and practically used lengths of time series for reliable estimation of $D_2$ in some publications is summarized in Table 1.

The recent study of Carvajal *et al.* [52] is a good example of finding the correlation dimension for the heart rate beyond the practical limit: $D_2$ between 8.4 and 10.6 for data segments of a length of $10^4$ beats! Moreover, obtaining high values of $D_2$ ($\approx 10$) for noisy experimental data is essentially the same as saying that the underlying system is stochastic. In that case the notion of correlation dimension is meaningless, and one should find better methods for characterizing the data. Note that there is no simple recipe for obtaining adequate long time series: whereas a long observation period often implies non-stationarities, oversampling emphasizes the noise.

|            | Ref. [21]   | Ref. [44]       | Ref. [25]   | Ref. [53]       | Ref. [52]       |
|------------|-------------|-----------------|-------------|-----------------|-----------------|
| $D_2$      | 5.5–6.3     | 9.6–10.2        | 2.8-5.8     | 4–7             | 8.4–10.6        |
| $N_{exp}$  | $10^3$      | $2 \cdot 10^4$  | $10^4$      | $2 \cdot 10^4$  | $10^4$          |
| $N_{req}$  | $10^4$      | $10^6$          | $10^4$      | $3 \cdot 10^4$  | $3 \cdot 10^5$  |

Table 1: The table compares the criterion given by Eq. (5) with the data of some papers devoted to the correlation dimension analysis. The table gives experimental values of correlation dimension ($D_2$), following by lengths of the underlying data sets ($N_{exp}$), and data-set lengths required for reliable estimation ($N_{req}$). Adopted from **Publication III** and extended with recent studies.

*Finally*, it has been found that the effect of nonlinear mapping from the time domain to the phase space may result in an overestimation of the correlation dimension [49].

In **Publication III**, the author of this thesis studied the effects of the finite resolution of the apparatus and a wide dynamic range of the mean heart rate to the scaling of correlation sum $C_2$. The author constructed a simple model of heart rate generation, which reproduces the scaling behaviour of the correlation sum of real medical data. **Publication III** showed that calculated values of scaling exponents for $C_2$ are mostly defined by the dynamics of the short-time variability. The conclusion was that whereas the scaling exponent can be used for quantitative characterization of short-time variability of HRV, it is not an invariant and, in order to obtain comparable values, time-resolution, record length, and the embedded dimension of the phase space have to be kept constant. These research results can be summarized as follows: Whereas the correlation sums of the human heart rate typically follow a scaling law, in most cases, the scaling exponents are *not* the correlation dimensions.

## 2 Entropy-based measures

The measures of deterministic chaos based on reconstructed phase space usually fail in describing a deterministic chaos inside the heart, because the dominantly deterministic dynamics is suppressed by essentially intermittent signals arriving from the autonomous nervous system and regulating the heart rhythm. However, some fine-tuned measures, e.g. various entropies, cf. [57, 63, 65, 70], can be useful in describing the level of short-time variability of the heart rhythm. Entropy-based measures, being essentially an average of the logarithm of a conditional probability, can be viewed as a *statistical* characteristics, which can be applied to both deterministic and stochastic processes. While not directly requiring the presence of a deterministic dynamics, they are ideologically related to the analysis of nonlinear dynamics (they deal with the dynamics in time delay space). These measures also reflect the rate of new pattern generation (irregularity of signal),

and are therefore closely related to the concepts of Shannon and Kolmogorov-Sinai entropies. They can be classified as extensions of those concepts, more suitable for characterization of experimentally measured time series.

## 2.1 Kolmogorov-Sinai entropy and its estimators

Kolmogorov-Sinai entropy ($K$) is defined as the mean rate of the change of entropy of the trajectory of an attractor in phase space due to the finer phase space partitioning within each iteration $n$:

$$K \equiv \lim_{n \to \infty} \frac{1}{n} S_n = \lim_{n \to \infty} S_{n+1} - S_n, \tag{6}$$

where $n$ is the index of partition and $S_n$ is the Shannon entropy of partition $n$. The Kolmogorov-Sinai entropy measures the mean rate of the creation of information, and therefore a positive value of $K$ may be used to define the existence of chaos. Unfortunately, there are a number of difficulties in directly calculating $K$ entropy for experimental time series [28, 70, 66], mainly because of the finite length of data and the presence of noise on small scales. However, several techniques have been suggested to estimate the Kolmogorov-Sinai entropy with reasonable precision, for example, Grassberger and Procaccia [55] suggested in 1983 a calculating measure they named $K_2$ entropy, which estimates the lower boundary of the $K$ entropy:

$$K_2 = - \lim_{N \to \infty} \lim_{m \to \infty} \lim_{r \to 0} \ln[C^{m+1}(r) - C^m(r)], \tag{7}$$

here $C^m(r)$ stands for the probability that any two points in phase space of dimension $m$ are closer to each other than some small $r$; $N$ stands for the length of data. In 1985, Eckmann and Ruelle [56] extended this technique and suggested calculating the Kolmogorov-Sinai entropy when characterizing low-dimensional chaotic systems as:

$$K_{ER} = \lim_{N \to \infty} \lim_{m \to \infty} \lim_{r \to 0} [\Phi^m(r) - \Phi^{m+1}(r)], \tag{8}$$

where $\Phi^m(r) \propto \sum_i \ln C_i^m(r)$ and $\Phi^m(r) - \Phi^{m+1}(r)$ depicts the probability that sequences of length $m$ that are similar within a fixed small tolerance $r$ remain similar for increased length $m+1$.

## 2.2 Approximate and sample entropy

The notion of *approximate entropy* ($ApEn$) and the calculation algorithm (based on previous work by Eckmann and Ruelle) was firstly proposed in 1991 by Pincus [57]. The motivation was the need to estimate values of $K$ for experimentally obtained data, usually noisier and shorter than would be suitable for accurate calculation. Although, $ApEn$ is defined as:

$$ApEn(m, r) = \lim_{N \to \infty} [\Phi^m(r) - \Phi^{m+1}(r)], \tag{9}$$

16

for finite $N$, the $ApEn$ is estimated by the measure:

$$ApEn(m, r, N) = \Phi^m(r) - \Phi^{m+1}(r),\tag{10}$$

Lower values of $ApEn$ indicate that the time series are more regular (deterministic); high values indicate randomness. $ApEn$ is mainly used in the analysis of heart rate variability [58, 59, 60, 61, 62], but is also often calculated for other biosignals, such as ECG, EEG, respiration, endocrine hormone release pulsatility. Time series shuffling greatly impacts the value of $ApEn$, whereas the value of standard deviation remains unaffected. Also note that $ApEn$ is not an *invariant*, and depends on the choice of threshold level $r$, and embedded dimension $m$, and on the length of data $N$. Comparisons between different time series can only be made with the same values of $m$, $r$, and $N$. Typically, pattern length $m$ is chosen to be 2-4, while tolerance $r$ is chosen to be 10-20% of the standard deviation of the time series.

In 2000, Richman and Moorman modified the algorithm for the calculation of $ApEn$ and suggested calculating a less biased measure, i.e., *sample entropy* ($SampEn$) [63]. The main advantage of $SampEn$ is that it is less dependent on the time series length and has a stronger property of relative consistency regarding the choice of parameters $r$ and $m$ than $ApEn$ has. Recently, it has been found that the decreased $SampEn$ calculated for neonatal heart rate is a good indicator of neonatal sepsis episodes [64]. The conclusion was that $SampEn$ may be used in medical practice as a general estimate of the health of the infant.

However, the algorithms mentioned above do not take into account the multiple time scales in variability of biological signals. Instead, they are effectively single-scale measures, reflecting only short-time dynamics. Such a limitation often leads to spurious results: higher values of entropy are estimated for time series representing certain pathology, i.e., atrial fibrillation, which is structurally less complex than the heart rate of healthy indivuduals (which is a signal of a physiologically complex state, adaptive to many inputs). In order to address the presence of multiple time scales in the temporal fluctuations of biological time series, several approaches were proposed.

## 2.3   Multiscale entropy

In 1991, Zhang [67] suggested the quantity $K$, which he named *complexity*. This complexity measure $K$, being effectively the sum of scale-dependent Shannon entropies over all possible scales $n$,:

$$K = \sum_n S_n,\tag{11}$$

assigns higher values to colored noise compared to white noise. However, Zhang's work was very theoretical; the quantity $K$ based on the Shannon entropy requires

a huge number of almost noise-free data points limiting its practical applicability in the case of noisy data of limited length.

In the approach of Costa *et al.* [65] (2002), the notion of *multiscale entropy* $MSE$ was introduced. In the $MSE$ method, one calculates the sample entropy $SampEn$ as a function of the scale: $SampEn(\tau)$. The coarse-grained time series corresponding to scale $\tau$ are obtained by averaging the data points within non-overlapping windows of length $\tau$ (so called "coarse-graining" process). $MSE$ addresses the question of how wide the range of dynamics for the mean heart rate is (averaged over a time $\tau$), depending on the time-scale $\tau$, which makes this measure closely related to the multifractal aspect of time series. The clinical usefulness of MSE is still unclear (apart from the fact that it has been claimed to be able to distinguish between healthy subjects and patients with congestive heart failure [65]).

The idea of *pattern entropy* ($S_p$) for HRV analysis was proposed in 1994 by Zebrowski *et al.* [69]. They motivated this measure by the fact that the calculation of ordinary (Shannon) entropy completely failed to distinguish healthy individuals from those with heart pathologies. Thus, pattern entropy was calculated as modified Shannon entropy:

$$S_p = -\sum_k p_k \log p_k, \tag{12}$$

where $p_k = p(t_{RR})p_\tau(t_{RR})$ for 2-dimensional phase space. Here $\tau$ is the integer time delay in beats used for phase space reconstruction, and $p(t_{RR})$, $p_\tau(t_{RR})$ are the probabilities of finding $RR$-interval of length $t_{RR}$ for corresponding coordinates in reconstructed phase space. Correspondingly, for 3-dimensional phase space $p_k = p(t_{RR})p_\tau(t_{RR})p_{2\tau}(t_{RR})$. By definition, pattern entropy is larger for stationary and ordered time series, this property is exactly the opposite for ordinary Shannon entropy. It has been found that the values of pattern entropy distinguished reasonably well between some pathologies and health, and overperformed the standard frequency- and time-domain analysis [69]. In the later paper, Zebrowski *et al.* [70] also found that the statistical order of heart rate time series measured by pattern entropy (calculated for sliding window) depends on age, especially for younger persons.

In order to get entropy estimates, which can be directly compared between different time series, the *renormalization* procedure was suggested by Kurths *et al* in 1995 [71]. In this approach, one renormalizes the entropy, estimated for certain time series, in such a manner that the mean effective energy for this time series remains the same as the energy obtained for some reference data.

To conclude, an analysis of HRV based on reconstructed phase space historically started from adapting of parameters from the theory of nonlinear deterministic systems, and resulted mainly in fine-tuned entropy-based measures. Such a shift in focus was motivated by the presence of relatively strong stochastic component in presumably deterministic heart rate generation. It is also important to note

18

that entropy-based measures of the complexity of HRV focusing on short-term variability do not reflect the aspect of long-range correlations in rhythm. Entropy-based measures should therefore be used in combination with other quantities.

# 3  Heart rhythm and respiration mode-locking analysis

This section discusses the effect of coupling between two oscillatory processes in cardiovascular dynamics, heart rate, and respiration activity. As it was mentioned above, respiration modulates the heart rhythm. The heart is most responsive with respect to the signals of the autonomous nervous system when the heart rate is unaffected by physical activity, i.e., when the patient is at rest. In that case, HRV is driven by weaker signals induced by respiration and baroreflex, which (due to their quasi-periodic nature) may lead to mode-locking. Indeed, recent studies [79, 80] confirmed the synchronization between three main rhythmic processes governing the cardiovascular dynamics: sinus rhythm (fundamental frequency is about 1 Hz), respiration (0.12 Hz – 0.25 Hz), and baroreflex (0.1 Hz). In the case of respiratory mode-locking, the heart rate is automatically slightly adjusted so that the respiration and heart beat periods relate to each other as (small) integers $\frac{n}{m}$. In practice, synchronization between two oscillators can be defined as:

$$|n\phi_1 - m\phi_2| < \epsilon, \tag{13}$$

where $\phi_1$, $\phi_2$ are phases of the oscillators, and $\epsilon$ is a small positive constant. The decorrelation time between the heart rhythm and respiration can be very long: it was reported that the $\frac{3}{1}$ synchronisation regime can be as long as $10^3$ seconds [72]. Other ratios like $\frac{5}{1}$, $\frac{5}{2}$, $\frac{7}{2}$ were observed for shorter periods ($\approx 1$ minute); some episodes of $\frac{4}{1}$-, $\frac{8}{3}$-, $\frac{11}{4}$-mode-locking were also documented [72, 75]. This effect of mode-locking causes the patterns (isolated clouds of points) observable in the reconstructed phase space (cf. **Publication III**, Fig. 6). These patterns can be easily misinterpreted as traces of an attractor of a nonlinear deterministic system.

The successful start to the modelling of cardiorespiratory synchronization can be attributed to the simple beat-to-beat model proposed by DeBoer *et al.* in 1987 [1]. This nonlinear model described dynamical properties of human *cardio-baroreceptor* control loop, i.e., relationship between heart rhythm, respiration, blood pressure, and peripheral vessels resistance. Further, this model has been elaborated by Seidel *et al.* [76] by taking into account phase dependency of the sinus node responsiveness to neural activity. Recently, a physiologically plausible model of cardiorespiratory synchronization was suggested by Kotani *et al.* [77]. This model exhibits stable synchronization between the heart rhythm and respiration even in the presence of noise.

The mode-locking effect has been studied numerically using bivariate data (simultaneous recordings of ECG and respiration activity) and the technique called

*cardiorespiratory synchrogram* [72, 73, 74]. Also, a univariate data analysis method using the *angle-of-return-times map* has been elaborated by Janson *et al.* [78]. In that case, only recording of the heart rate is used to reconstruct the phase of forcing (breathing) and the phase of the oscillator (heart). These phases are plotted versus each other; in the case of mode-locking, disjoint clouds of points will appear. In **Publication III**, an independent, intuitive and easy to use method of mode-locking detection from univariate data (NN-interval sequence) is developed. The method is based on calculating the amplitudes of the oscillatory component of the fluctuation function $F(n)$ for one-hour segments of 24-hour heart rate recording (cf. **Publication III**, Fig. 7). The fluctuation function $F(n)$ (introduced in 1993 by Peng *et al.* in [91]) is defined as:

$$F(n) \equiv \langle |t_{NN}(k + n) - t_{NN}(k)| \rangle_k \tag{14}$$

here $\langle \ldots \rangle_k$ denotes an average over all intervals $k$. For the patients with isolated clouds of points in phase space, the function $F(n)$ had significant oscillations at small values of $n$ (see **Publication III**, Fig. 7), revealing the causal relationship between mode locking and the presence of "satellite clouds". Indeed, the oscillations of fluctuation function $F(n)$ were not observed for data forming single-clouds in reconstructed phase space. Thus, the amplitudes of the short-scale components of the discrete Fourier transform were chosen to characterize the patterning in phase space. In order to minimize the influence of the long-scale components, the transform was applied to the function $G(n) \equiv F(n) - \langle F(n) \rangle$. Here $\langle F(n) \rangle$ denotes the smoothed (averaged and interpolated) fluctuation function $F(n)$.

It is also important to note that this approach of synchronization detection is very simple and does not require synchronous respiration rhythm recording (as compared with the bivariate techniques, cf. [72, 79, 80]), and can be conveniently used to find relatively short ($\approx 10$ minutes) locking periods from a nonstationary 24-hour recording. These periods were characterized by a low heart rate and a high respiration-driven short-time variability. Besides, the devised technique provides a natural measure to quantify the degree of $\frac{n}{m}$ mode-locking (unlike the qualitative univariate approach of Janson *et al.* [78]), i.e., the amplitude $\Phi(\alpha)$ of the oscillatory component of $F(n)$ at a given wavelength $\alpha = \frac{n}{m}$. The method is very sensitive: the ratio of the Fourier transform amplitude of the locked mode $\Phi(\alpha)$ to the root-mean-square of the amplitudes of the other modes is typically between 10 and 30. The heart and the respiratory complex act as a system of coupled oscillators; however, by no means does this imply that there is a deterministic chaos inside the heart: since the mode locking occurs during a relatively small fraction of the whole recording time, it has almost no effect on the scaling behavior of the correlation sum, which has been tested by calculating the correlation sum for different time-windows: including and excluding the mode-locking periods.

To conclude, the coupling in cardiovascular system, being a "bridge" between spontaneous sinus rhythm and respiration, allows to exchange information between these oscillatory processes by adapting them to a changing environment. This important aspect of appropriate functioning of the cardiovascular system can be certainly used in clinical practice as an independent approach in the diagnostics of pathologies in the autonomic nervous system. Thus the complete lack of synchronization in cardiorespiratory dynamics can be attributed to some failures in the mechanism controlling heart activity, alerting possible pathologies.

# 4 Scale-independent measures

In this Section we will discuss the scale-invariant properties of HRV. Recent studies have shown that scale-invariant characteristics can be successfully applied to the analysis of the heart rate variability [91, 82, 86, 92]. However, this conclusion has been disputed, and certain scale-dependent measures (particularly, the amplitude of the wavelet spectra at a specific time-scale) have been claimed to provide better results [87]. The scale-independent methods have been believed to be more universal, subject-independent, and to reflect directly the dynamics of the underlying system, unlike the scale-dependent methods which may reflect characteristics that are specific to the subject and/or to the method of analysis [92]. The opposing argument has been that certain heart disorders affect the heart rate variability at a specific scale or range of scales; owing to this circumstance, at the properly chosen time-scale, scale-dependent measures may provide useful information [87].

## 4.1 Hurst exponents

One of the possibilities to describe inhomogeneous and nonstationary time series of the heart rate on a scale-independent level is to measure its *fractality*. The simplest relevant fractal measure is the *Hurst exponent $H$*, which is used to describe statistically self-affine random functions $x(t)$ of one or more variables. Here, the author presents a theoretical background for describing the stochastic processes in terms of fractality and, more generally, *multifractality*. Stochastic processes are usually described via the probability density function $p(x, t)$, where $p$ is the probability that at time $t$, the system will be in state $x$. Stochastic process $x(t)$ is called *self-similar*, when its probability distribution function $p(x, t)$ is invariant under suitable scaling in time and space [93]:

$$p(x, at) = p(bx, t). \tag{15}$$

The simplest example of self-similar stochastic processes is the one-dimensional ordinary Brownian motion. The stricter form of self-similarity is called *self-*

21

*affinity* and defined as follows:

$$p(x, ct) = p(c^H x, t), \tag{16}$$

where the exponent $H$ is called the exponent of self-similarity, scaling exponent, or self-affinity index. The self-affine process is *nonstationary* by definition, because it is not invariant under time shift. However, if the increments of such a process are *stationary*:

$$p[x(t + \tau) - x(t)] = p[x(\tau) - x(0)], \tag{17}$$

the *structure function* of order $q$ (a concept borrowed from the theory of the fully-developed turbulence) for nonstationary process $x(t)$ can be defined as the $q$-th moment of the increments of $x(t)$:

$$S_q(\tau) \equiv \langle |x(t + \tau) - x(t)|^q \rangle, \tag{18}$$

here $\langle \ldots \rangle_k$ denotes an average over all values of (discrete) time $t$. The structure function $S_p(\tau)$ for a scale-invariant and self-affine process is expected to scale over some *inertial* range of time lags $\tau$:

$$S_q(\tau) \propto \tau^{\zeta(q)}, \tag{19}$$

where $\zeta(q)$ is the exponent of the structure function. Stochastic statistically self-similar processes can be classified by means of scaling exponents $\zeta(q)$ or self-similarity exponents $H(q)$ (in fact, Hurst exponent), which are related to each other as:

$$\zeta(q) = qH(q). \tag{20}$$

The classification is as follows:

- A trivial case, when the process $x(t)$ is stationary, there is no scaling ($\zeta(q) = H(q) = 0$), because $x(t)$ has scale-independent increments and, therefore, is invariant under translation in time.

- A more interesting case, when the nonstationary process $x(t)$ with a constant $H(q)$ ($\zeta(q)$ linearly depends on $q$), is *monofractal*. The monofractal process has the property of monoscaling, i.e., it is described by the single Hurst exponent $H(q) = H$.

- A general case, when the nonstationary process $x(t)$ with a $q$-dependent $H(q)$ (nonlinear $\zeta(q)$) is *multifractal*. The multifractal process is described by a *spectra* of Hurst exponents $H(q)$.

Plotting the scaling $qH(q)$ versus $q$ provides a straightforward way to check for multifractality: fitting the dependence on $q$ by a straight line indicates monofractal

data. Thus, the calculation of $H(q)$ spectra for time series allows for the straightforward identification of the stationary/nonstationary and monofractal/multifractal nature of the process. Moreover, values of the Hurst exponent quantitatively characterize long-time correlations. Following the original work of Hurst [102], in the case of $H < \frac{1}{2}$, there is a negative long-range correlation (antipersistence) between the increments of the function $x(t)$, whereas $H > \frac{1}{2}$ corresponds to a positive correlation (persistence).

Historically, the scaling of the 2nd-order structure function $S_2(\tau)$ was studied and the corresponding process was referred to as *fractional Brownian motion* (*fBm*):

$$\left\langle |x_{fBm}(t+\tau) - x_{fBm}(t)|^2 \right\rangle = \tau^{2H}, 0 < H < 1. \tag{21}$$

Such a generalisation (introducing a memory, also known as the *Joseph effect*) of Brownian motion was firstly described by Kolmogorov in 1940 [94] and later popularised by Mandelbrot in 1968 [95], who introduced the term *fractional Brownian motion* (*fBm*). Note that $H = \frac{1}{2}$ is a special case of ordinary Brownian motion, i.e., the increments of the function are delta-correlated (uncorrelated random process), and $x(t)$ can be viewed as the displacement of the Brownian particle as a (self-affine) function of time $t$:

$$\left\langle |x_{Bm}(t+\tau) - x_{Bm}(t)|^2 \right\rangle = \tau. \tag{22}$$

with

$$\left\langle |x_{Bm}(t+\tau) - x_{Bm}(t)| \right\rangle = 0. \tag{23}$$

Besides the scaling of structure functions $S_p(\tau)$, there are a number of different methods to calculate the Hurst exponent $H$ for experimentally obtained time series, including rescaled range analysis (also referred as R/S-statistic, technique originally introduced by Hurst) [102, 103], scaled windowed variance [105], and dispersional analysis [104].

Many phenomena in nature exhibit this kind of scale-invariance, revealing nontrivial long-range correlation, and lead to fractional Brownian time series [95]. The same is true for the heart rate variability: after filtering out short-scale components with a period of less than 30 seconds (corresponding to rhythm modulated by respiration and baroreflex), the fluctuation function $F(n)$, defined in Eq. (14) revealed a good scaling behavior in a broad physiologically relevant time scale (200 – 4000 beats, cf. [91]):

$$F(n) \propto n^\alpha \tag{24}$$

Note, that $F(n)$ is a structure function of order 1 ($q = 1$), and therefore the obtained scaling exponent $\alpha$ directly corresponds to the Husrt exponent $H$ ($\alpha \equiv H$). While for healthy patients, the increments of the heart rhythm were found to be significantly anticorrelated resulting in $H < \frac{1}{2}$, the heart rhythm of the patients with dilated cardiomyopathy was essentially Brownian with $H \approx \frac{1}{2}$ [91]. The conclusion was that the lack of *nontrivial* long-range correlations in physiological

23

systems reveals a failure in the ability to adapt to a changing environment, and therefore may indicate a diseased state.

The early scale-invariant studies of HRV were based on power spectra [96, 97], an aspect also closely related to the scaling exponent $H$. Recently, various techniques, such as detrended fluctuation analysis (DFA) [82], detrended time series analysis (DTS) [89], and wavelet amplitude analysis [85] have been proposed to fine-tune the Hurst-exponent-based approach.

### 4.1.1 Detrended fluctuation analysis

When studying the scale-invariance of some process, one generally is not interested in long-range correlations that are simply footprints of (nonstationary) drifts. Therefore, it is important to test the stationarity of the data record, and to exclude nonstationary segments, which tend to give biased estimates of $H$ close to 1. Another way to address such drifts is to *detrend* time series locally; this approach is used in the DFA method. The DFA method was first proposed in 1994 by Peng *et al.* [81] in the study of long-range correlations for noncoding regions in DNA sequences. Later, this approach has been used in the analysis of the heart rate [82].

In this method, one first integrates (or accumulates) nonlinear time series $x(i)$, obtaining integrated data $y(i)$. Further, $y(i)$ divided into segments of equal length $n$. The trend for every segment is defined by the linear fitting of $y(i)$ on this segment to $y_n(i)$. The root-mean-square fluctuation of integrated time series $y(i)$ around detrended data is calculated for the whole recording of length $N$, cf. [82]:

$$F(n) = \sqrt{\frac{1}{N} \sum_i [y(i) - y_n(i)]^2}. \tag{25}$$

For a process with long-range correlations, $F(n)$ is expected to scale as $F(n) \propto n^\alpha$. The DFA method works well on signals with slowly varying trends, i.e., with circadian rhythms. However, one should be aware that certain types of nonstationarity can affect the results [83]. Thus, when correlation properties change in time, the resulting value of scaling exponent $\alpha$ is a superposition of the local scalings of the different segments [83]. Recently, scaling exponents $\alpha$ were calculated for a wide range of physiological time series, including DNA sequences [81], HRV [82], human gait [84], etc.

A slightly different approach to detrend time series (DTS) was proposed by Ashkenazy *et al.* in 1999 [89]. In that method, one produces a locally detrended time series simply by finding the differences between the signal and the local average, calculated on a moving window of size $n$. The standard deviation (calculated for windows of various lengths) also reveals a good scaling with $n$. Note that scaling exponents $\alpha$ calculated by the DTS technique are highly correlated with those obtained by DFA [90].

### 4.1.2 Multiresolution wavelet analysis

The technique of multiresolution wavelet analysis for HRV time series was apparently first applied by Ivanov *et al.* [85]. In this method, one finds the wavelet (weight) coefficients for signal $x_i$ via discrete wavelet transform:

$$W(m,n) = 2^{-m/2} \sum_{i<N} x_i \psi(2^m i - n), \qquad (26)$$

where $m$ is a scale parameter, $n$ is a position parameter and $\psi(m,n)$ is a basis function of the wavelet. The wavelet transform extracts the frequency components of a signal as a function of time, and easily removes polynomial components. These properties make this technique naturally suited to handle nonstationary signals. The choice of wavelet usually depends on properties of the time series; Haahr or Daubechies wavelets are mostly used for HRV analysis. The obtained 2-dimensional distribution of coefficients $W(m,n)$ characterizes the signal in both time and frequency space. Ivanov *et al.* found that the distribution $W(m,n)$ is stable over a wide range of time scales for healthy subjects and does not exist for a group with cardiopulmonary instability [85].

Later, Thurner *et al.* [87] extended this approach by measuring the variance (standard deviation) of calculated $W(m,n)$-sequence for fixed time-scale $m$:

$$\sigma^2(m) = \frac{1}{N-1} \sum_{n<N} (W(m,n) - \mid W(m,n) \mid)^2, \qquad (27)$$

It has been found that values of $\sigma$ for scales 4 and 5 (correspondingly, 16 and 32 heartbeat intervals), completely separated two groups of patients. The Thurner's group even claimed that they found a "*clinically* significant measure of the finding of heart failure with 100% sensitivity at 100% specificity" [87]. However, the performance of this method was later tested on a different set of data, and the separation was found to be less than perfect [88].

Further, the method was slightly extended by Ashkenazy *et al.* [88] via the addition of a filtering procedure. Filtering was done by an inverse wavelet transform for scales $1 < m < 6$, discarding wavelet coefficients related to higher scales. The standard deviation was then calculated for the inversely transformed signal, which resulted in remarkably better discrimination between healthy subjects and patients with heart failure.

Note that the multiresolution wavelet analysis actually detrends the signal (i.e., can be used instead of DFA) by removing the polynomially interpolated components of higher order (the order being given by the order of the wavelet). Also, calculating the structure function $S_q(\tau)$ is essentially the same as applying the wavelet transform with the wavelet constructed from two delta functions with opposite signs and being at distance $\tau$ from each other: $\psi(t,\tau) = \delta(t) - \delta(\tau + t)$. On the other hand, this method is a natural choice when analysing the *multifractal* structure of HRV [86], as it enables to obtain the spectra of local Hurst exponents in a straightforward way.

## 4.2 Multifractality of heart rate

Complex non-stationary time series cannot be described by a single global scaling exponent $H$. Indeed, simple scaling behavior is expected if there is a Gaussian distribution of increments. However, even in the case of Gaussian functions, the scaling exponent is not necessarily constant over the whole range of scales. Instead, it can be a slow (eg. logarithmic) function of the scale, so that other descriptions (such as stretched exponentials) may be required. Physiological time series are typically non-Gaussian [91]. For such functions, scale-invariance can be very complicated. Therefore, it is not surprising that the human heart rate signal was found to obey a multi-affine structure [92, 86]. A non-exhaustive way to describe such behavior is to calculate the multifractal spectrum of Hurst exponents [98].

Qualitatively, a multifractal time series behaves as follows. If the whole time series is divided into short segments, each segment can be characterized by its own *local* Hurst exponent $h$ (referred to as the *Lipschitz-Hölder exponent*). Then, the distribution of segments of fixed values of $h$ is self-similar, and is described by a fractal dimension $f(h)$. Technically, the spectrum $f(h)$ can be calculated by the means of wavelet transform, cf. [92]. This scheme includes the calculation of the scaling exponents $\tau(q)$ (referred to as the *mass exponents*), which describe how the $q$-th moment of the wavelet transform amplitude scales with the wavelet width. The multifractal spectrum $\tau(q)$ is related to the singularity spectrum $f(h)$, through a *Legendre transform*:

$$f(h) = qh - \tau(q), \tag{28}$$

with $h = \frac{d\,\tau(q)}{d\,q}$. The degree of the signal's multifractality can be qualitatively characterized by the width of the spectrum $f(h)$. It has been reported that the spectrum $f(h)$ for heart rate time series is broader for healthy individuals (revealing multifractal properties of signal), and narrow for subjects with congestive heart failure (displaying monofractality) [86]. Also, the scaling exponents $\tau(2)$ and $\tau(5)$ have been found to have a significant prognostic value (for the post-infarction prognosis) [92]. The wavelet transform amplitudes, calculated for a specific wavelet width ($\approx$ 5 min), have been claimed to be of even higher prognostic value [87]. However, independent studies have shown that the scale-invariant measures seem to be superior tools [99]. It should also be noted that the wavelet transform amplitude at a fixed time-scale is closely related to the linear measure SDANN (see **Appendix 1**). Substituting the robust standard deviation by a wavelet transform amplitude is technical fine-tuning which cannot be expected to result in qualitatively new information.

The multifractal structure of the heart rate signal has several consequences. Thus, the $q$-th order structure function $S_q$ (defined in Eq. 18) of the heart rate interval has a scaling behavior, with the scaling exponent $\zeta(q)$ being a function of $q$ [100]. Note that this spectrum of exponents $\zeta(q)$ is very closely related to the above-mentioned $\tau(q)$ spectrum (both describing the same physical phenomenon,

differences being of a technical kind). However, the technique based on wavelet transform makes a more complete utilization of the underlying data, and therefore, the $\tau(q)$ spectrum can be expected to yield somewhat superior prognostic and/or diagnostic results.

Several recent studies addressed the important question of the origin of multifractal properties for heart rate time series [109, 111]. In these studies, parasympathetic blockade led to the loss of multifractal properties; thus the presence of multifractality was attributed mainly to the intrinsic dynamics of the *parasympathetic* branch of the autonomic nervous system and not to changes in external stimulation. Amaral *et al.* in [111] partly motivated this conclusion by the fact that the width of the singularity spectrum $f(h)$ was not dependent on the daily habits of the observed individuals. Struzik *et al.* in [109] confirmed the strong dependency of scaling properties on the functioning of the autonomic nervous system, and proposed the idea of a *"behavioral-independent"* marker for HRV. This idea is based on the observed effects of autonomic neuroregulation on the heart rate (summarized in Table 2).

|                 | global scaling ($H$) | multifractality (width of $f(h)$) |
|-----------------|:--------------------:|:---------------------------------:|
| SNS suppression | increases ↗          | preserves →                       |
| PNS suppression | increases ↗          | decreases ↘                       |

Table 2: The effects of suppression of sympathetic (SNS) and parasympathetic (PNS) autonomic nervous systems on scaling and multifractal properties of heart rate, for details, cf. [109].

The robust scale invariance in the probability density function of increments in healthy human heart rate was reported by Struzik *et al.* in [110]: scale invariance of PDF in a wide range of time lags between 10 and $10^3$ seconds was *preserved* in both quiescent and dynamic conditions. This result might indicate that autonomic neuroregulation constantly converges the heart to a critical state [110]. An analogy with other critical phenomena supports the hypothesis that the regulatory system of the heart rate maximizes the ability of the heart to function under continually changing external conditions.

## 4.3   Intermittency of heart rate

Multifractal spectrum addresses only one aspect of the non-Gaussianity of the time series increments by revealing the possible range of scaling laws for the long-range [at time-scale of many ($\gg$ 1) heartbeat intervals] dynamics of the mean heart rhythm. However, the short-time variability of the heart rhythm is also fluctuating in a complex manner. It has been pointed out that the NN-sequences of healthy subjects consist of intertwined high- and low-variability periods [23]. This conclusion can be easily verified by a simple visual observation of the NN-sequences, see Fig. 8 in **Publication IV**. The multifractal spectra fail to reflect

*all* the features of the intertwining phenomena: the long-term correlations in the dynamics of short-time variability ([112], **Publication V**), and the clustering of periods of a similar mean heart rate [101]. The latter aspect was recently studied by Ivanov *et al.*: they showed that there is a power-law segment-length distribution of the segments with different mean heart rates, into which the heart rate signal can be divided [101]. Switching between low and high levels of short-term variability is another physiologically important aspect, because, typically, low levels are caused by the heart being in a stressed state. The scale-invariant aspects of such a behavior can be addressed by studying the length-distribution of the low-variability periods.

## 4.4 Low-variability periods analysis

Here, the author provides a brief overview of the method based on the analysis of low-variability periods in intermittent time series. The author first developed this method for the analysis of HRV in 2001 (cf. [113]), and presented it at the *Euroattractor* conference in 2002 (cf. **Publication I**). The author presented a further study of low-variability periods distribution using this technique at the *Frontier Science* conference in 2003 and published his results in **Publication V**. Devising this method is a major part of the author's research on short-time HRV, or, to put it more generally, on multifractal intermittent time series.

In this approach, one defines local heart rate variability $\delta(i)$ for each $i$-th interbeat interval as a deviation of the heart rate from the local average:

$$\delta(i) = \frac{|t_{NN}(i) - \langle t_{NN}(i)\rangle_\tau|}{\langle t_{NN}(i)\rangle_\tau}, \tag{29}$$

where $t_{NN}(i)$ is the interval between two adjacent (with indices $i$ and $i+1$) non-arrhythmic beats. The angular braces $\langle\ldots\rangle_\tau$ denote the local average over a window of width $\tau$. In the study, the local average was calculated using a narrow (5 beats wide) Gaussian weight function. The $i$-th interval is said to have low variability in respect to some threshold $\delta_0$ if its local variability does not exceed $\delta_0$:

$$\delta(i) \leq \delta_0. \tag{30}$$

The *low-variability* period is defined as a set of consecutive low-variability interbeat intervals; its length $l$ is measured in the number of heartbeats (see Fig. 1 in **Publication V**). Finally, the cumulative distribution function $r(\tau)$ is defined as the number of periods with length $l > \tau$. Typically, the distribution $r(\tau)$ for heart rate reveals *multiscaling* properties, i.e., within a certain range of scales, the power law

$$r(\tau) \propto \tau^{-\gamma(\delta_0)}. \tag{31}$$

is observed, the scaling exponent $\gamma$ being a function of the threshold level $\delta_0$. For a very low threshold parameter $\delta_0$, all the low-variability periods are very

short, because it is difficult to satisfy the stringent condition (30). Also, in that case, the inertial range of scales is too short for meaningful scaling. Contrary, for a very high value of $\delta_0$, there is a single low-variability period occupying the entire heart rate recording. Between these two extreme cases, there is such a range of the values of $\delta_0$, which typically leads to a non-trivial scaling (see Fig. 2b in **Publication V**).

In fact, the procedure of obtaining distribution $r(\tau)$ for low-variability periods in the heart rate is equivalent to the procedure that was originally done by Harvard linguist George K. Zipf in 1949 when studying the frequency-rank distribution of the words in natural languages [114]. First, for a given language (e.g. English), one can calculate the frequency of each word on the basis of a large set of texts. Further, words are ranked according to their frequency $f$: the most frequent word obtains rank $r = 1$, the second frequent $- r = 2$, etc. It turns out that for a wide range of ranks (starting with $r = 1$), there is a power law $f(r) \propto r^{-\alpha}$ (*Zipf's law*), where $\alpha \approx 1$. Zipf's law is universal; it holds for all the natural languages and for a wide variety of texts. Furthermore, similar scaling laws describe the rank-distribution of many other classes of objects as well. Thus, when cities are arranged according to their population $s$, the population of a city $s \propto r^{-\alpha}$, with $\alpha \approx 1$ [115]. Another example is the income-rank relationship for companies (*Pareto distribution*); here we have again $\alpha \approx 1$. In the most general form (*Zipf-Mandelbrot law*), the law can be formulated as $f \propto (r + r_0)^{-\alpha}$, and $\alpha$ is not necessarily close to unity [98]. The Zipf-Mandelbrot law was found to apply to the distribution of scientific articles according to their citation index [116], for the distribution of internet sites according to the number of visitors [117], etc.

It is not surprising that the scaling behaviour (and Zipf's law) is not perfect. Indeed, the heart rhythm is a non-stationary signal affected by the non-reproducible daily activities of the subjects. The non-stationary pattern of these activities, together with their time-scales, is directly reflected in the distribution $r(\tau)$. This distribution can also have a fingerprint of the characteristic time-scale (10–20 seconds) of the blood pressure oscillations, which modulate the level of HRV [72]. It should be emphasized that the problem of non-reproducible daily activities also affects the reliability of the other scale-invariant measures, and is probably the main obstacle preventing the clinical application of the seemingly extremely efficient diagnostic and prognostic techniques. Finally, there is a generic reason why scaling is nonperfect at big lengths $\tau$: while Zipf's law is a statistical law, each distribution curve is based only on a single measurement. In particular, there is only one longest low-variability period (likewise, only one most-frequent word), the length $\tau$ of which is just as long as it happens to be; there is no averaging whatsoever. For small lengths $\tau$, the relative statistical uncertainty can be estimated as $1/\sqrt{r}$.

In **Publication V**, the author found that the scaling exponent $\gamma(\delta_0)$ (31), and the width of the scaling range are mostly personal characteristics weakly correlated with diagnosis (see Table 2 in **Publication V**). However, the distribution

function of the low-variability periods $r(\tau)$ still contains a significant amount of diagnostically valuable information: the overall number of low-variability periods $r_{max}$ (which is small, if there are a lot of long low-variability periods) and the coordinates of specific points of the $r(\tau)$-curve provided a remarkable resolution between the groups of patients (see Table 2 in **Publication V**). Found quantities characterize the complex structure of the human HRV signal, where the short-time variability level fluctuates intermittently, an aspect which is not addressed by the other methods of HRV analysis (such as multifractal analysis based on fractional Brownian motion).

One can argue that the analysis of $r(\tau)$ distribution in intermittent time series is a simple alternative to conventional multifractal analysis providing higher time-resolution. Indeed, in multifractal formalism, each point corresponding to time $t + \tau$ of the multi-affine time series $x(t)$ is characterized by its *local* Hurst exponent $h$:

$$|x(t + \tau) - x(t)| \propto \tau^h, \tau \gg \tau_0 \tag{32}$$

Here $\tau \gg \tau_0$ states that increments of process $x(t)$ are studied for time lags much greater than some small cut-off scale $\tau_0$. Thus, the effective time resolution $\tau_{min}$ is limited by this requirement to as low as $\tau_{min} \gg \tau_0$. Contrary, the approach of low-variability periods has the effective time resolution of as high as cut-off scale $\tau_0$ ([118]). Also, it is shown that for the multifractal time series, the scaling exponents $\gamma(\delta_0)$ are in one-to-one correspondence with multifractal spectra of the underlying time series ([118]).

The developed method is not limited to heart rate analysis only. It has been proven to be useful for the analysis of various intermittent nonstationary time series like financial data ([118, 119]), and EEG multichannel analysis (**Publication VI** and **Publication VII**). The latter papers focus on the detection of subtle changes in the intensity and time-variability of the human EEG at rest, produced by low-level microwave exposure. These studies evaluate the hypothesis that microwave exposure affects the power spectrum and increases the variability of the human EEG signal (*null* hypothesis is that EEG recordings of subjects under exposure cannot be distinguished from sham signals). In convenient EEG multichannel analysis, one estimates the power spectral density $W$ of the EEG signal for certain frequency bands: theta (4-8 Hz), alpha (8-13 Hz), and beta (13-40 Hz) rhythms. Possible influence of microwave exposure is expected to be reflected in the change of corresponding $W$-values. This approach detects the difference between signals in frequency domain with good accuracy; meanwhile, its resolution in time is limited by the window size (usually $\approx 10^3$ data points), and therefore cannot adequately describe changes in the intermittency of intensity. The method based on the distribution of low-variability periods was selected for the time-variability analysis of the EEG signals, and resulted in the detection of a statistically significant effect of microwave exposure to the EEG signal for about 11% of subjects and for none of the subjects in the case of sham recordings (see Table 1 in **Pub-**

**lication VII**). The formalism of low-variability periods was successfully applied and elaborated further by Kitt and Kalda in their studies of financial time series: currency rates and stock prices time series (c.f. [118]), as well as stock trading volume time series (c.f. [119]).

## Abstract

The thesis *Intermittency and long-range structurization of heart rate* focuses on the analysis of the human heart rate by methods of nonlinear dynamics. In this thesis, the author gives an overview of the main research results in the study of HRV during the last decades, and summarizes his own original results in this field.

Section 1 provides a summary of the approach of phase-space reconstruction and addresses the skepticism in regard to estimating of the correlation dimension of the heart rhythm. **Publication III** also discusses the interpretation of the scaling exponent of the correlation sum in the case of the human heart rate. The paper shows that in the case of the human heart rate (perhaps, excluding subjects with severe heart pathologies), the scaling behavior of the correlation sum is a result of the interplay of various factors: finite resolution of the apparatus, a wide dynamic range of the mean heart rate, and the amplitude of short-time variability, which is a decreasing function of the mean heart rate.

The author devises a simple but sensitive method for detecting the presence of mode-locking between the heart rhythm and respiration. This quantitative method is based on the univariate heart rate data analysis and thus does not require synchronous recording of respiration rhythm. The approach is summarized in Section 3, and the detailed description with the obtained results are provided in **Publication III** and **Publication IV**.

Section 4 provides a comprehensive overview of the scale-independent approach to the study of the heart rate. The author elaborates a new aspect of the multifractality of *intermittent* nonlinear time series: the scale-invariance of low-variability periods. **Publication I** and **Publication II** showed that the length-distribution of low variability periods in the activity of the human heart rate typically has multi-scaling properties. This scale-invariance describes the long-term dynamics of the short-time variability level of the heart rate, which is not addressed by classical multifractal analysis of HRV (**Publication V**). The rank-length distribution contains a significant amount of diagnostically valuable information and efficiently discriminates between several heart pathologies (**Publication IV**). The method is universal: it was succesfully applied in analysis of EEG signals (**Publication VI**, **Publication VII**) and financial data. Therefore, one can argue that this novel approach is a simple alternative to conventional multifractal analysis.

31

# Kokkuvõte

Käesolev väitekiri *Südamerütmi pikamastaabiline kord ja juhumuutlikkus* on kokkuvõte autori tööst viimase nelja aasta jooksul Tallinna Tehnikaülikooli Küberneetika Instituudi mehaanika ja rakendusmatemaatika osakonnas. Suur osa uuringutest on tehtud tihedas koostöös Tallinna Diagnostika Keskusega. Doktoritöö käsitleb inimese südamerütmi löögisageduse muutlikkust (SLM, inglise keeles *heart rate variability, HRV*) mittelineaarse dünaamika meetodite abil. Väitekirjas antakse ülevaade SLM-i analüüsi peamistest tulemustest, mis on saadud viimaste aastakümnete jooksul, ning tehakse kokkuvõtte autori originaaluuringutest selles valdkonnas.

Esimeses osas antakse ülevaade lühiajalise muutlikkuse mittelineaarsetest mõõtudest, mis põhinevad rekonstrueeritud faasiruumil. Kriitilise pilguga on vaadeldud nende mõõtude rakendatavust südamerütmi analüüsi jaoks. **Publikatsioonis III** on uuritud korrelatsioonisumma skaleeruvuse näitaja rakendatavust SLM-i kirjeldamisel ja on näidatud, et inimese SLM-i puhul ei ole alust rääkida madaladimensionaalse deterministliku kaose avaldumisest. Seega formaalselt arvutatud korrelatsioonidimensioon (mis on dünaamilise kaootilise süsteemi vabadusastmete arv) ei peegelda südame sisemist deterministlikut dünaamikat ja korrelatsioonisumma skaleeruvus on erinevate faktorite (mõõtmistehnika lõplik resolutsioon, keskmise südamerütmi lai dünaamiline diapasoon ja lühiajalise muutlikkuse amplituudi sõltuvus keskmisest südamerütmist) koosmõju tulemus.

On arendatud lihtne kuid tundlik meetod hingamise ja südametöö vahelise sünkronisatsiooni leidmiseks. Meetodi idee on tutvustatud kolmandas osas ning detailne kirjeldus ja saadud tulemused on toodud **Publikatsioonis III** ja **Publikatsioonis IV**.

Neljandas osas antakse ülevaade mastaabi-invariantsetest meetoditest SLM-i uurimistes. Tutvustatakse juhumuutlike mittelineaarsete aegridade multifraktaalsuse uus aspekt: väikese muutlikkusega perioodide mastaabi-invariantsus. On näidatud, et südamerütmi madala muutlikkusega perioodide jaotus nende kestvuse järgi tüüpiliselt vastab multiskaleeruvale astmeseadusele (**Publikatsioon I** ja **Publikatsioon II**). Selline mastaabi-invariantsus kirjeldab lühiajalise SLM-i pikaajalist dünaamikat, mida SLM-i klassikalised multifraktaalsed meetodid ei käsitle (**Publikatsioon V**). Väikese muutlikkusega perioodide jaotusfunktsioon sisaldab diagnoostiliselt kasulikut olulist lisainformatsiooni, võimaldades eristada patsiente nende diagnoosi järgi (**Publikatsioon IV**). Arendatud meetod on universaalne ja seda on kasutatud inimese EEG signaali (**Publikatsioon VI** ja **Publikatsioon VII**) ning majanduslike aegridade analüüsis, mis tähendab, et see kujutab ennast klassikalise multifraktaalse analüüsi lihtsat alternatiivi.

# References

[1] R. DeBoer, J. Karemaker, J. Strackee, *Hemodynamic fluctuations and baroreflex sensitivity in humans: a beat-to-beat model.* Am. J. Physiol. Heart. Circ. Physiol. (1987), **253**, 680–689.

[2] A. Malliani, M. Pagani, F. Lombardi, S. Cerutti, *Cardiovascular neural regulation explored in the frequency domain.* Circulation (1991), **84**, 2, 482–492.

[3] E. Hon, S. Lee, *Electronic evaluations of the fetal heart rate patterns preceding fetal death, further observations.* Am. J. Obstet. Gynec. (1965), **87**, 814–826.

[4] M. Wolf, G. Varigos, D. Hunt, J. Sloman, *Sinus arrhythmia in acute myocardial infarction.* Med. J. Australia (1978), **2**, 52–53.

[5] S. Akselrod, D. Gordon, F. Ubel, D. Shannon, A. Barger, R. Cohen, *Power spectrum analysis of heart rate fluctuation: a quantitative probe of beat to beat cardiovascular control.* Science (1981), **213**, 220–222.

[6] R. Kleiger, J. Miller, J. Bigger, A. Moss, The Multi-center Post-Infarction Research Group, *Decreased heart rate variability and its association with increased mortality after acute myocardial infarction.* Am. J. Cardiol. (1987), **59**, 256–262.

[7] M. Malik, T. Farrell, T. Cripps T, A. Camm, *Heart rate variability in relation to prognosis after myocardial infarction: selection of optimal processing techniques.* European Heart Journal (1989), **10**, 1060–1074.

[8] A. Kiviniemi, M. Tulppo, A. Hautala, T. Mäkikallio, T. Seppänen, H. Huikuri, *A novel heart rate variability index of cardiac vagal outflow predicts sudden cardiac death after an acute myocardial infarction.* Heart Rhythm (2005), **2**, 5, S55

[9] A. Goldberger, D. Rigney, J. Mietus, E. Antman, S. Greenwald, *Nonlinear dynamics in sudden cardiac death syndrome: heart rate oscillations and bifurcations.* Experientia (1988), **44**, 983–987.

[10] *Task Force of The European Society of Cardiology and The North American Society of Pacing and Electrophysiology: Heart rate variability: standards of measurement, physiological interpretation, and clinical use.* European Heart Journal (1996), **17**, 354–381.

[11] Z. Struzik, *Revealing local variability properties of human heartbeat intervals with the local effective Hölder exponent.* Fractals (2001), **9**, 77–93.

[12] http://www.physionet.org, *An on-line repository of recorded biomedical signals and open-source software for analyzing them.*

[13] A. Goldberger, L. Amaral, L. Glass, J. Hausdorff, P. Ivanov, R. Mark, J. Mietus, G. Moody, C. Peng, H. Stanley, *PhysioBank, PhysioToolkit, and PhysioNet: Components of a new research resource for complex physiologic signals.* Circulation (2000), **101**, 23, E215–E220.

[14] B. van der Pol, J. van der Mark, *The heartbeat considered as a relaxation oscillation, and an electrical model of the heart.* Phil. Mag. (1928), **6**, 763–775.

[15] D. Noble, *A modification of the Hodgkin-Huxley equations applicable to Purkinje fiber action and pacemaker potential.* J. Physiol. (1962), **160**, 317–352.

[16] B. West, A. Goldberger, G. Rooner, V. Bhargava, *Nonlinear dynamics of the heartbeat. 1. The av junction: passive conduct on active oscillator.* Physica D (1985), **17**, 198–206.

[17] A. Karma, *Electrical alternans and spiral wave breakup in cardiac tissue.* Chaos (1994), **4**, 461–472.

[18] J. Engelbrecht, O. Kongas, *Driven oscillators in modelling of heart dynamics.* Applicable Anal. (1995) **57**, 119–144.

[19] M. Courtemanche, *Complex spiral wave dynamics in a spatially distributed ionic model of cardiac electrical activity.* Chaos (1996), **6**, 579–600.

[20] P. McSharry, G. Clifford, L. Tarassenko, L. Smith, *A dynamical model for generating synthetic electrocardiogram signals.* IEEE Transactions on Biomedical Engineering. (2003) **50**, 3, 289–294. The software implementation of this model is available on http://www.physionet.org/physiotools/ecgsyn

[21] A. Babloyantz, A. Destexhe, *Is the normal heart a periodic oscillator?* Biol. Cybern. (1988), **58**, 203–211.

[22] J. Bassingthwaighte, L. Liebovitch, B. West, *Fractal Physiology*, Oxford Univ. Press, New York 1994.

[23] C. Poon, C. Merrill, *Decrease of cardiac chaos in congestive heart failure.* Nature (1997), **389**, 492–495.

[24] A. Voss, J. Kurths, H. Kleiner, A. Witt, N. Wessel, P. Saparin, K. Osterziel, R. Schurath, R. Dietz, *The application of methods of non-linear dynamics for the improved and predictive recognition of patients threatened by sudden cardiac death.* Cardiovasc. Res. (1996), **31**, 419–433.

[25] R. Govindan, K. Narayanan, M. Gopinathan, *On the evidence of deterministic chaos in ECG: Surrogate and predictability analysis.* Chaos (1998), **8**, 495–502.

[26] F. Takens. *Detecting strange attractors in turbulence* in: D.A. Rand, L.-S. Young (Eds.), Dynamical Systems and Turbulence, Lecture Notes in Mathematics, vol. 898, Springer, New York, 1981.

[27] T. Sauer, J. Yorke, M. Casdagli, *Embedology.* J. Stat. Phys. (1991), **65**, 579–616.

[28] H. Kantz, T. Schreiber, *Nonlinear time series analysis.* Cambridge Univ. Press, Cambridge, 1997.

[29] T. Schreiber, H. Kantz, *Observing and predicting chaotic signals: Is 2% noise too much?* in *Predictability of Complex Dynamical Systems*, Springer, New York, 1996.

[30] P. Mansier, J. Clairambault, N. Charlotte, C. Mèdigue, C. Vermeiren, G. LePape, F. Carrè, A. Gounaropoulou, B. Swynghedauw, *Linear and nonlinear analyses of heart rate variability: a minireview,* Cardiovasc. Res. (1996), **31**, 371–379.

[31] G. Sugihara, R. May, *Nonlinear forecasting as a way of distinguishing chaos from measurement error in time series.* Nature (1990), **344**, 734–741.

[32] K. Chon, J. Kanters, R. Cohen, N. Holstein-Rathlou, *Detection of chaotic determinism in times series from randomly forced maps.* Physica D (1997), **99**, 471–486.

[33] P. Bryant, R. Brown, H. Abarbanel, *Lyapunov exponents from Observed Time Series.* Phys. Rev. Lett. (1990), **65**, 1523–1526.

[34] M. Rosenstein, J. Collins, C. De Luca, *A practical method for calculating largest Lyapunov exponents from small data sets.* Physica D (1993), **65**, 117–134.

[35] H. Kantz, *A robust method to estimate the maximal Lyapunov exponent of a time series.* Phys. Lett. A (1994), **185**, 77–87.

[36] A. Wolf, J. Swift, H. Swinney, J. Vastano, *Determining Lyapunov exponents from a time series.* Physica D (1985), **16**, 285–317.

[37] M. Sano, Y. Sawada, *Measurement of the Lyapunov spectrum from a chaotic time series.* Phys. Rev. Lett. (1985), **55**, 1082–1085.

[38] J.-P. Eckmann, S. Kamphorst, D. Ruelle, S. Ciliberto, *Lyapunov exponents from time series.* Phys. Rev. A (1986), **34**, 4971–4979.

[39] R. Stoop, P.F. Meier, *Evaluation of Lyapunov exponents and scaling functions from time series.* J. Opt. Soc. Am. B (1988), **5**, 1037–1045.

[40] R. Stoop, J. Parisi, *Calculation of Lyapunov exponents avoiding spurious elements.* Physica D (1991), **50**, 89–94.

[41] R. Ganz, G. Weibels, K. Stacker, P. Faustmann, C. Zimmermann, *The Lyapunov exponent of heart rate dynamics as a sensitive marker of central autonomic orgainization: an exemplary study of early multiple sclerosis.* Int. J. Neurosci. (1993), **71**, 29–36.

[42] H. Kantz, T. Schreiber, *Dimension estimates and physiological data.* Chaos (1995), **5**, 1, 143–154.

[43] L. Smith, *Intrinsic limits on dimension calculations.* Phys. Lett. A (1988), **133**, 283–288.

[44] J. Kanters, N. Holstein-Rathlou, E. Agner, *Lack of evidence for lowdimensional chaos in heart rate variablity.* J. Cardivasc. Electrophys. (1994), **5**, 591–601.

[45] A. Bezerianos, T. Bountis, G. Papaioannou, P. Polydoropoulus, *Nonlinear time series analysis of electrocardiograms.* Chaos (1995), **5**, 95–101.

[46] R. Berne, N. Levy, *Cardiovascular physiology. Eighth edition.* Mosby, New York, 2001.

[47] D. Kaplan, M. Talajic, *Dynamics of heart rate.* Chaos (1991), 1, 251–256.

[48] M. Rosenblum, J. Kurths, *A model of neural control of the heart rate.* Physica A (1995), **215**, 439–450.

[49] A. Stefanovska, S. Strle, P. Kroselj, *On the overestimation of the correlation dimension.* Physics Letters A (1997), **235**, 24–30.

[50] P. McClintock, A. Stefanovska, *Noise and determinism in cardiovascular dynamics.* Physica A (2002), **314**, 69–76.

[51] J. Theiler, *Spurious dimension from correlation algorithms applied to limited time-series data.* Phys. Rev. A (1986), **34**, 2427–2432 .

[52] R. Carvajal, N. Wessel, M. Vallverdù, P. Caminal, A. Voss, *Correlation dimension analysis of heart rate variability in patients with dilated cardiomyopathy.* Comp. Methods Programs Biomed. (2005), **78**, 2, 133–140

[53] S. Guzzetti, M. Signorini, C. Cogliati, S. Mezzetti, A. Porta, S. Cerutti, A. Malliani, *Non-linear dynamics and chaotic indices in heart rate variability of normal subjects and heart-transplanted patients.* Cardiovasc. Res. (1996), **31**, 441–446.

[54] M. Casdagli, *Chaos and deterministic versus stochastic non-linear modelling.* J. R. Statist. Soc B (1991), **54**, 303–328.

[55] P. Grassberger, I. Procaccia, *Estimation of the Kolmogorov entropy from a chaotic signal.* Phys. Rev. A (1983), **28**, 2591–2593.

[56] J.-P. Eckmann, D. Ruelle, *Ergodic theory of chaos and strange attractors.* Rev. Mod. Phys. (1985), **57**, 617–656.

[57] S. Pincus, *Approximate entropy as a measure of system complexity.* Proc. Natl. Acad. Sci. USA (1991), **88**, 2297–2301.

[58] S. Pincus, *Heart rate control in normal and aborted-SIDS infants.* Am. J. Physiol. (1991), **33**, R638–R646.

[59] D. Kaplan, M. Furman, S. Pincus, S. Ryan, L. Lipsitz, A. Goldberger., *Aging and the complexity of cardiovascular dynamics.* Biophys. J. (1991), **59**, 945–949.

[60] S. Pincus, *Physiological time series analysis: What does regularity quantify?* Am. J. Physiol. (1994), **266**, H1643–H1656.

[61] D. Sapozhnikov et al. *Detection of regularities in heart rate variations by linear and nonlinear analysis: Power spectrum versus approximate entropy.* Comput. Methods Programs Biomed. (1995), **48**, 201–209.

[62] S. Pincus, *Approximate entropy (ApEn) as a complexity measure.* Chaos (1995), **5**, 110–117.

[63] J. Richman, J. Moorman, *Physiological time-series analysis using approximate entropy and sample entropy.* Am. J. Physiol. (2000), **278**, H2039–H2049.

[64] D. Lake, J. Richman, M. Griffin, J. Moorman, *Sample entropy analysis of neonatal heart rate variability.* Am. J. Physiol. (2002), **283**, 3, R789–R797.

[65] M. Costa, A. Goldberger, C.-K. Peng, *Multiscale entropy analysis of complex physiologic time series.* Phys. Rev. Lett., (2002), **89**, 068102 (4 pages).

[66] M. Costa, A. Goldberger, C.-K. Peng, *Multiscale entropy analysis of biological signals.* Phys. Rev. E, (2005), **71**, 021906 (18 pages).

[67] Y.-C. Zhang, *Complexity and 1/f noise:  a phase space approach.* J. Phys. I France, (1991), **1**, 971–977.

[68] P. Grassberger, J. Procaccia, *Measuring the strangeness of a strange attractor.* Physica D (1983), **9**, 189–195.

[69] J. Zebrowski, W. Poplawska, R. Baranowski, *Entropy, pattern entropy, and related methods for the analysis of data on the time intervals between heartbeats from 24-h electrocardiograms.* Phys. Rev. E (1994), **50**, 5, 4187–4205.

[70] J. Zebrowski, W. Poplawska, R. Baranowski, T. Buchner, *Symbolic dynamics and complexity in a physiological time series.* Chaos, Solitons, Fractals (2000), **11**, 1061–1075.

[71] J. Kurths, A. Voss, P. Saparin, A. Witt, H. Kleiner, N. Wessel, *Quantitative analysis of heart rate variability.* Chaos (1995), **5**, 88–94.

[72] C. Schäfer, M. Rosenblum, J. Kurths, H. Abel, *Heartbeat synchronized with ventilation.* Nature (1998), **392**, 239–240.

[73] M. Rosenblum, J. Kurths, A. Pikovsky, C. Schäfer, P. Tass, H. Abel, *Synchronization in noisy systems and cardiorespiratory interaction.* IEEE Eng. Med. Biol. Mag. (1998), **17**, 46–53.

[74] C. Schäfer, M. Rosenblum, H. Abel, J. Kurths, *Synchronization in the human cardiorespiratory system.* Phys. Rev. E (1999), **60**, 857–870.

[75] M. Lotric, A. Stefanovska, *Synchronization and modulation in the human cardiorespiratory system.* Physica A (2000), **283**, 451–461.

[76] H. Seidel, H. Herzel, *Bifurcations in a nonlinear model of the baroreceptor-cardiac reflex.* Physica D (1998), **115**, 145–160.

[77] K. Kotani, K. Takamasu, Y. Ashkenazy, H. Stanley, Y. Yamamoto, *Model for cardiorespiratory synchronization in humans.* Phys. Rev. E (2002), **65**, 051923 (9 pages).

[78] N. Janson, A. Balanov, V. Anishchenko, P. McClintock, *Phase synchronization between several interacting processes from univariate data.* Phys. Rev. Lett. (2001), **86**, 1749–1752.

[79] F. Censi, G. Calcagnini, S. Cerutti *Coupling patterns between spontaneous rhythms and respiration in cardiovascular variability signals.* Comp. Meth. Prog. Biomed. (2002), **68**, 1, 37–47.

[80] M. Prokhorov, V. Ponomarenko, V. Gridnev, M. Bodrov, A. Bespyatov, *Synchronization between main rhythmic processes in the human cardiovascular system.* Phys. Rev. E (2003), **68**, 4. 041913

[81] C. Peng, S. Buldyrev, S. Havlin, M. Simons, H. Stanley, A. Goldberger, *Mosaic organization of DNA nucleotides.* Phys. Rev. E (1994), **49**, 1685–1689.

[82] C. Peng, S. Havlin, H. Stanley, A. Goldberger, *Quantification of scaling exponents and crossover phenomena in nonstationary heartbeat time series.* Chaos (1995), **5**, 82–87.

[83] Z. Chen, P. Ivanov, K. Hu, H. Stanley, *Effect of nonstationarities on detrended fluctuation analysis.* Phys. Rev. E (2002), **65**, 041107 (15 pages)

[84] J. Hausdorff, C. Peng, Z. Ladin, J. Wei, A. Goldberger, *Is walking a random walk? Evidence for long-range correlations in the stride interval of human gait.* J. Appl. Physiol. (1995) **78**, 349–358.

[85] P. Ivanov, M. Rosenblum, C. Peng, J. Mietus, S. Havlin, H. Stanley, A. Goldberger, *Scaling behaviour of heartbeat intervals obtained by wavelet-based time-series analysis.* Nature (1996), **383**, 323–327.

[86] P. Ivanov, M. Rosenblum, L. Amaral, Z. Struzik, S. Havlin, A. Goldberger, H. Stanley, *Multifractality in Human Heartbeat Dynamics*, Nature (1999), **399**, 461–465.

[87] S. Thurner, M. Feurstein, M. Teich, *Multiresolution Wavelet Analysis of Heartbeat Intervals Discriminates Healthy Patients from Those with Cardiac Pathology.* Phys. Rev. Lett. (1998), **80**, 1544–1547.

[88] Y. Ashkenazy, M. Lewkowicz, J. Levitan, H. Moelgaard, P. Thomsen, K. Saermark, *Discrimination of the healthy and sick cardiac autonomic nervous system by a new wavelet analysis of heartbeat intervals.* Fractals (1998), **6**, 3, 197–203.

[89] Y. Ashkenazy, M. Lewkowicz, J. Levitan, S. Havlin, K. Saermark, H. Moelgaard, P. Thomsen, *Discrimination between healthy and sick cardiac autonomic nervous system by detrended heart rate variability analysis.* Fractals (1999), **7**, 1, 85–91.

[90] Y. Ashkenazy, M. Lewkowicz, J. Levitan, S. Havlin, K. Saermark, H. Moelgaard, P. Thomsen, M. Moller, U. Hintze, H. Huikuri, *Scale specific and scale independent measures of heart rate variability as risk indicators.* arXiv:physics/9909029 v2 22 Nov 2000.

[91] C. Peng, J. Mietus, J. Hausdorff, S. Havlin, H. Stanley, A. Goldberger, *Long-range anticorrelations and non-Gaussian behavior of the heartbeat.* Phys. Rev. Lett., (1993), **70**, 1343–1347.

[92] L. Amaral, A. Goldberger, P. Ivanov, H. Stanley, *Scale-independent measures and pathologic cardiac dynamics.* Phys. Rev. Lett., (1998), **81**, 2388–2391.

[93] P. Embrechts and M. Maejima, *Selfsimilar Processes*, Princeton Univ. Press, Princeton 2002.

[94] A. Kolmogorov, *Wienersche Spiralen und einege andere interessante Kurven in Hilbertische Raum.* C.R. (Dokl.) Acad. Sci. URSS, (1940), **26**, 115–118.

[95] B. Mandelbrot, J. van Ness. *Fractional Brownian motions, fractional noises and applications.* SIAM Review **10**, 422–437, (1968), reprinted in *Selecta vol. H*

[96] M. Kobayashi, T. Musha, *1/f fluctuation of heart beat period.* IEEE Trans. Biomed. Eng. (1982), **29**, 456–457.

[97] Y. Yamamoto, R. Hughson, *Coarse-graining spectral analysis: new method for studying heart rate variability.* J. Appl. Physiol. (1991), **71**, 1143–1150.

[98] B. Mandelbrot, *The Fractal Geometry of Nature.* Freeman, San Francisco, 1983.

[99] K. Saermark, M. Moellery, U. Hintzey, H. Moelgaard, P. Thomsen, H. Huikuri, T. Mäkikiallio, J. Levitan, M. Lewkowicz, *Comparison of recent methods of analyzing heart rate variability.* Fractals (2000) **8**, 315–322.

[100] D. Lin, R. Hughson, *Modeling heart rate variability in healthy humans: a turbulence analogy.* Phys. Rev. Lett. (2001), **86**, 1650–1653.

[101] P. Bernaola-Galvàn, P. Ivanov, L. Amaral, H. Stanley, *Scale invariance in the nonstationarity of human heart rate.* Phys. Rev. Lett. (2001), **87**, 168105 (4 pages).

[102] H. Hurst, *The long-term storage capacity of reservoirs.* Trans. Am. Soc. Civ. Eng. (1951), **116**, 770–808.

[103] B. Mandelbrot, J. Willis, *Noah, Joseph and operational hydrology.* Water Resour. Res. (1968), **4**, 909–918, reprinted in *Selecta vol. H*

[104] J. Bassingthwaighte, G. Raymond, *Evaluation of the dispersional analysis method for fractal time series.* Ann. Biomed. Eng. (1995), **23**, 491–505.

[105] M. Cannon, D. Percival, D. Caccia, G. Raymond, J. Bassingthwaighte, *Evaluating scaled windowed variance methods for estimating the Hurst coefficient of time series.* Physica A (1997), **241**, 606–626.

[106] P. Ivanov, Z. Chen, K. Hu, H. Stanley, *Multiscale aspects of cardiac control* Physica A (2004), **344**, 3–4, 685–704.

[107] Y. Ashkenazy, S. Havlin, P. Ivanov, C. Peng, V. Schulte-Frohlinde, H. Stanley, *Magnitude and sign scaling in power-law correlated time series.* Physica A (2003), **323**, 19–41.

[108] J. Zebrowski, R. Baranowski, *Type I intermittency in nonstationary systems – models and human heart rate variability.* Physica A (2004), **336**, 1-2, 74–83.

[109] Z. Struzik, J. Hayano, S. Sakata, S. Kwak, Y. Yamamoto, *1/f scaling in heart rate requires antagonistic autonomic control.* Phys. Rev. E (2004), **70**, 050901 (4 pages).

[110] K. Kiyono, Z. Struzik, N. Aoyagi, S. Sakata, J. Hayano, Y. Yamamoto, *Critical scale invariance in a healthy human heart rate.* Phys. Rev. Lett (2004), **93**, 17, 178103 (4 pages).

[111] L. Amaral, P. Ivanov, N. Aoyagi, I. Hidaka, S. Tomono, A. Goldberger, H. Stanley, Y. Yamamoto, *Behavioral-independent features of complex heartbeat dynamics.* Phys. Rev. Lett (2001), **86**, 26, 6026–6029.

[112] J. Kalda, M. Vainu, M. Skki, *The methods of nonlinear dynamics in the analysis of heart rate variability for children.* Med. Biol. Eng. Comp. (1999), **37**, 69–72.

[113] J. Kalda, M. Skki, M. Vainu, M. Laan, *Zipf's law in human heartbeat dynamics.* arXiv:physics/0110075 v1 26 Oct 2001.

[114] G. Zipf, *Human Behaviour and the Principle of Least-Effort.* Addison-Wesley, Cambridge MA, 1949.

[115] X. Gabaix, Y. Ioannides, *The evolution of city size distributions*, in *Handbook of Urban and Regional Economics*, Volume 4, Chapter 53 (North-Holland), 2341–2378, 2004.

[116] Z. Silagadze, *Citations and the Zipf-Mandelbrot's law.* Complex Syst. (1997), **11**, 487–499.

[117] J. Pitkow, *Summary of WWW characterizations,* Computer Networks and ISDN Systems (1998), **30**, 551–558.

[118] R. Kitt, J. Kalda, *Properties of low-variability periods in financial time series.* Physica A (2005), **345**, 622–634.

[119] R. Kitt, J. Kalda, *Scaling analysis of multi-variate intermittent time series.* Physica A (2005), **353**, 480–492.

[120] C. Bonferroni, *Teoria statistica delle classi e calcolo delle probabilita.* Pubblicazioni del R Istituto Superiore di Scienze Economiche e Commerciali di Firenze (1936), **8**, 3–62.

[121] J. Shaffer, *Multiple Hypothesis Testing.* Ann. Rev. Psych. (1995), **46**, 561–584.

[122] A. Sankoh, M. Huque, S. Dubey, *Some comments on frequently used multiple endpoint adjustments methods in clinical trials.* Statistics in Medicine (1997), **16**, 2529–2542.

[123] T. Perneger, *What's wrong with Bonferroni adjustments.* Brit. Med. J. (1998), **316**, 1236–1238.

[124] J. Jaccard, C. Wan, *LISREL approaches to interaction effects in multiple regression.* Sage Publications, Thousand Oaks, CA, 1996.

**Publication I**

# ON THE ZIPF'S LAW IN HUMAN HEARTBEAT DYNAMICS.

M. SÄKKI, J. KALDA, M. VAINU, M. LAAN.

# On the Zipf's Law in Human Heartbeat Dynamics

*M. Säkki, J. Kalda*

*Institute of Cybernetics, Tallinn Technical University, Estonia*

*It is shown that the distribution of low variability periods in the activity of human heart rate typically follows a multi-scaling Zipf's law. The presence or failure of a power law, as well as the values of the scaling exponents, are personal characteristics depending on the daily habits of the subjects. Meanwhile, the distribution function of the low-variability periods as a whole discriminates efficiently between various heart pathologies. This new technique is also applicable to other non-linear time-series and reflects these aspects of the underlying intermittent dynamics, which are not covered by other methods of linear- and non-linear analysis.*

*Key words: medical physics, data analysis*

## 1. Introduction

The non-linear and scale-invariant aspects of the heart rate variability (HRV) have been studied intensively during the last decades. This continuous interest to the HRV can be attributed to the controversial state of affairs: on the one hand, the non-linear and scale-invariant analysis of HRV has resulted in many methods of very high prognostic performance (at least on test groups) [1-4]; on the other hand, practical medicine is still confident to the traditional "linear" methods. The situation is quite different from what has been observed three decades ago, when the "linear" measures of HRV became widely used as important non-invasive diagnostic and prognostic tools, soon after the pioneering paper [5]. Apparently, there is a need for further evidences for the superiority of new methods and for the resolution of the existing ambiguities.

During recent years the main attention of studies has been focused on the analysis of the scale-invariant methods. It has been argued that measures related to a certain time-scale (e.g. 5 min) are less reliable, because the characteristic time-scales of physiological processes are patient-specific. The scale-invariant measures are often believed to be more universal and sensitive to life-threatening pathologies [1, 2]. However, carefully designed time-scale-related measures can be also highly successful, because certain physiological processes are related to a specific time scale [3].

The scale invariance has been exclusively seen in the heart rhythm following the (multi)fractional Brownian motion (fBm) [6]. It has been understood that the heart rhythm in a very complex manner and reflects the activities of the subject (sleeping, watching TV, walking etc.) [7, 9] and cannot be adequately described by a single Hurst exponent of a simple fBm. In order to reflect the complex behaviour of the heart rhythm, the multi-affine generalization of the fBm has been invoked [1, 2]; it has been claimed that the multifractal scaling exponents are of a significant prognostic value.

The approach based on fBm addresses long-time dynamics of the heart rhythm while completely neglecting the short-scale dynamics on time scales less than one minute (the respective frequencies are typically filtered out [6]). The short-time variability has been described only by the so called linear measures, such as $p_{NN50}$ (the probability that two adjacent normal heart beat intervals differ more than 50 milliseconds). Meanwhile, the level of the short-time variability of the human heart rate varies in a very complex manner, the high- and low-variability periods are deeply intertwined [7]. This is a very important aspect, because the low-variability periods are the periods when the heart is in a stressed state, with high level of signals arriving from the autonomous nervous system. The conventional linear measures are not appropriate for describing such a complex behaviour. Thus, there is a clear need for suitable non-linear methods.

## 2. Problem Formulation

Our analysis is based on ambulatory Holter-monitoring data (recorded at Tallinn Diagnostic Centre) of 218 patients with various diagnoses. The groups of patients are shown in Table 1. The sampling rate of ECG was 180 Hz. The patients were monitored during 24 hour under normal daily activities. The preliminary analysis of the ECG recordings was performed using the commercial software; this resulted in the sequence of the normal-to-normal (NN) intervals $t_{NN}$ (measured in milliseconds), which are defined as the intervals between two subsequent normal heartbeats (i.e. normal QRS complexes).

Originally, the Zipf's law addressed the distribution of words in a language [11]: every word has assigned a rank, according to its "size" $f$, defined as the relative number of occurrences in some long text (the most frequent word obtains rank $r = 1$, the second frequent $r = 2$, etc). The empirical size-rank distribution law $f(r) \sim r^{-\alpha}$ is surprisingly uni-

Tab. 1: Test groups of patients. Abbreviations are as follows: IHD - Ischemic Heart Disease (Stenocardia); SND - Sinus Node Disease; VES - Ventricular Extrasystole; PCI - Post Cardiac Infarction; RR - Blood Pressure Disease; FSK - Functional Disease of Sinus Node.

|  | Healthy | IHD | SND | VES | PCI | RR | FSK |
|---|---|---|---|---|---|---|---|
| No of patients | 103 | 8 | 11 | 16 | 7 | 11 | 6 |
| Mean age | 45.5 | 65.4 | 50.0 | 55.9 | 47.3 | 55.5 | 11.7 |
| Std. dev. of age | 20.5 | 11.4 | 19.3 | 14.3 | 11.6 | 14.4 | 4.6 |

versal: in addition to all the tested natural languages, it applies to many other phenomena.

The scaling exponent is often close to one (e.g. for the distribution of words). Typically, the Zipf's law is applicable to a dynamical system at statistical equilibrium, when the following conditions are satisfied: (a) the system consists of elements of different size; (b) the element size has upper and lower bounds; (c) there is no intermediate intrinsic size for the elements. As already mentioned, the human heart rhythm has a complex structure, where the duration $\tau$ of the low-variability periods varies in a wide range of scales, from few to several hundreds of heart beats. Thus, one can expect that the distribution of the low-variability periods follows the Zipf's law

$$r \sim \tau^{-\gamma}. \tag{1}$$

However, the scaling behaviour should not be expected to be perfect. Indeed, the heart rate is a non-stationary signal affected by the non-reproducible daily activities of the subjects. The non-stationary pattern of these activities, together with their time-scales, is directly reflected in the above mentioned distribution law.

This distribution law can also have a fingerprint of the characteristic timescale (around ten to twenty seconds) of the blood pressure oscillations. Finally, there is a generic reason why the Zipf's law fails (or is non-perfect) at small rank numbers. The Zipf's law is a statistical law; meanwhile, each rank-length curve is based on a single measurement. Particularly, there is only one longest low-variability period (and likewise, only one most-frequent word), the length of which is just as long as it happens to be, there is no averaging whatsoever.

To begin with, we define the local variability for each ($i$-th) interbeat interval as the deviation of the heart rate from the local average,

$$\delta(i) = |t_{NN}(i) - [t_{NN}(i)]| / [t_{NN}(i)]. \tag{2}$$

The angular braces denote the local average, calculated using a narrow (5 beats wide) Gaussian weight function. Further, we introduce a threshold value $\delta_0$; $i$-th interbeat interval is said to have a low variability, if the condition

$$\delta(i) < \delta_0 \tag{3}$$

is satisfied. A low-variability period is defined as a set of consecutive low-variability intervals; its length $\tau$ is measured in the number of heartbeats. Finally, all the low-variability periods are arranged according to their lengths and associated with ranks. The rank of a period is plotted versus its length in a logarithmic graph, see Fig. 1; Zipf's law would correspond to a straight descending line.
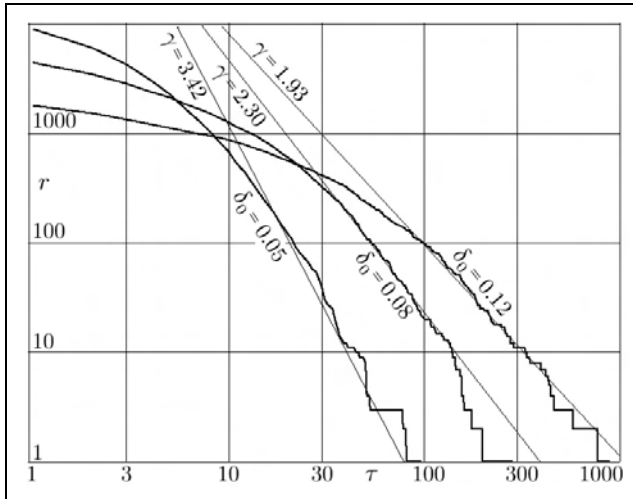
Fig. 1: Multi-scaling distribution of the low-variability periods: the rank r of a period is plotted versus its duration τ (measured in heartbeats) for different values of the threshold parameter $\delta_0$.
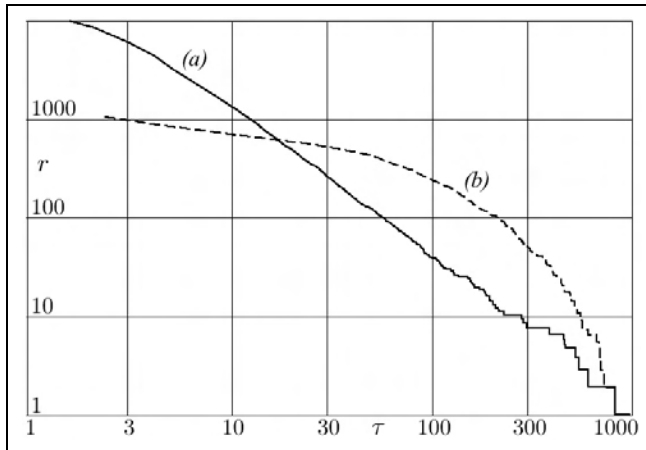


Fig. 2: Rank-length curves for a patient with a good power law (a) and for a patient with no power law (b). In both cases, the threshold parameter $\delta_0 = 0.05$.

# 3. Problem Solution

For a very low threshold parameter $\delta_0$, all the low-variability periods are very short, because it is difficult to satisfy the stringent condition (3). In that case, the inertial range of scales is too short for a meaningful scaling law. On the other hand, for a very high value of $\delta_0$, there is a single low-variability period occupying the entire HRV-recording. Between these two cases, there is such a range of the values of $\delta_0$, which leads to a non-trivial rank-length law. For a typical healthy patient, the $r(\tau)$-curve is reasonably close to a straight line, and the scaling exponent  is a function of the threshold parameter $\delta_0$. Thus, unlike all the other well-known applications of the Zipf's law, we are dealing with a multi-scaling law.

Recently, Ivanov et al. [2] have reported that anomalous multifractal spectra of the HRV signal indicate an increased risk of sudden cardiac death. Therefore, it is natural to ask, does the presence or failure of the multiscaling behaviour indicate the healthiness of the patient? In what follows we discuss a somewhat more general question: what is the relationship between the properties of the distribution function of the low variability periods and the diagnosis of the patient. Testing the prognostic significance for predicting sudden cardiac death, which is also of a great importance, has been postponed due to the nature of our test groups.

First, let us analyse the correlation between the diagnosis of a patient and the scaling exponent To begin with, we have to determine the optimal value for the threshold parameter $\delta_0$. For a meaningful analysis, the scaling behaviour should be as good as possible. It turned out that for a typical patient, the best approximation of the function $r(\tau)$ with a power law is achieved for $\delta_0 = 0.05$ (see Fig. 2a); in what follows, all the values of the exponent  are calculated for $\delta_0 = 0.05$. It should be noted that for some patients, the length-rank distribution is still far from a power law (see Fig. 2b).

The slope of a curve on the logarithmic plot is calculated using root-mean-square (rms) fit for such a range of lengths $[\tau_{start}; \tau_{end}]$, for which the $r(\tau)$-curve is nearly a power law, and the scaling range width $\Delta = \ln \tau_{end} - \ln \tau_{start}$ is as large as possible. Bearing in mind the statistical nature of the Zipf's law and non-stationarity of the underlying signal, we have chosen a not very stringent definition of what is "nearly a power law", see Fig. 3. Around the rms-fit-line, two limit lines are drawn; $\tau_{start}$ and $\tau_{end}$ end correspond to the points, where the $r(\tau)$-curve crosses the limit lines.

Note that the precise placement and shape of the limit lines is arbitrary, i.e. small variations do not lead to qualitative effects. Here, the distance of the limit lines from the central line has been chosen to be $\ln 2$ at $\tau = \tau_{max}$, and zero at $\tau = 1$, where $\tau_{max}$ is the length of the longest low-variability period. Admitting mismatch $\ln 2$ at $\tau = \tau_{max}$ is motivated by the observation that due to the lack of any statistics, the longest low-variability period could have been easily twice as long as we measured it to be.

However, the above mentioned effect of the non-stationary pattern of the subjects daily activities makes the situation more complicated. There is no easy way to quantify this effect and therefore, we opted for the simplest possible solution, simple straight limit lines.
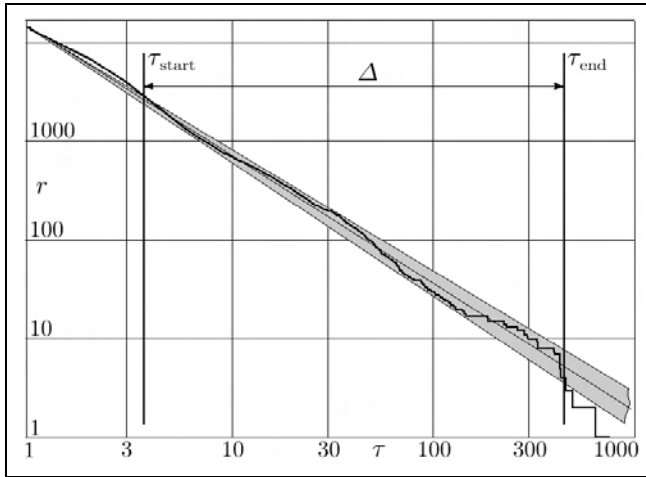
Fig. 3: Definition of the width of the scaling interval Δ. The rank-length curve is fitted with a power law; the boundaries of the scaling interval are defined as the intersection points of limit lines and $r(\tau)$-curve.
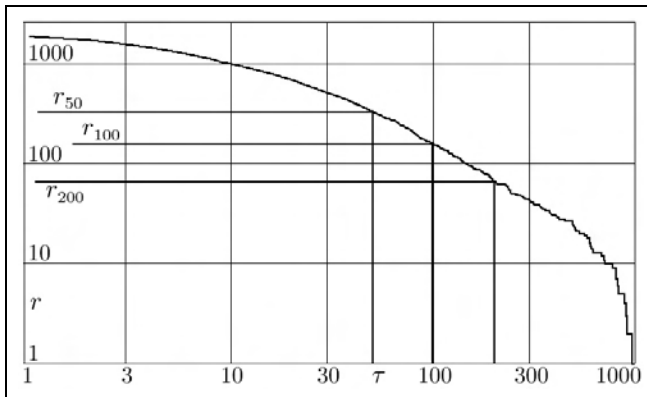


Fig. 4: Definition of the parameters $r_{50}$, $r_{100}$, and $r_{200}$.

The scaling exponent has been calculated for all the patients and Student test was applied to every pair of groups. In most cases, the significance was quite low; two best distinguishable groups were RR and FSK, the result of Student test being 5.7%. Therefore, one can argue that the slopes of linear parts are highly personal characteristics depending also on the daily habits of the subjects, which are weakly correlated with diagnosis. Further we tested, how is the failure of the power law correlated with the diagnosis. The width of the scaling range Δ was used as a measure of how well the curve is

*Tab. 2: p-values of the Student test. Data in the topmost triangular region (with label A) are calculated using the parameter ln $\tau_{end}$. Triangular region B corresponds to the parameter ln $r_{max}$, region C - to ln $r_{100}$, and region D - to ln $\tau_{40}$. Gray background highlights small p-values, $p < 10\%$.*

| p (%) | Healthy | IHD | SND | VES | PCI | RR | FSK |
|---|---|---|---|---|---|---|---|
| Healthy | *B*   *A* | 0.06 | 17.21 | 0.02 | 0.07 | 1.59 | 1.55 |
| IHD | 0.36 | | 2.85 | 96.79 | 97.62 | 21.93 | 20.05 |
| SND | 2.99 | 59.10 | | 2.10 | 3.04 | 25.77 | 25.57 |
| VES | 0.08 | 91.60 | 63.79 | | 94.18 | 17.59 | 16.20 |
| PCI | 25.27 | 21.61 | 46.37 | 22.89 | | 22.50 | 20.62 |
| RR | 0.14 | 73.57 | 77.69 | 80.49 | 28.90 | | 98.20 |
| FSK | 46.48 | 5.20 | 8.72 | 5.52 | 20.06 | 6.45 | |
| Healthy | *D*   *C* | 1.27 | 43.12 | 0.01 | 6.27 | 87.40 | 73.99 |
| IHD | 4.82 | | 4.87 | 90.04 | 27.13 | 6.11 | 5.83 |
| SND | 47.91 | 6.37 | | 3.81 | 12.31 | 55.50 | 63.46 |
| VES | 0.34 | 81.67 | 6.02 | | 11.04 | 3.69 | 4.43 |
| PCI | 38.38 | 18.24 | 27.25 | 12.40 | | 20.45 | 17.37 |
| RR | 85.74 | 6.80 | 59.23 | 4.01 | 42.81 | | 88.81 |
| FSK | 65.87 | 9.45 | 81.38 | 9.53 | 38.30 | 77.74 | |

corresponding to a power law. The Student test results for the parameter $\Delta$ turned out to be similar to what has been observed for the parameter the correlation between the failure of the power law and diagnosis was weak. Thus, a rank-length curve resembling the one depicted by a dashed line in Fig. 2, does not hint to heart pathology. It should be also noted that the dashed curve in Fig. 2 can be considered as a generalized form of scale-invariance with scale-dependent differential scaling exponent.

Finally, we analysed the diagnostic significance of the parameters ln $\tau_{end}$ and ln $\tau_{start}$. This analysis does make sense, because typically, the start- and end-points of the scaling range correspond to certain physiological time-scales. The parameter ln $\tau_{end}$ provided, indeed, a remarkable resolution between the groups of patients, see Table 2.

According to the Student test, the healthy patients, were distinct from five heart pathology groups with probability $p < 1.6\%$. The parameter ln $\tau_{start}$ was diagnostically less significant.

Unfortunately, the calculation of the parameter $\tau_{end}$ is technically quite a complicated task, not suited for clinical practice. Therefore, we aimed to find a simpler alternative to it. Basically, the strategy was to find a simple parameter reflecting the behaviour of the rightmost (large-$\tau$) part of the r($\tau$)-curve. An easy option is ln $\tau_{max}$, which has been already analysed [10]. This parameter has indeed a considerable diagnostic value, but its reliability is decreased by the above discussed statistical fluctuations. Better alternatives are provided by (*a*) the overall number of low-variability periods $r_{max}$ (which is small, if there are lot of long low-variability periods); (*b*) the coordinates of specific points of the rank-length curve. Here we chose a set of critical ranks $R = 10$, 20 or 40, and determined

the respective lengths $\tau_R$ so that $r(\tau_R) = R$. We also fixed a set of critical length values, $T$ = 50, 100, or 200, and determined the respective rank numbers $r_T = r(T)$, see Fig. 4. Both techniques turned out to be of high diagnostic performance; illustrative $p$-values are given in Table 2. Parameters $\tau_{10}$ and $\tau_{20}$ performed less well than $\tau_{40}$ (for instance, the $p$-values for the healthy and VES-subject groups were 0.60%, 0.58% and 0.34%, respectively), and are not presented in tabular data. Similarly, $r_{100}$ turned out to be more efficient than $r_{50}$ and $r_{200}$ (the respective healthy and VES-group $p$-values being 0.02%, 0.01%, and 0.09%). It also outperforms $\tau_{40}$, but is sometimes less efficient than $r_{max}$ or $\tau_{end}$ (see Table 2). Hence, various heart pathologies seem to affect the heart rate dynamics at the time scale around 100 heart beats (one to two minutes).

## 4. Conclusion

In conclusion, new aspect of non-linear time-series has been discovered, the scale-invariance of low-variability periods. We have shown that the distribution of low variability periods in the activity of human heart rate typically follows a multi-scaling Zipf's law. The presence or failure of a power law, as well as the values of the scaling exponents, are personal characteristics depending on the daily habits of the subjects. Meanwhile, the distribution function of the low-variability periods as a whole contains also a significant amount of diagnostically valuable information, the most part of which is reflected by the parameters $r_{100}$, $r_{max}$, and $\tau_{end}$, see Table 2. These quantities characterize the complex structure of HRV signal, where the low- and high variability periods are deeply intertwined, aspect which is not covered by the other methods of heart rate variability analysis (such as fractional Brownian motion based multifractal analysis). This new technique is also applicable to other non-linear time-series, such as EEG signals and financial data [8]. As a future development, it would be of great importance to analyse the prognostic value of the above mentioned parameters for patients with sudden cardiac death.

## References

1. Amaral, L. A. N., Goldberger, A. L., Ivanov, P. Ch., Stanley, H. E. (1998). Phys. Rev. Lett., 81, 2388
2. Ivanov, P. Ch. et al. (1999). Nature, 399, 461
3. Thurner, S., Feurstein, M. C., Teich, M. C. (1998). Phys. Rev. Lett., 70, 1544
4. Saermark, K. et al. (2000). Fractals, 8, 315
5. Hon, E. H., Lee, S. T. (1965). Am. J. Obstet. Gynec., 87, 814
6. Peng, C. K. et al. (1993). Phys. Rev. Lett., 70, 1343
7. Poon, C. S., Merrill, C. K. (1997). Nature, 389, 492
8. Kalda, J., Säkki, M., Kitt, R. (unpublished)
9. Struzik, Z. R. (2001). Fractals, 9, 77
10. Kalda, J., Vainu, M., Säkki, M. (1999). Med. Biol. Eng. Comp., 37, 69

11. Zipf, G. K. (1949). Human Behavior and the Principle of Least Effort. Cambridge: Addison-Wesley

# Nonlinear methods of heart rate variability in patients with heart disease using ambulatory ECG monitoring.

## M. Vainu, J. Kalda, M. Laan, M. Säkki

# Mittelineaarsed meetodid südame löögisageduse muutlikkuse hindamisel kardioloogilistel patsientidel ambulatoorse EKG monitooringu andmetel

**Meelis Vainu[1], Jaan Kalda[2], Mari Laan[3], Maksim Säkki[2]** – [1]Tallinna Diagnostikakeskus, [2]TTÜ küberneetika instituut, [3]Tallinna Lastehaigla

südame löögisageduse muutlikkus, HRV, ambulatoorne EKG monitooring, mittelineaarne dünaamika

**Südame löögisagedus ja südame löögisageduse muutlikkus on südamehaiguste puhul olulised parameetrid, mida kasutatakse nii diagnostilistel eesmärkidel kui prognoosi määramisel. Seni on nimetatud otstarbel kasutatud valdavalt lineaarseid meetodeid standarditud eeskirjade alusel. Artiklis on antud teoreetiline ülevaade südame löögisageduse muutlikkuse mittelineaarsetest karakteristikutest ning tehtud kokkuvõte autorite originaaluuringutest mittelineaarsete meetodite rakendamisel südame löögisageduse muutlikkuse määramisel südamehaigetel.**

Tänapäeval kasutatakse hulgaliselt väga erinevaid meetodeid, et välja selgitada krooniliste haiguste seni veel tundmatuid riskitegureid. Paljud lihtsalt määratavad näitajad, mida on võimalik jälgida pikema aja vältel, on arvatud oluliste riskifaktorite hulka, kuigi nende usaldusväärsus ja prognostiline tähendus igapäevases arstipraktikas on sageli veenvalt tõestamata. Südame löögisagedus ja südame löögisageduse muutlikkus (SLM, *heart rate variability – HRV*) kui erinevate krooniliste haiguste riskitegurid on viimastel aastakümnetel olnud paljude uurimistööde huviobjektiks. SLMi mõõdetakse ja analüüsitakse standarditud eeskirjade alusel, kasutades selleks üldjuhul vaid lineaarseid meetodeid (1). SLM lineaarseid meetodeid ning nende osa erinevate südame- ja veresoonkonnahaiguste puhul on ka Eesti Arstis varem põhjalikult käsitletud (2). Mittelineaarsete meetodite osas on viimase kümne aasta jooksul toimunud olulised nihked arusaamades ja kohati on uurimistöö tulemused olnud väga paljulubavad. Artikli **eesmärgiks** on anda ülevaade olulisematest saavutustest selles valdkonnas ning teha kokkuvõte oma originaaluuringutest, mille sihiks oli õppida mõõtma ja analüüsida diagnostilise tähenduse seisukohast selliseid SLM aspekte, mille

iseloomustamist pole seni tuntud meetodid võimaldanud.

SLM mittelineaarsed karakteristikud võib liigitada järgmiselt:

1. Rekonstrueeritud faasiruumil põhinevad mõõdud (mitmesugused entroopiad, korrelatsioonidimensioon, Ljapunovi astmenäitajad jms): suurused, mis kirjeldavad lühiajalist muutlikkust.

2. Mastaabi-invariantsed mõõdud (Hursti astmenäitaja, multifraktaalne spekter, multi-mastaabiline entroopia jms): mõõdud, mis kirjeldavad südame löögisageduse muutuste pikemaajalisi seoseid.

3. Mastaabi-spetsiifilised mõõdud: teatud kindla ajamastaabiga seotud lainekeste amplituud.

4. Juhumuutlikke aspekte kirjeldavad mõõdud, mis tuginevad teatud ajaintervallide pikkusjaotusele (Zipfi seadus); ajaintervallid võivad olla saadud kas vähese muutlikkuse või keskmise südamelöögi intervalli alusel fragmenteerimise tulemusel.

Allpool on vastavalt toodud klassifikatsioonile vaadeldud neid mõõte lähemalt.

**1. Rekonstrueeritud faasiruumil põhinevad mõõdud.** See et siinussõlme ja atrioventrikulaarse sõlme poolt moodustuv südamerütmi genereeriv süsteem on vaadeldav seostatud mittelineaarsete

ostsillaatoritena (piltlikult nagu kaks pendlit, mis on omavahel kummipaelaga ühendatud), on üldtunnustatud asjaolu (3, 4). See mudel kirjeldab edukalt mitmeid nähtusi (nt Wenckebachi ja Mobitzi II tüüpi südame-rütmihäireid ja bistabiilset käitumist (4)).

Niisiis võiks arvata, et mittelineaarse dünaamika meetodid on sobilikud ka SLM kirjeldamiseks. Selliseks meetodiks on näiteks korrelatsioonidimensiooni arvutamine: see on suurus, mis kirjeldab dünaamilise kaootilise süsteemi vabadusastmete arvu ja mida võib vaadelda ka süsteemi keerulisuse määrana. Teisteks olulisteks mõõtudeks on Ljapunovi eksponendid ja Kolmogorovi entroopia (s.o suurima Ljapunovi eksponendi keskväärtus). Suurim Ljapunovi eksponent kirjeldab seda, kui tundlik on süsteem algtingimuste suhtes (s.t kui muuta vähesel määral algtingimusi, siis millise aja pärast on see muutus kasvanud oluliselt tuntavaks); neid võib vaadelda kui kaootilisuse määrasid. Ka Shannoni, ligikaudne (*approximate*), kujundi- (*pattern*) jt entroopiad on süsteemi kaootilisuse mõõtudeks.

Esimesed südame löögisageduse mittelineaarsust uurivad tööd olidki pühendatud mainitud suurustele, sh teedrajav uurimus (5). Jõuti järeldusele, et terve süda on kaootilisem kui haige süda. Terve südame puhul leiti, et korrelatsioonidimensioon on vahemikus 3,6 kuni 5,2.

Tänaseks päevaks on aga aru saadud, et tegelikult mängivad SLM korral määravat rolli autonoomsest närvisüsteemist saabuvad impulsid, mis oma loomult ei ole deterministlikud (s.t ei ole pendli või muu mehaanilise süsteemi sarnase käitumisega) ja mida on kõige õigem vaadelda juhumuutliku mürana. Niisiis, formaalselt võib küll arvutada mittelineaarse dünaamika mõõte (korrelatsioonidimensiooni jt), kuid need ei kirjelda seda, mille kirjeldamiseks nad on välja mõeldud.

On küll tõsi, et terve süda käitub üldjuhul haigest südamest näiliselt kaootilisemalt, kuid see pole tingitud mitte sellest, et mittelineaarsel ostsillaatoril südame sees on vabadusastmeid rohkem või Ljapunovi astmenäitaja on suurem. Põhjuseks on

see, et terve süda suudab kohaneda märksa ulatuslikuma autonoomsest närvisüsteemist saabuva südame löögisagedust reguleeriva signaalidevooga, kui seda teeb haige süda. Seega suudab terve süda muuta löögisagedust kiiremini ja suuremas vahemikus. Nimetatud asjaolu tõttu on ka terve südame korrelatsioonidimensioon (jmt parameetrid) suurem. Korrelatsioonidimensioon on konstrueeritud, et kirjeldada teistsugust füüsilist olukorda, seega pole ta kaugeltki optimaalseks SLMi kirjeldavaks suuruseks ja allpool kirjeldatud suurused on märksa adekvaatsemad.

Vaadeldud suuruste arvutamiseks kasutatakse nn rekonstrueeritud faasiruumi, mille dimensioonide arv N võib olla milline tahes (kuid mitte väga suur, N >6 puhul muutub arvutatavate suuruste statistiline usaldatavus faktiliselt olematuks). Korrelatsioonidimensiooni arvutamisel tuleb vaadelda mitmeid N väärtusi (N = 2, 3, 4, 5, 6). Sageli piirdutakse kolmemõõtmelise ruumiga (nt mitmesuguste entroopiate arvutamisel). Kolmemõõtmelise rekonstrueeritud faasiruumi puhul määravad kolm järjestikust südamelöögi intervalli ära ruumipunkti: esimene neist on punkti x-koordinaadiks, teine y-koordinaadiks ja kolmas z-koordinaadiks. Mõnikord kasutatakse rekonstrueeritud faasiruumi asendajana sümbolarvutust: südamelöögi intervallile omistatakse teatav täht (a, b jne) vastavalt intervalli pikkusele; järjestikused tähed moodustavad sõna.

Kokkuvõtteks: kõik rekonstrueeritud faasiruumil põhinevad suurused mõõdavad südamerütmi lühiajalist (mõne sekundi jooksul toimuvat) muutlikkust, pakkudes seega alternatiivi lineaarsele mõõdule pNN50 ning sellega seoses võivad omada teatavat (kuid mitte revolutsiooniliselt uut) diagnostilist väärtust (vt nt viide 6).

**2. Mastaabi-invariantsed, Hursti astmenäitajal põhinevad mõõdud** annavad lineaarsete suurustega võrreldes uudset informatsiooni, kirjeldades seda, kuidas toimub ajamastaabi kasvades löögisageduse muutlikkuse kasv. Uurimaks keskmise löögiintervalli dünaamikat

vabanetakse esmalt muutlikkuse kõrgsageduslikust (mõnesekundilisest) komponendist. Edasi uuritakse, kuidas sõltub ajavahemiku T jooksul täheldatava löögiintervalli muutuse ruutkeskmine väärtus $\Delta t$ ajavahemikust T. Kui $\Delta t$ on võrdeline T teatava astmega H, siis nimetatakse H-d Hursti astmenäitajaks. Mitmed uurimused kinnitavad, et kas vahetult või teatud täiustatud tehnikat kasutades leitud H väärtus võimaldab prognoosida südamepuudulikkusega patsientide suremust (7–9). Täiustatud tehnikana mainigem trendi eemaldavat fluktuatsioonianalüüsi (*detrended fluctuation analysis*, DFA) (8) ja lainekeste teisenduse meetodit (9).

Veelgi täiuslikumaks meetodiks on Hursti astmenäitaja multifraktaalse spektri arvutamine (10, 11). Kui iga ajahetke jaoks arvutada lokaalne (väikest aja-akent kirjeldav) Hursti astmenäitaja h, siis võib arvutada teatava h väärtusega punktide hulga fraktaalse dimensiooni f. Funktsiooni f(h) nimetataksegi multifraktaalseks spektriks (ka Lipschitzi-Hölderi astmenäitajaks). Selle spektri leidmiseks kasutatakse harilikult nn massi-astmenäitajaid $\tau(q)$, mis kirjeldavad lainekeste teisenduse amplituudi q-nda astme keskväärtuse sõltuvust lainekeste pikkusest (s.t ajamastaabist). On leitud, et massi-astmenäitajad ise võivad olla heaks prognostiliseks mõõduks (11). Massiastmenäitajaga on väga tihedalt seotud q-ndat järku struktuurifunktsiooni astmenäitaja $\zeta(q)$ (12), mille erinevus funktsioonist $\tau(q)$ on peamiselt tehnilist laadi. Struktuurifunktsiooni mõiste on pärit tugeva turbulentsi teooriast.

Mastaabi-invariantseks mõõduks on ka nn multimastaabiline entroopia (13), mis on eespool mainitud astmenäitajatest suhteliselt sõltumatu, sarnanedes nendega siiski selle poolest, et kirjeldab samuti üle ajaperioodi T keskmistatud südamelöögi intervalli muutlikkuse taset sõltuvuses perioodist T. On leitud, et see suurus võimaldab hästi eristada südamepuudulikkusega patsiente.

**3. Mastaabi-invariantsete muutlikkuse mõõtude** puhul arvatakse, et kuivõrd nad iseloomustavad muutlikkuse trendi ja ei ole seotud

ühegi konkreetse ajamastaabiga, siis ei sõltu nad patsiendispetsiifilistest detailidest, vaid näitavad eeskätt patoloogilisi muutusi (11). Samas on juhitud tähelepanu, et mõned patoloogiad võivad mõjutada südamelöögi intervalli muutlikkust teatud kindla ajamastaabi juures ja sellisel korral tuleks kasutada just mastaabispetsiifilisi mõõte (14). Nii on leitud, et lainekeste spektri amplituud teatava lainekese pikkuse (nt 5 min) juures annab häid prognostilisi tulemusi (14). Võrreldes lineaarsete mõõtudega ei anna see amplituud aga kardinaalselt uut informatsiooni; pigem on tegemist suuruse SDANN peenviimistletud variandiga. Sõltumatud uurimused (15) on siiski näidanud, et mastaabi-invariantsed suurused annavad prognostiliselt paremaid tulemusi.

**4. Juhumuutlikke aspekte kirjeldavad mõõdud.** SLM on tugevalt mittestatsionaarne ja juhumuutlik. Veidi lihtsustatult tähendab see, et olles uurinud tema dünaamikat teatava ajavahemiku jooksul, on võimatu usaldusväärselt ennustada järgmise samasuguse perioodi jooksul toimuvat. Teatud perioodi jooksul võib olla löögisageduse muutlikkus hästi väike, seejärel aga võib löögisagedus hakata kiiresti muutuma. Keskmine löögisagedus võib olla pikka aega väike, seejärel hüpata sageli üles-alla. Sellise käitumise kirjeldamiseks on uuritud niisuguste perioodide pikkusjaotust, mille kestel on keskmine löögisagedus enam-vähem konstantne (16). Nähtuse teine aspekt on see, et ka väikse muutlikkusega perioodid jaotuvad pikkuse järgi suhteliselt keerulisel moel ning vastavat jaotusseadust kirjeldavaid parameetreid võib kasutada diagnostilistel eesmärkidel (17). Informatsioon, mida need parameetrid pakuvad, on uudne, sest vaadeldav jaotusseadus kirjeldab SLM niisuguseid aspekte, mida ei kirjelda ei lineaarsed ega ka teised mittelineaarsed mõõdud – seda, kuidas käitub lühiajaline muutlikkus pikema perioodi jooksul. Oma uurimistöös (vt allpool) oleme kasutanud juhumuutlikke aspekte kirjeldavate mõõtude hulka kuuluvaid SLM parameetreid.

Füsioloogiliste signaalide keerukuse (*complexity*) määramine tervetel isikutel ja teatud haiguste (sh ka südamehaiguste) korral on olnud väga paljude kliiniliste uurimistööde huviobjektiks (13, 19). Selleks on kasutatud lisaks traditsioonilistele SLM parameetritele ka uuemaid meetodeid, mida on rakendatud eelkõige mittelineaarse dünaamika (kaoseteooria) ja fraktaalanalüüsi valdkonnas (19–21). Ka meditsiinis on kasutusele võetud aproksimaalse entroopia (ApEn) mõiste kui süsteemi "keerukust" iseloomustav näitaja (22). Seda on rakendatud inimloote südametegevuse ning loote üldseisundi hindamisel kliinilises praktikas enam kui 15 aasta vältel (23, 24). Peale traditsiooniliste uurimismeetodite on näiteks uuritud patsientide hingamissageduse karakteristikuid mittelineaarse dünaamika meetoditega avastamaks erinevusi normaalsete isikute ning paanikahäiretega patsientide vahel (25). Lisaks tavapärastele meetoditele rakendatakse mittelineaarseid SLM parameetreid edukalt ka südamelihase infarkti põdenud haigete prognoosi määramiseks (26, 27). Analüüsiks kasutatakse nii EKG lühiajalise registreerimise (5 min, 15 min, 1000 QRS-kompleksi) kui ka 24tunnise ambulatoorse EKG monitooringu tulemusi (21).

**Uurimistöö eesmärk** on rakendada uusi ja seni veel kasutamata mittelineaarseid SLM parameetreid erinevate südamehaiguste puhul registreeritud 24 tunni ambulatoorse EKG monitorjälgimise andmete analüüsil.

## Uurimismaterjal ja -metoodika

Uuringusse kuulus 156 patsienti. Patsiendid jagati vastavalt kliinilisele diagnoosile kuude rühma: I rühm (n = 103) – terved isikud; II (n = 8) – südame isheemiatõvega haiged; III (n = 11) – siinussõlme nõrkuse sündroomiga haiged; IV (n = 16) – ventrikulaarse ekstrasüstooliaga haiged; V (n = 7) – müokardiinfarkti põdenud haiged, VI (n = 11) – hüpertooniatõbe põdevad haiged. Andmed uuritavate rühmade kohta on esitatud tabelis 1. Patsiendid kasutasid uuringu vältel ravimeid tavapärases annuses ja režiimis.

**Tabel 1. Uuritud patsiendirühmad**

|  | Terved | IHD | SND | VES | PCI | RR |
|---|---|---|---|---|---|---|
| Patsientide arv | 103 | 8 | 11 | 16 | 7 | 11 |
| Keskmine vanus | 45,5 | 65,4 | 50,0 | 55,9 | 47,3 | 55,5 |
| Vanuse standardhälve | 20,5 | 11,4 | 19,3 | 14,3 | 11,6 | 14,4 |
| 24 t keskmine südame löögisagcdus | 72,7 | 68,4 | 64 | 74,5 | 65,7 | 63,2 |
| Sageduse standardhälve | 10,7 | 7,4 | 11,3 | 9,8 | 8,5 | 9,8 |

IHD – südame isheemiatõvega haiged, SND – siinussõlme nõrkuse sündroomiga haiged, VES – ventrikulaarse ekstrasüstooliaga haiged, PCI – müokardiinfarkti põdenud haiged, RR – hüpertooniatõbe põdevad haiged.

Kõigile uuritavatele tehti 24 tunni ambulatoorne EKG monitorjälgimine (Holteri monitooring) Tallinna Diagnostikakeskuses. Kasutati firma Rozinn (USA) kolmekanalist jälgimissüsteemi modifitseeritud lülitustega II, V1 ja V5. EKG signaali mõõtmissagedus (*sampling rate*) oli 180 Hz ja signaali ajaline lahutusvõime (*resolving power*) 6 ms. Kasutades kommertstarkvara, toimus rütmihäirete ning artefaktide elimineerimine kardioloogi poolt enne RR-intervallide määramist (NN). Andmete analüüsimisel rakendati 24 tunni vältel registreeritud parameetreid. Andmeid töödeldi vastavalt joonisel 1 esitatud skeemile.

Uuriti vähese muutlikkusega perioodide pikkusjaotust (17). Esmalt tehti kindlaks väikse muutlikkusega intervalli kui sellise intervalli, mille suhteline erinevus libisevast keskmisest on suurem kui teatav fikseeritud väärtus $\delta_0$. Libisev keskmine leitakse lühiajalise, 5sekundilise aknaga; allpool toodud tulemuste puhul on kasutatud väärtust $\delta_0 = 5\%$. Väikse muutlikkusega perioodiks nimetame järjestikuste väikse muutlikkusega intervallide hulka (s.t suure muutlikkusega intervall lõpetab väikse muutlikkusega perioodi). Järjestades väikse muutlikkusega perioodid pikkuse l järgi (kus l on perioodis sisalduvate intervallide arv) ning omistades igale perioodile järjekorranumbri r (nii et pikim periood omab järjekorranumbrit r = 1), saame sõltuvuse r(l). Joonisel 2 on toodud see sõltuvus logaritmilises teljestikus, kus astmeseadusele $r = Al^{-\gamma}$ vastaks sirgjoon (sirge tõus on määratud astmenäitajaga $\gamma$). Paljudel patsientidel ongi väikse muutlikkusega perioodide pikkusjaotuseks astmeseadus, kuid sageli on sellest ka

**Tabel 2. p-väärtused vastavalt Studenti testile**

| p (%) | Terved | IHD | SND | VES | PCI | RR |
|---|---|---|---|---|---|---|
| Terved | B\A | 0,06 | 17,21 | 0,02 | 0,07 | 1,59 |
| IHD | 0,36 | | 2,85 | 96,79 | 97,62 | 21,93 |
| SND | 2,99 | 59,10 | | 2,10 | 3,04 | 25,77 |
| VES | 0,08 | 91,60 | 63,79 | | 94,18 | 17,59 |
| PCI | 25,27 | 21,61 | 46,37 | 22,89 | | 22,50 |
| RR | 0,14 | 73,57 | 77,69 | 80,49 | 28,90 | |
| Terved | D\C | 7,01 | 10,01 | 0,01 | 0,98 | 4,34 |
| IHD | 3,89 | | 2,70 | 45,88 | 62,20 | 74,98 |
| SND | 0,64 | 0,10 | | 1,44 | 3,40 | 3,23 |
| VES | 8,83 | 64,71 | 0,15 | | 3,46 | 16,26 |
| PCI | 14,93 | 0,99 | 3,31 | 1,98 | | 12,63 |
| R R | 21,58 | 1,07 | 1,94 | 2,38 | 70,25 | |

Kolmnurgas A toodud arvud vastavad karakteristikule $\ln(l_{end})$, kolmnurgas B $\ln(r_{max})$-le, kolmnurgas C pnn50-le ja kolmnurgas D SDNN-le. Arvu taust on hall siis, kui modifitseeritud Bonferroni meetodi järgi korrigeeritud p-väärtus jääb alla 10%.



**Joonis 1. Mittelineaarsete karakteristikute uurimisel kasutatav andmetöötluse tüüpskeem.**

märgatavaid kõrvalekaldeid (vt jn 2). Selgub, et astmeseaduse olemasolu või selle puudumine ei ole diagnoosiga märkimisväärses korrelatsioonis, vaid sõltub eeskätt patsiendi igapäevastest tegevustest ja harjumustest – sellest, millises vahekorras on kehaliselt aktiivne tegevus, istumine, söömine, lamamine jm (vt ka 18); siiski peitub vaadeldavas jaotusseaduses ka olulist diagnostilist informatsiooni. Loomulikult mõjutavad igapäevased harjumused ka kõiki teisi eelmainitud mittelineaarseid mõõte, see asjaolu on aga sageli jäänud piisava tähelepanuta. Võib öelda, et teatud SLM mõõt on seda parem, mida tundlikum on see patoloogiate suhtes ning mida vähem tundlik patsiendi igapäevaste harjumuste ja tegevuste suhtes.

## Uurimistulemused ja arutelu

Tabelis 2 on toodud Studenti testi tulemused väikse muutlikkusega perioodide jaotust kirjeldavate parameetrite $\ln(l_{end})$ ja $\ln(r_{max})$ järgi (tegemist on naturaallogaritmidega suurusest $l_{end}$ ja $r_{max}$; esimene neist on logaritmilises teljestikus lineaarse osa lõpp-punkti l-koordinaat, teine aga suurim järjekorranumber, mis on seda väiksem, mida rohkem on väikse muutlikkusega pikki perioode). Võrdluseks on toodud kaks lineaarset karakteristikut, pnn50 ja SDNN. Võtmaks arvesse nn nullhüpoteesi võimalikkust (reaalset korrelatsiooni pole, väikesed

p-väärtused on juhuslik tulemus: kui on arvutatud palju p-väärtusi, siis need jaotuvad ühtlaselt skaalal nullist üheni ning seega on mõned neist üsna väikesed) on rakendatud modifitseeritud Bonferroni korrektsiooni, kus korrigeeritud p-väärtuse leidmiseks korrutatakse algne p-väärtus testide arvuga (siin 60) ning jagatakse n-ga, kus n näitab mitmes väiksuselt on antud p-väärtus. Tabelis tähistab hall taust seda, et korrigeeritud p-väärtus on alla 10%. Et Studenti test eeldab normaaljaotust, siis kontrolliti, kas see eeldus on põhjendatud. Selleks arvutati vaadeldud suuruste jaotuse asümmeetria ja ekstsess. Tulemused näitasid, et normaaljaotus on tõepoolest piisavalt heaks
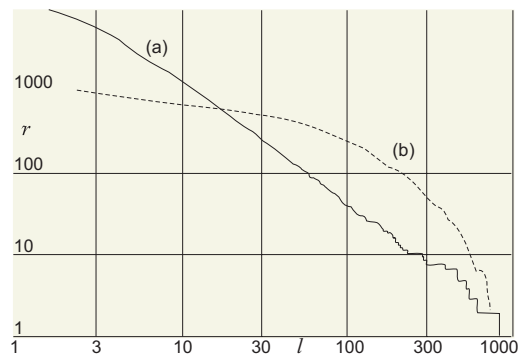


**Joonis 2. Madala muutlikkusega perioodide järjekorranumbri r sõltuvus pikkusest l on esitatud logaritmilises teljestikus. Patsiendil (a) on tegemist astmeseadusega (graafik on lähedane sirgjoonele), patsiendil (b) on aga märgata olulist kõrvalekallet astmeseadusest.**

aproksimatsiooniks (näiteks tervete rühma ja suuruse ln(I_end) korral oli asümmeetria 0,24 ja asümmeetria –0,58).

Nagu tabelist näha, võimaldavad vaadeldud mittelineaarsed suurused eristada tervete rühma kõigist teistest rühmadest peale SND-grupi. Samal ajal võimaldasid klassikalised meetodid eristada just nimelt SND-rühma tervetest (ja mõnest patoloogiast – IHD ja VES rühmast). Niisiis võib vaadeldud lähtematerjali põhjal väita, et väikse muutlikkusega perioodide jaotusseadus pakub võrreldes klassikaliste SLM karakteristikutega olulist lisainformatsiooni, võimaldades eristada eeskätt just terveid patsiente.

## Kokkuvõte

Mittelineaarsete SLM karakteristikute hulgas on kahtlemata väga perspektiivikaid suurusi (nii prognostilisi kui ka diagnostilisi eesmärke silmas pidades). Osa neist valgustavad täiesti uusi SLM aspekte, osa aga dubleerivad suures osas lineaarsete mõõtude poolt pakutavat infot (võimalik, et pakuvad siiski veidi paremat patoloogiatesse puutuva ja patsiendispetsiifilise info suhet just tänu peenviimistletud matemaatilisele käsitlusele). Kliinilised rakendused on takerdunud selle taha, et pole tehtud piisavalt laiaulatuslikke ja homo-geenseid patsiendirühmi hõlmavaid uuringuid. Väikse muutlikkusega perioodide jaotust kirjel-davad suurused kuuluvad diagnostiliselt pers-pektiivsete karakteristikute hulka, mille edasisel uurimisel tuleks keskenduda 1) prognostilisusele infarktijärgsete patsientide juures; 2) suuruse ln(I_end) jaoks lihtsamini arvutatava alternatiivi otsimisele; 3) laiemate patsiendigruppide vaatlemisele.

## Kirjandus

1. Heart rate variability. Standards of measurement, physiological interpretation and clinical use. Task Force of the European Society of Cardiologu and the North American Society of Pacing and Electrophysiology. Circulation 1996;93:1043–65.
2. Ristimäe T, Teesalu R. Südame löögisageduse muutlikkus. Eesti Arst 1999;1:34–40.
3. West BJ, Goldberger AL, Rooner G, Bhargava V. Nonlinear dynamics of the heartbeat. 1. The av junction: passive conduct on active oscillator. Physica D 1985; 17:198–206.
4. Engelbrecht J, Kongas O. Driven oscillators in modelling of heart dynamics. Applicable Anal. 1995;57:119–44.
5. Babloyantz A, Destexhe A. Is the normal heart a periodic oscillator? Biol Cybern. 1988;58:203–11.
6. Zebrowski JJ, Poplawska W, Baranowski R, Buchner T. Symbolic dynamics and complexity in a physiological time series. Chaos, Solitons, Fractals 2000;11:1061–75.
7. Peng CK, Mietus J, Hausdorff JM, Havlin S, Stanley HE, Goldberger AL. Log-range anticorrelations and non-Gaussian behavior of the heartbeat. Phys Rev Lett 1993; 70:1343–7.
8. Peng CK, Havlin S, Stanley HE, Goldberger AL. Quantification of scaling exponents and crossover phenomena in nonstationary heartbeat time series. Chaos 1995;5:82–7.
9. Ashkenazy Y, Lewkowicz M, Levitan J, Moelgaard H, Bloch Thomsen PE, Saermark K. Discrimination of the healthy and sick cardiac autonomic nervous system by a new wavelet analysis of heartbeat intervals. Fractals 1998;6:197–203.
10. Ivanov PCh, Rosenblum MG, Amaral LAN, Struzik Z, Havlin S, Goldberger AL, Stanley HE. Multifractality in human heartbeat dynamics. Nature 1999;399:461–5.
11. Amaral LAN, Goldberger AL, Ivanov PCh, Stanley HE. Scale-independent measures and pathologic cardiac dynamics. Phys Rev Lett 1998;81:2388–91.
12. Lin DC, Hughson RL. Modeling Heart Rate Variability in Healthy Humans: A Turbulence Analogy. Phys Rev Lett 2001;86:1650–3.
13. Costa M, Goldberger AL, Peng C-K. Multiscale entropy analysis of complex physiologic time series. Phys Rev Lett 2002;89:068102–1–4.
14. Thurner S, Feurstein MC, Teich MC. Multiresolution wavelet analysis of heartbeat intervals discriminates healthy patients from those with cardiac pathology. Phys Rev Lett 1998;80:1544–7.
15. Saermark K *et al.* Comparison of recent methods of analyzing heart rate variability. Fractals 2000;8:315–22.
16. Bernaola-Galván P, Ivanov PCh, Amaral LAN, Stanley HE. Scale invariance in the nonstationarity of human heart rate. Phys Rev Lett 2001;87:168105–14.

17. Kalda J, Säkki M, Vainu M, Laan M. Zipf's law in human heartbeat dynamics. e-print 2001; physics/0110075 (http://arxiv.org/abs/physics/0110075, 4 pages).
18. Struzik ZR. Revealing local variability properties of human heartbeat intervals with the local effective hölder exponent. Fractals 2001;9:77–93.
19. De Vito G, Galloway SDR, Nimmo MA, Maas P, McMurray JJV. Effects on central sympathetic inhibition on heart rate variability during steady-state exercise in healthy humans. Clin Physiol & Func Im 2002;22:32–38.
20. Routledge HC, Chowdhary S, Townend JN. Heart rate variability – a therapeutic target? J Clin Pharm Ther 2002;27:85–92.
21. Pikkujamsa S, Makikallio T, Sourander L et al. Cardiac interbeat interval dynamics fromchildhood to senescence: comparison of conventional and new measures based on fractals and chaos theory. Circulation 1999;100:393–99.
22. Pincus SM, Viscarello RR. Approximate entropy: a regularity measure for fetal heart rate analysis. Obstet Gynecol 1992;79:249–55.
23. Groome L, Mooney D, Holland S, Smith L, Atterbury J, Loizou P. Human fetuses have nonlinear cardiac dynamics. J Appl Physiol. 1999;87;2:530–37.
24. Lake D, Richman J, Griffin P, Morman R. Sample entropy analysis of neonatal heart rate variability. Am J Physiol Regul Integr Comp Physiol 2002;283:789–97.
25. Yeragani VK, Radhakrishna RKA, Tancer M, Uhde T. Nonlinear measures of respiration: Respiratory irregularity and increased chaos of respiration in patients with panic disorder. Neuropsychobiology 2002;46;3:111–20.
26. Sosnowski M, MacFarlane PW, Czyz Z, Skrzypek-Wanha J, Boczkowska-Gaika E, Tendera M. Age-adjustment of HRV measures and its prognostic value for risk assessment in patients late after myocardial infarction. Inter J Cardiol 2002;86(2–3):249–58.
27. Perkiomäki J, Zareba W, Daubert J, Couderc JP, Corsello A, Kremer K. Fractal correlation properties of heart rate dynamics and adverse events in patients with implantable cardioverter-defibrillators. Am J Cardiol 2001;88:17–22.

**Summary**

**Nonlinear methods of heart rate variability in patients with heart disease using ambulatory ECG monitoring**

Heart rate and heart rate variability are important tools used in patients with heart disease for obtaining diagnostic and prognostic information. So far mainly standardized linear methods of heart rate variability have been employed in clinical practice. The present article reviews the nonlinear aspects of heart rate variability and presents the results of the authors' studies based on nonlinear methods of heart rate variability in patients with heart disease.

meelis@dk.ee

# WHAT DOES MEASURE THE SCALING EXPONENT OF THE CORRELATION SUM IN THE CASE OF HUMAN HEART RATE?

M. SÄKKI, J. KALDA, M. VAINU, M. LAAN

# What does measure the scaling exponent of the correlation sum in the case of human heart rate?

M. Säkki[a] and J. Kalda
*Institute of Cybernetics, Tallinn Technical University, Akadeemia tee 21, 12618 Tallinn, Estonia*

M. Vainu
*Tallinn Diagnostic Center, Pärnu mnt. 104, Estonia*

M. Laan
*Nõmme Children Hospital, Laste 1, Tallinn, Estonia*

It is shown that in the case of human heart rate, the scaling behavior of the correlation sum (calculated by the Grassberger–Procaccia algorithm) is a result of the interplay of various factors: finite resolution of the apparatus (finite-size effects), a wide dynamic range of mean heart rate, the amplitude of short-time variability being a decreasing function of the mean heart rate. This is done via constructing a simple model of heart rhythm: a signal with functionally modulated Gaussian noise. This model reproduces the scaling behavior of the correlation sum of real medical data. The value of the scaling exponent depends on all the above-mentioned factors, and is a certain measure of short-time variability of the signal. © *2004 American Institute of Physics.*
[DOI: 10.1063/1.1636151]

**Correlation dimension has been one of the most popular nonlinear measures of heart rate variability. However, due to various factors (noise, nonstationarity, limited time-resolution of apparatus), the finiteness of the correlation dimension fails to be a proof of the presence of an underlying deterministic dynamics. Here we suggest a simple heart rhythm model (a signal with functionally modulated Gaussian noise) which reproduces the scaling behavior of the correlation sum of real medical data. This gives us a key on how to interpret the clinical values of this scaling exponent.**

## I. INTRODUCTION

Heart rate variability (HRV) has been often thought to be driven by deterministic chaos inside the heart. Such a belief lies upon the mathematical models of the complex of sino-atrial and atrio-ventricular nodes, which is responsible for the heart rhythm generation and has been treated as a system of nonlinear coupled oscillators.[1,2] As a consequence, the measures of deterministic chaos, such as correlation dimension, Lyapunov exponents, Kolmogorov entropy, etc., have been thought to be important tools of HRV analysis, cf. Refs. 3 and 4. Meanwhile, the heart rate is known to be regulated by the signals arriving from the autonomous nervous system, which fluctuate intermittently, cf. Refs. 5–7. The level of these signals is high enough to suppress the possible underlying nonlinear deterministic dynamics; in particular, the signals due to respiration (and mediated by the phenomenon known as baroreflex[6]) have a strong fingerprint on the short-

time variability of the heart rate and can lead to the mode-locking between the heart rate and respiration.[8,9]

Despite the above-mentioned advances in understanding of the nature of HRV, the measures of deterministic chaos (correlation dimension, Lyapunov exponents, and Kolmogorov entropy, etc.) are still being calculated in a considerable number of papers devoted to HRV. Besides, various entropies (Shannon, renormalized, Renyi, pattern, approximate, etc., cf. Refs. 10 and 11) are persistently popular research topics; while not directly requiring the presence of a deterministic dynamics, they are ideologically related to the analysis of nonlinear dynamics (both deal with the dynamics in time delay space). In order to be able to interpret correctly the results of these numerous studies, it is important to know *which physical aspects of HRV signal are actually being measured by the measures of nonlinear dynamics.* In this paper, we study the case of the correlation dimension (we shall use the term ''scaling exponent of the correlation sum,'' in order to emphasize that we are not assuming the presence of an underlying deterministic dynamics).

It has been pointed out that even in the case of a really existent and nonsuppressed deterministic dynamics, nonstationarity and noisiness (which are typical to physiological time series) make a reliable calculation of the correlation dimension impossible.[12–14] Furthermore, it has been emphasized that a reasonable fitting of a correlation sum to a power law does not necessarily mean that the obtained exponent is the correlation dimension of the underlying dynamical system; instead, thorough nonautomatable verification procedure has to be done.[15] All this leads us to the conclusion that the formally calculated correlation dimension of a heart rhythm *does not correspond to the dimensionality of an intrinsic attractor.* Meanwhile, the correlation sums of human heart rate follow typically a scaling law, cf. Ref. 4, and, as

[a]Electronic mail: max@cens.ioc.ee
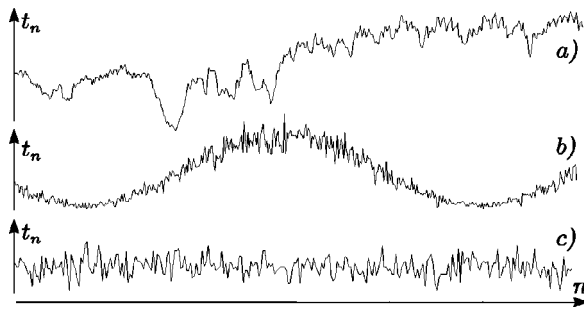
FIG. 1. Heart beat intervals (in arbitrary units) are plotted vs the beat number: (a) a real patient; (b) model time series (functionally modulated Gaussian noise); (c) plain Gaussian noise added to a constant "heart" rate. The time window is 1250 heart beats.



FIG. 2. The same as in Fig. 1, except that the time window is 37 700 heart beats and curve (c) corresponds to the model-time-series with $1/f$ power spectrum [given by Eqs. (4)–(6)].

pointed out in the pioneering paper of Babloyantz and Destexhe,[3] the high values of the scaling exponent ("correlation dimension") indicate the healthiness of the heart. Hence, it is natural to ask, what does measure the scaling exponent of the correlation sum, and how is it related to the healthiness of the heart.

Our answer to the posed question is based on very simple observations, which are valid for healthy patients: (a) the long-time variability of the interbeat intervals (which is typically around 500 ms) is typically much higher than the variability on the time scale of few heart beats ($\sim 50$ ms), see Figs. 1(a) and 2(a); (b) for those periods, when the mean heart rate is high (i.e., when the subject is performing a physical exercise) the heart rate variability is low; (c) the heart rate is controlled by nondeterministic and effectively random signals arriving from the autonomous nervous system. As a consequence, in time delay coordinates, an HRV time series generates an elongated conical cloud of points (the narrow tip of which is directed toward the origin). Although the theoretical (and correct) value of the correlation dimension of such a cloud is infinite, the finite resolution of the recording apparatus, finite length of the time series, and the linear structure of the cloud result in a smaller value. This is evident for a very narrow "cone," which is efficiently one dimensional. In what follows we show that the "correlation dimension" reflects the geometrical size of such a cloud of points.

The layout of the paper is as follows. First, we give the details of the HRV database used for this study. Second, we provide a short overview of the research results related to the correlation dimension of human heart rhythm. Third, we construct simple model time series, the correlation sum of which scales almost identically to that of real HRV data. Fourth, we
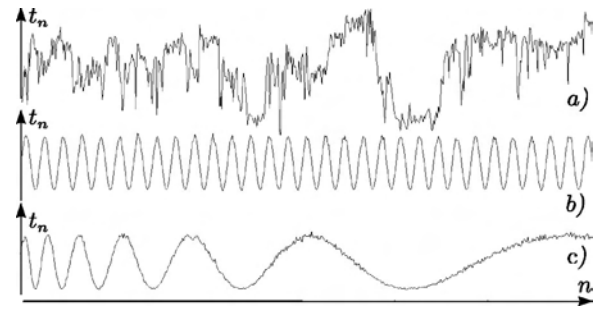
discuss the phenomenon of mode locking between heart rhythm and respiration. Finally, we discuss the universality and implications of our model.

## II. EXPERIMENTAL DATA

The experimental data analyzed in this paper have been recorded at Tallinn Diagnostic Center. The recordings of ambulatory Holter-monitoring (24 h, approximately 100 000 data points) were obtained during regular diagnostical examinations and covered over 200 patients with various clinically documented diagnoses (including also many healthy subjects). The main groups of patients are shown in Table I. The resolving power of original ECG recordings was 6 ms (sampling rate of 180 Hz). The diagnostics and data verification has been made by a qualified cardiologist; the data preprocessing included also filtering of artifacts and arrhythmias.

Our study would have been certainly benefitted from using higher resolution data. In the case of short-term ($<1$ h) recordings, a free access to the high resolution (above 250 Hz) data is provided by public databases (e.g., at www.physionet.org). However, the length of these recordings is not suitable for the correlation sum scaling analysis when the scaling exponent is larger than four (see below, cf. Table II). In the case of Holter-monitoring (24 h), the recordings at www.physionet.org are recorded at 128 Hz; this resolution is often adopted for the studies of long-term dynamics of RR intervals, cf. Ref. 16. The most modern and advanced Holter-monitoring recorders do provide sampling rates up to 500 Hz. Unfortunately, our research group did not have access to such recordings. For our purposes, 180 Hz seems to be still acceptable, because the resolution 6 ms is smaller than the variability on the time scale of few heart beats $\sim 50$ ms. This

TABLE I. Test groups of patients. Abbreviations are as follows: IHD—ischemic heart disease (stenocardia); SND—sinus node disease; VES—ventricular extrasystole; PCI—post cardiac infarction; RR—blood pressure disease; FSK—functional disease of sinus node.

|                   | Healthy | IHD  | SND  | VES  | PCI  | RR   | FSK  |
|-------------------|---------|------|------|------|------|------|------|
| No. of patients   | 103     | 8    | 11   | 16   | 7    | 11   | 6    |
| Mean age          | 45.5    | 65.4 | 50.0 | 55.9 | 47.3 | 55.5 | 11.7 |
| Std. dev. of age  | 20.5    | 11.4 | 19.3 | 14.3 | 11.6 | 14.4 | 4.6  |

TABLE II. Data from papers devoted to the correlation dimension analysis: experimental values of correlation dimension, lengths of the underlying data sets, and data-set lengths required by Eq. (3).

|  | Ref. 3 | Ref. 13 | Ref. 19 | Ref. 20 |
|---|---|---|---|---|
| Correlation dimension | 5.5–6.3 | 9.6–10.2 | 2.8–5.8 | 4–7 |
| Length of the data set | $10^3$ | $2 \times 10^4$ | $10^4$ | $2 \times 10^4$ |
| Required length | $10^4$ | $10^6$ | $10^4$ | $3 \times 10^4$ |

conclusion is supported by the fact that the effect of data downsampling to the correlation sum scaling behavior is small (see Sec. IV).

## III. BACKGROUND INFORMATION AND BASIC ASSUMPTIONS

The concept of correlation dimension, introduced by Grassberger and Procaccia,[17] is designed to reflect the number of degrees of freedom of a deterministic system (more precisely, the dimensionality of an attractor, which, in principle, can be fractal). For empirical time series, the phase variables are typically not known. It is expected that the attractors in the phase space are topologically equivalent to the attractors in a reconstructed phase space with time-lag coordinates $\{x(T), x(T+\tau), \ldots, x[T+(m-1)\tau]\}$, as long as the embedding dimensionality $m$ (the dimensionality of the reconstructed phase space) exceeds the dimensionality of the attractor $D$; here $T$ is the time, $x(T)$ is the signal, and $\tau$ is a reasonably chosen time lag. This circumstance is exploited by the Grassberger–Procaccia method[17] for the calculation of the correlation dimension. To begin with, the second-order correlation sum is defined as

$$C_2(r) = \frac{2}{N(N-1)} \sum_{i<j} \theta(r - |\mathbf{r}_i - \mathbf{r}_j|), \tag{1}$$

where $\theta(r)$ is the Heaviside function, $\mathbf{r}_i = \{x(T_i), x(T_i + \tau), \ldots, x[T_i + (m-1)\tau]\}$ is a point in the reconstructed phase space, and $i, j = 1, 2, \ldots, N$ count the moments of discretized time. In the case of HRV analysis, the time is typically measured in the number of heart beats (so that $T_j \equiv j$), and unit time lag is used, $\tau = 1$. In what follows we use the notation $x(j) \equiv t_j$ for the duration of $j$th normal heart beat. For small $r$, the correlation sum is expected to scale as $C_2(r) \propto r^{D_2}$, assuming that $D_2 < m$. The exponent $D \equiv D_2$ is called the *correlation dimension* of the system.

A nonlinear dynamical system may be chaotic and then the phase trajectory fills certain subset of the phase space. In that case, the correlation dimension $D$ is expected to be equal to the number of degrees of freedom (the dimensionality of the phase space minus the number of conservation laws). This is why $D$ is often considered as a measure of the complexity of the system. Babloyantz and Destexhe[3] studied the correlation dimension of the sequence of $NN$ intervals (intervals between normal heartbeats) of human heart rhythm. For healthy patients and data series consisting of 1000 intervals, they found $D = 5.9 \pm 0.4$. It is widely recognized that life-threatening heart pathologies lead to the reduction of the complexity of the HRV signal, cf. Ref. 4. Correspondingly,

the correlation dimension of the heart rate has been often believed to measure the healthiness of the heart.

However, the heart is not an isolated system. Although the heart rhythm is generated by the complex of oscillatory elements, its rate is controlled by *nondeterministic inputs* arriving from the autonomous nervous system. In particular, these inputs lead to the increase of the heart rate when the subject is under a physical stress, and to slowing down when the subject is at rest, cf. Ref. 6. Healthy heart responds easily to these signals, and is able to adapt to a wide range of beating rates. This responsiveness gives rise to the high variability of the heart rate. Severe heart diseases decrease the responsiveness of the heart with respect to the whole spectrum of signals arriving from the autonomous nervous system; this leads to the loss of the apparent complexity of the HRV signal.

The heart is more responsive with respect to the signals of the autonomous nervous system when the heart rate is slow, i.e., when the patient is at rest. In that case, the heart rate variability is driven by weaker signals, like the ones generated by respiration and blood-pressure oscillations. These two stimuli are quasiperiodic, the periods being, respectively, a few and 10–20 s. While the 10–20 s period is too long to affect essentially the dynamics in time delay spaces (unless the dimensionality is very large, 10 or more), the few-second (quasi-)periodicity has a strong fingerprint in the distribution of points in the reconstructed phase space.

## IV. FUNCTIONALLY MODULATED GAUSSIAN NOISE

Our model of the heart rhythm generation is as follows. The possibly nonlinear deterministic dynamics inside the heart is almost completely suppressed by the signals arriving from the autonomous nervous system. These signals control the mean heart rate, but obey also a noise-like component, the amplitude of which decreases with increasing mean heart rate. This noise-like component is a mixture of the respiration-induced signal (which, if not mode-locked, decorrelates quickly, and from the standpoint of the distribution of points in time-delay space, is effectively random; the mode-locking phenomenon will be discussed later). In the case of correlation sum analysis, this noise-like component is indistinguishable from a Gaussian noise. Therefore, theoretically, the correlation dimension is infinite. The reported relatively small values of the correlation dimension are to be attributed to the finite length of the time series and, most important, to the finite resolution of the recording apparatus. Too short record length can be the cause of a false detection of the correlation sum scaling exponent saturation effect. Indeed, typically, the correlation dimension has been found to be at the limit (or beyond) of a credible analysis.[12,18] It has been suggested[12,18] that the calculation of the correlation dimension $D$ is reliable, if the number $N$ of data points in the time series

$$N \gtrsim 10^{D/2+1}. \tag{2}$$

In Table II, this criterion is compared with the data of some papers.

In order to test our hypothesis we aimed to construct such model time series (using an algorithm as simple as possible), the correlation sum of which is similar to the correlation sums of the time series of real patients. An alternative approach could have been to create surrogate data by shuffling the real clinical data. The advantages of using model time series are as follows. (a) There is no risk of creating artifacts by data shuffling; (b) interpretation of the results is more straightforward and reliable, because there are no unknown statistical features (higher order correlations, intermittency) of the time series; (c) the relationship between the observed scaling exponent values and the statistical properties of the underlying data set can be easily studied by adjusting the control parameters (e.g., the noise amplitude) of the model.

To begin with, we analyzed the sequences of NN intervals extracted from the ECG recordings. The scaling exponent was found as the slope of a root-mean-square fit of the correlation sum [Eq. (1)] in log–log plot using the best scaling range, i.e., such a range which is as wide as possible, and for which the mismatch between the curve and fitting line is smaller than the statistical uncertainties. The statistical uncertainties have been estimated by Monte Carlo method: 30 different time series [Eqs. (3) and (4)] were generated, and the corresponding variance of $C_2(r)$ was calculated.

First we discuss the case of embedding dimensionality $m=6$, because on the one hand, this is the dimensionality at which the exponent saturation has been observed;[3] on the other hand, higher values of $m$ would not be applicable to the majority of the studies presented in Table II, due to the shortness of the respective underlying data series.

Reliable correlation sum analysis is possible only for more or less stationary time series, cf. Ref. 12. Meanwhile, HRV signal is highly nonstationary, as evidenced by the multifractal structure of its long-time dynamics.[21] The most stationary period in the heart rate dynamics is the sleeping time. This is why we studied only the nocturnal part of the HRV records. The scaling exponent was determined as the slope of the correlation sum $C_2(r)$ in log–log plot by performing root-mean-square fit for the almost linear part (at small values of $r$) of the curve, see Fig. 3. Note that the leftmost horizontal part of the curve is due to the limited resolving power (6 ms) of the medical equipment: if two NN intervals differ less than 6 ms, they are recorded to be of the same length. For $m=6$, the scaling exponents ranged from $D=4.2$ to $D=5.1$ and were almost uncorrelated with the diagnoses (see Table III).

Further we generated two model time series with Gaussian noise: (i) plain Gaussian noise added to a constant signal [see Fig. 1(c)]; (ii) time series with variable mean "heart rate" and modulated noise, generated according to

$$t_n = a + b \sin(fn) + c g(n) \sqrt{1.1 + \sin(fn)}, \qquad (3)$$

see Figs. 1(b) and 2(b). Here, $t_n$ denotes the duration of $n$th interval; $g(n)$ is a random uncorrelated time series with unit variance, zero mean, and Gaussian distribution of values. The term $b \sin(fn)$ models the variability of the mean heart rate due to physiological processes (physical activity, blood pressure oscillations, etc.). The term $\sqrt{1.1 + \sin(fn)}$ reflects
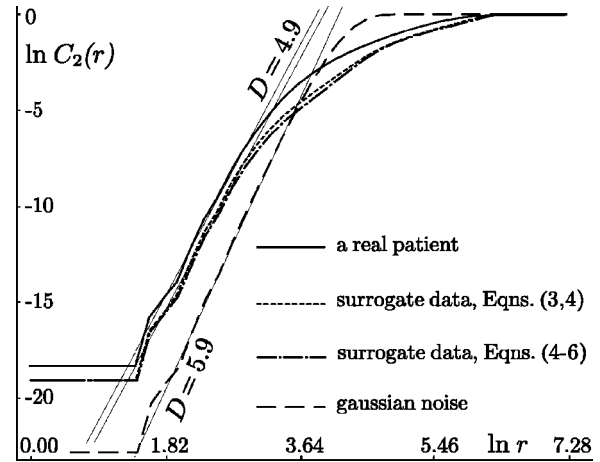


FIG. 3. Correlation sums of a typical healthy patient, a plain Gaussian signal, and functionally modulated Gaussian signals in logarithmic plot. Embedding dimensionality $m=6$.

the empirical observation that the short-time variability of the heart rhythm increases together with the mean heart beat interval. A good similarity between the correlation sums of clinical and model data is achieved for the following set of parameters

$$a=700 \text{ ms}, \quad b=110 \text{ ms}, \quad f=0.005, \quad c=3.5 \text{ ms}; \qquad (4)$$

the values of $t_n$ have to be rounded to the nearest multiple of the "resolving power," 6 ms.

It should be emphasized that both the square-root and sinusoidal dependencies have been completely arbitrary choices; here, the selection criterion has been the simplicity of the model. The sinusoidal trend of the model data is not intended to (and does not) match the intermittent pattern of real HRV (cf. Refs. 21 and 22), because the correlation sum is not sensitive with respect to this pattern (neither with respect to the modulation frequency $f$). Indeed, as long as the characteristic time scale of the fluctuations is longer than $\sim 10$ s, the intermittency has no effect on the distribution of points in time delay space. So, due to the robustness of the model, the sinusoid can be substituted by any other function which varies between 1 and $-1$, and has no high-frequency ($\lesssim 1$ Hz) components. In order to demonstrate the expected robustness, we generated a slightly different model time series [see Fig. 2(c)],

$$t_n = a + b \sin[\phi(n)] + c g(n) \sqrt{1.1 + \sin[\phi(n)]}, \qquad (5)$$

where

TABLE III. $p$-values of the student test for the seven groups of patients. Abbreviations are explained in Table I.

| $p$, % | IHD | SND | VES | PCI | RR | FSK |
|---|---|---|---|---|---|---|
| Healthy | 89.4 | 21.9 | 3.5 | 18.4 | 2.4 | 71.5 |
| IHD | | 34.1 | 12.0 | 17.6 | 7.1 | 69.4 |
| SND | | | 66.8 | 52.9 | 45.7 | 54.4 |
| VES | | | | 73.0 | 67.6 | 25.2 |
| PCI | | | | | 95.7 | 26.7 |
| RR | | | | | | 15.9 |
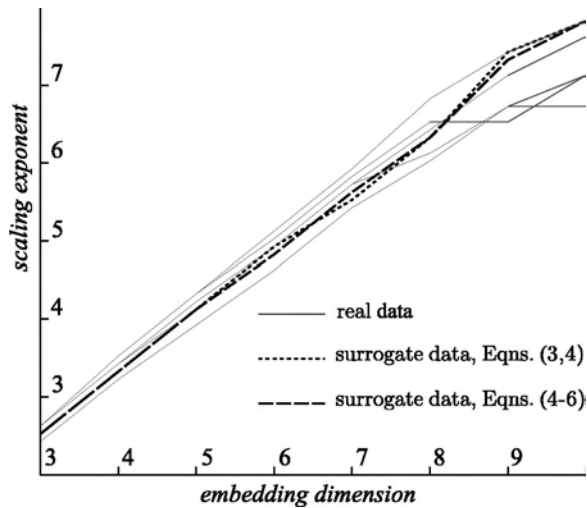
FIG. 4. Correlation sum scaling exponents for five typical patients and for the model time series are plotted vs the embedding dimensionality.



FIG. 5. The effect of the ECG resolving power on the correlation sum scaling exponent is demonstrated by downsampling the raw data of three randomly selected subjects. The effect is weak; however, lower sampling rate decreases systematically the scaling exponent values.

$$\phi(n) = fn/(1 + 0.0001n), \tag{6}$$

and the definitions of $a$, $b$, $c$, $f$, and $g(n)$ are the same as in the case of Eq. (3). This time series has $1/f$ power spectrum, similar to what is observed for real clinical data.[23]

As mentioned earlier, the square root function in Eqs. (3) and (5) mimics the dependence of the short-time variability level on the mean heart rate. While the correlation sum scaling properties can be expected to be sensitive with respect to the dynamic range of this dependence, the specific functional form is of lesser importance. So, $\sqrt{x}$ can be substituted by some other monotonically increasing function $f(x)$, assuming that the dynamic range remains unchanged, i.e., $f(0.1) = \sqrt{(0.1)}$, and $f(2.1) = \sqrt{(2.1)}$.

For a Gaussian signal, the correlation dimension is infinite, and the scaling exponent should be equal to the embedding dimension $m = 6$. This is exactly what is observed for plain unmodulated Gaussian time series, see Fig. 3. However, for the noise of modulated amplitude, the finite size effects are significant: the scaling exponent $D$ of such time series depends on the model parameters $a$, $b$, $c$, $f$, and on the resolving power. By adjusting the parameters $b$, $c$, and the resolving power, we were able to obtain the values ranging from $D = 4$ to $D = 6$. At the resolving power of 6 ms, and with the parameter set being given by Eq. (4), there was almost no difference between the correlation sums of the two model signals [Eqs. (3) and (5)], and the correlation sums of real patients, see Fig. 3. This is in a complete agreement with the theoretical expectations.

The similarity between the correlation sums of our signal with functionally modulated Gaussian noise and real physiological data extends beyond the six-dimensional embedding space. We have studied the time delay spaces with dimensionalities ranging from 3 to 10. The scaling exponents have been calculated for the real data, and for model time series (3), (5). The results presented in Fig. 4 show that the scaling exponent of the correlation sum increases persistently toward large embedding dimensionalities. The similarity between the $D(m)$ curves of the generated time series and the real
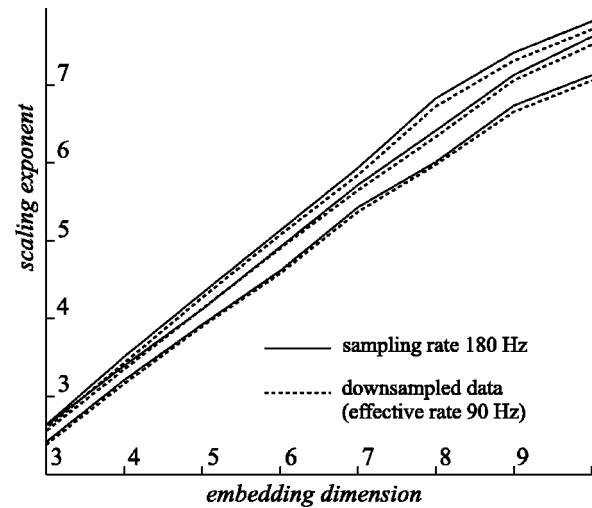
data is quantitative, and in the case of some patients, nearly perfect, see Fig. 4. Note that for large embedding dimensionalities and (too) short data series, this increase is not smooth, due to high statistical uncertainties. Strong enough fluctuations [which are expected when condition (2) is violated] form random "plateaus" of the $D(m)$ curve; which can be falsely interpreted as the signs of saturation of the scaling exponent. The effect of the resolving power of the recording apparatus is demonstrated in Fig. 5, where the correlation sums of raw clinical data are compared with that of the downsampled data (with the effective resolving power of 11 ms).

## V. MODE LOCKING

Finally, we discuss the phenomenon of mode locking between the respiration and heart rate, which has been demonstrated by simultaneous recording of ECG and respiration activity, together with the technique called cardiorespiratory synchrogram[8] (and which has been also detected using univariate HRV time series[9]). In the case of simple respiration-induced HRV, the decorrelation time between respiration and heart rhythm is of the order of 10 s; mode locking increases this time by an order of magnitude. The ratio of the mode-locked periods is typically small, 2:1, 3:1, 5:2, etc., and the phenomenon gives rise to specific patterns in the reconstructed phase space (satellite clouds around the central elongated conical cloud of points), see Fig. 6. These patterns can be easily misinterpreted as traces of an attractor of a nonlinear deterministic system.

In order to show the causal relationship between the mode locking and the presence of "satellite clouds," we devised a quantitative method for the detection of mode locking; as compared with the alternative univariate technique,[9] our method is simpler, more intuitive, and equally sensitive. To begin with, let us introduce the fluctuation function

$$F(\nu) = \langle |t_n - t_{n+\nu}| \rangle \tag{7}$$
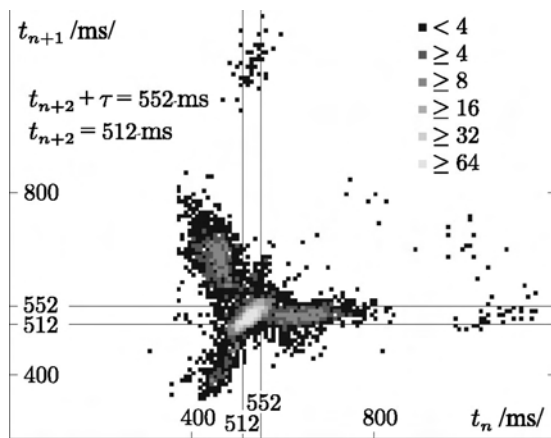
FIG. 6. Two-dimensional intersection of three-dimensional reconstructed phase space for a patient with pronounced mode locking between heart rate and respiration. The number of points per unit cell is given in gray-scale coding.

(angular brackets denote averaging over $n$). Unlike in the case of "single-cloud-patients," the fluctuation function of the patients with satellite clouds revealed a presence of an oscillatory component, see Fig. 7(b). As a quantitative measure of the amplitude of such oscillations, the discrete Fourier transform amplitude can be used; $n:m$ mode locking is related to the Fourier transform amplitude $\Phi_\alpha$ at the wavelength $\alpha = n/m$. In order to reduce the influence of non-mode-locked respiration (and thereby attain a better sensitivity with respect to the mode-locking), the small values of the delay $\nu$ have to be ignored. For instance, a good sensitivity is achieved when the Fourier transform is applied to the range $5 \lesssim \nu \lesssim 30$ (the range length must be a multiple of $n$).

By dividing the entire 24 h HRV record into 1 h intervals, and calculating the amplitude of the oscillatory component of the fluctuation function for each interval, we were able to locate the periods responsible for the satellite clouds in the reconstructed phase space, see Fig. 7(b). These were always the periods before falling asleep, around 10 or 11 pm, characterized by a low heart rate and a high respiration-driven short-time variability. The phase between the heart

rate and respiration is locked during tens of seconds, confirming the observations of Kurths et al.[8] Thus, in a certain sense, the heart and respiratory complex act as a system of coupled oscillators, cf. Ref. 9; however, by no means does this imply that there is a deterministic chaos inside the heart. Since the mode locking occurs during a relatively small fraction of the whole recording time, it has almost no effect on the scaling behavior of the correlation sum (as has been tested by calculating the correlation sum for different time-windows: including and excluding the mode locking periods).

Note that our method of mode-locking detection is very simple, and does not require synchronous respiration rhythm recording (unlike the thorough method[8]). Besides, it can be conveniently used to find relatively short ($\gtrsim 10$ min) locking periods from a 24 h recording, because, unlike in the case of the alternative univariate data analysis technique,[9] there is a simple quantitative measure of the effect, the amplitude of the oscillatory component of the fluctuation function $F(\nu)$. The sensitivity of the method is high: the ratio of the Fourier transform amplitude of the locked mode $\Phi_{\alpha_0}$ to the root-mean-square of the amplitudes of the other modes is typically between 10 and 30.

## VI. CONCLUSION

Comparative analysis of real and model data showed that in the case of human heart rate, the correlation sum properties are defined by the interplay of the following factors: (a) finite resolution of the recording equipment (which leads to finite-size effects); (b) a significant level of long-time variability (the dynamical range of the mean heart rate exceeds the typical level of short-time variability); (c) the fact that the amplitude of short-time variability is a decreasing function of the mean heart rate. As a result, the correlation sum exhibits a scaling behavior, and the scaling exponent can be noticeably less than the dimensionality of the time-delay space. The scaling exponent value is mostly defined by the dynamics of the short-time variability, but depends also on the resolving power of the recording apparatus and is an increasing function of the embedding dimensionality. Therefore, the scaling exponent can be used as a certain measure of short-time variability of the signal (however, in order to obtain comparable values, time-resolution, record length, and the dimensionality of the time-delay space have to be kept constant). The diagnostic and/or prognostic value of this measure is possible, but has been found to be nonsignificant for our patient groups (see Table II). We have also shown that the above-drawn conclusion remains valid even in these cases, when a mode locking between the respiration and heart rhythm leads to "satellite clouds" in the time-delay space (see Fig. 6). Finally, we have devised a simple method of detecting the presence of the mode locking, based on the fluctuation function (7).

## ACKNOWLEDGMENTS

FIG. 7. Patient with 3:1 mode locking between heart rate and respiration: (a) heart beat intervals (in milliseconds) plotted vs the beat number. Heart rate has a pronounced oscillatory component; vertical lines mark the period of three heart beats, horizontal lines indicate the sequences with coherent phase. (b) Fluctuation function (arbitrary units) is plotted vs the time lag $\nu$ (in heart beats); the oscillating component is magnified.

[1] L. Glass, M. R. Guevara, A. Shrier, and R. Perez, Physica D **7**, 89 (1983).

[2] B. West, A. Goldberger, G. Rooner, and V. Bhargava, Physica D **17**, 198 (1985).

[3] A. Babloyantz and A. Destexhe, Biol. Cybern. **58**, 203 (1988).

[4] J. B. Bassingthwaighte, L. S. Liebovitch, and B. J. West, *Fractal Physiology* (Oxford University Press, New York, 1994).

[5] R. M. Berne and N. M. Levy, *Cardiovascular Physiology*, 8th ed. (Mosby, New York, 2001).

[6] D. L. Kaplan and M. Talajic, Chaos **1**, 251 (1991).

[7] M. Rosenblum and J. Kurths, Physica A **215**, 439 (1995).

[8] C. Schäfer, M. G. Rosenblum, J. Kurths, and H. H. Abel, Nature (London) **392**, 240 (1998).

[9] N. B. Janson, A. G. Balanov, V. S. Anishchenko, and P. V. E. McClintock, Phys. Rev. Lett. **86**, 1749 (2001).

[10] J. J. Zebrowski, W. Poplawska, R. Baranowski, and T. Buchner, Chaos, Solitons Fractals **11**, 1061 (2000).

[11] A. Voss *et al.*, Cardiovasc. Res. **31**, 419 (1996).

[12] H. Kantz and T. Schreiber, Chaos **5**, 143 (1995).

[13] J. K. Kanters, N. H. Holstein-Rathlou, and E. Agner, J. Cardivasc. Electrophysiol. **5**, 591 (1994).

[14] A. Bezerianos, T. Bountis, G. Papaioannou, and P. Polydoropoulus, Chaos **5**, 95 (1995).

[15] H. Kantz and T. Schreiber, *Nonlinear Time Series Analysis* (Cambridge University Press, Cambridge, 1997).

[16] V. Schulte-Frohlinde, Y. Ashkenazy, P. Ch. Ivanov, L. Glass, A. L. Goldberger, and H. E. Stanley, Phys. Rev. Lett. **87**, 068104 (2001).

[17] P. Grassberger and J. Procaccia, Physica D **9**, 189 (1983).

[18] L. Smith, Phys. Lett. A **133**, 283 (1988).

[19] R. Govindan, K. Narayanan, and M. Gopinathan, Chaos **8**, 495 (1998).

[20] S. Guzzetti, M. G. Signorini, C. Cogliati, S. Mezzetti, A. Porta, S. Cerutti, and A. Malliani, Cardiovasc. Res. **31**, 441 (1996).

[21] P. Ch. Ivanov, M. G. Rosenblum, L. A. N. Amaral, Z. Struzik, S. Havlin, A. L. Goldberger, and H. E. Stanley, Nature (London) **399**, 461 (1999).

[22] P. Bernaola-Galván, P. Ch. Ivanov, L. A. N. Amaral, and H. E. Stanley, Phys. Rev. Lett. **87**, 168105 (2001).

[23] M. Kobayashi and T. Musha, IEEE Trans. Biomed. Eng. **29**, 456 (1982).

# NON-LINEAR AND SCALE-INVARIANT ANALYSIS OF THE HEART RATE VARIABILITY.

J. KALDA, M. SÄKKI, M. VAINU, M. LAAN

# Nonlinear and scale-invariant analysis of heart rate variability

Jaan Kalda[a], Maksim Säkki[a], Meelis Vainu[b], and Mari Laan[c]

[a] Institute of Cybernetics at Tallinn Technical University, Akadeemia tee 21, 12618 Tallinn, Estonia; kalda@ioc.ee
[b] Tallinn Diagnostic Centre, Suur-Ameerika 18, 10122 Tallinn, Estonia
[c] Tallinn Children Hospital, Tervise 28, 13419 Tallinn, Estonia

**Abstract.** Human heart rate fluctuates in a complex and nonstationary manner. Elaborating efficient and adequate tools for the analysis of such signals has been a great challenge for the researchers during last decades. Here, an overview of the main research results in this field is given. The following questions are addressed: What are the intrinsic features of the heart rate variability signal? What are the most promising nonlinear measures, bearing in mind clinical diagnostic and prognostic applications?

**Key words:** heart rate variability, nonlinear time-series, intermittency.

## 1. INTRODUCTION

The heart rate of healthy subjects fluctuates in a complex manner. These non-stationary and nonlinear fluctuations are related mainly to a nonlinear interaction between competing neuroautonomic inputs: parasympathetic input decreases and sympathetic stimulation increases the heart rate. Meanwhile, heart pathologies may decrease the responsiveness of the heart and lead to a failure to respond to the external stimuli. Evidently, such pathologies lead to an overall reduction of heart rate variability (HRV). Understanding the diagnostic and prognostic significance of the various measures of HRV has great importance for the cardiology as a whole, because unlike the invasive methods of diagnostics, the required measurements are low-cost and harmless for patients. A particularly important application is the prognostics of the patients with increased risk of sudden cardiac death. While the "linear measures" of HRV are nowadays widely used in clinical practice, the

importance of more complicated measures has been hotly disputed in the scientific literature during the recent decades.

The structure of this review is as follows. In Section 2, general aspects of the heart rate generation, electrocardiogram (ECG) structure, and data acquisition are discussed. In Section 3, we give a brief overview of the "linear era" of the HRV analysis. Section 4 is devoted to the early studies of the nonlinearity of HRV, i.e. to the methods based on the reconstructed phase-space analysis. Here we also provide the modern view on the applicability of these methods. In Section 5, we discuss the self-affine and multi-affine aspects of HRV (including the wavelet-transform-based techniques). Section 6 deals with the phenomenon which can be referred to as "intertwining of low- and high-variability periods". Section 7 examines the effect of synchronization between the heart rate and respiration. Section 8 provides a brief conclusion.

## 2. HEART RATE GENERATION, ECG, AND DATA ACQUISITION

The quasi-periodic contraction of the cardiac muscle is governed by the electrical signal, which is generated by the sino-atrial (SA) node – a set of electrically active cells in a small area of the right atrium. The signal spreads through the atrial muscle leading to its contraction. It also spreads into a set of specialized cells – the atrio-ventricular (AV) node. Further the signal spreads via the His-Purkinje bundle (which is a fractal-like set of electrically conductive fibres) to the myocardial cells causing their contraction. The ECG is measured as the electrical potential between different points at the body surface. The activity of the SA node by itself is not reflected on the ECG. The electrical activation of the atrial cells leads to the appearance of the P-wave of the ECG. The Q, R, S, and T waves (see Fig. 1) are caused by the electrical activity of the ventricular muscle. The heart rate is generally measured as the RR-interval $t_{RR}$ – the time-lag between two subsequent R-pikes (R-pike itself corresponds to the ventricular contraction). For the HRV analysis, only the normal heart activity is taken into account. All the QRS-complexes are labelled as normal or arrhythmic. Note that even for healthy patients, some heartbeats can be arrhythmic. Normal-to-normal (NN) interval $t_{NN}$ is defined as the value of $t_{RR}$ for such heartbeats, which have both starting and ending R-pikes labelled as normal (see Fig. 1).

Typically, HRV analysis is based on the 24-hour recordings of the *Holter-monitoring*. Shorter ECG recordings can be used for this purpose as well; however, in that case it is impossible to observe the long-scale variations and compare the sleep-awake differences in the heart rhythm. Portable apparatus stores the ECG data as the time-dependent voltage $U(t)$ either on a tape or on a PC flash card; the sampling rate is 125 Hz or higher. The data are later analysed by computer software. Typical commercial software allows visualization of the ECG recording, automated or semiautomated recognition of arrhythmias and artifacts, and the calculation of the standard "linear" characteristics of HRV. Most often, a research
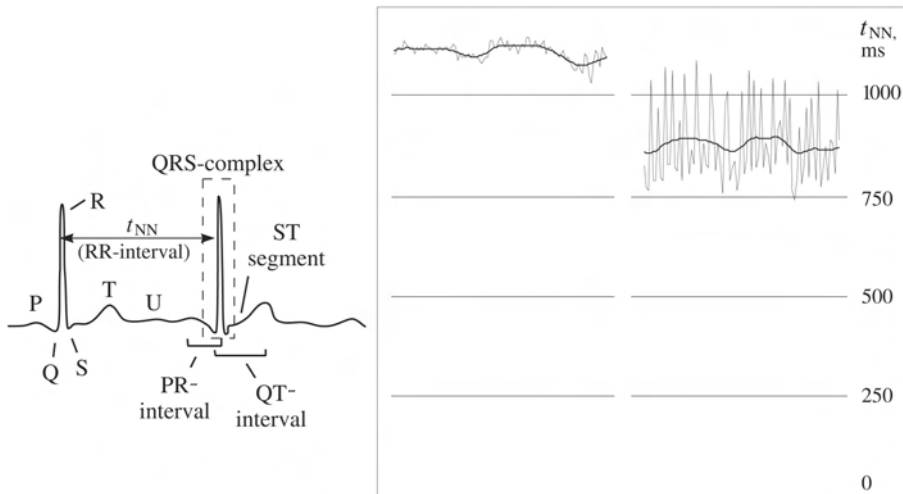
**Fig. 1.** Left image: normal ECG recording. Image on the right: $t_{NN}$ sequences of low and high variability.

devoted to the methods of nonlinear dynamics is based on plain sequences of NN-intervals and disregards the details of the continuous ECG recordings. Other aspects of the ECG, e.g. the clustering of arrhythmic beats [1] and dynamics of QT intervals [2] (pp. 13–16) are also of high clinical importance, but remain beyond the scope of this review.

The experimental data serving as the basis of the original research performed by the authors of the review were recorded (a) at the Tallinn Nõmme Hospital (children) and (b) Tallinn Diagnostic Centre (adult subjects). The scheme of data acquisition is presented in Fig. 2. For group (a), the recordings of ambulatory Holter-monitoring covered 12 healthy subjects of mean age $11.5 \pm 3.3$ years, 6
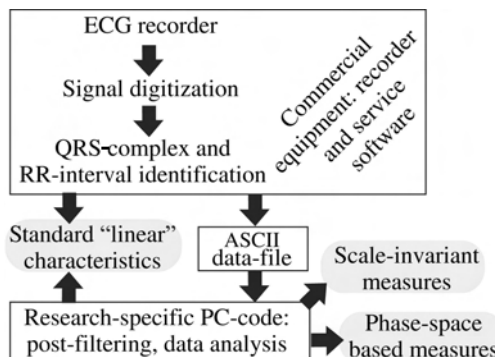


**Fig. 2.** The analysis of heart rate variability: the scheme of data acquisition and analysis.

**Table 1.** Test groups of patients. Abbreviations are as follows: IHD – ischemic heart disease (stenocardia); SND – sinus node disease; VES – ventricular extrasystole; PCI – post cardiac infarction; RR – blood pressure disease; FSK – functional disease of sinus node

|                 | Healthy | IHD  | SND  | VES  | PCI  | RR   | FSK  |
|-----------------|---------|------|------|------|------|------|------|
| No. of patients | 103     | 8    | 11   | 16   | 7    | 11   | 6    |
| Mean age        | 45.5    | 65.4 | 50.0 | 55.9 | 47.3 | 55.5 | 11.7 |
| Std. dev. of age| 20.5    | 11.4 | 19.3 | 14.3 | 11.6 | 14.4 | 4.6  |

children with clinically documented sinus node disease (mean age $11.5 \pm 1.9$ years), and 12 subjects with miscellaneous diagnosis. The sampling rate of the ECG was 125 Hz. For group (b), specifics are given in Table 1. These data have been obtained during regular diagnostical examinations of more than 200 patients using the *Rozinn* equipment; the ECG sampling rate has been 180 Hz. It is known that there can be significant differences between the HRV dynamics of young and adult subjects. The primary goal of including the children groups has been to test the universality (age-independence) of the scaling behaviour of HRV qualitatively. The diagnostics and data verification have been made by a qualified cardiologist. The data preprocessing included filtering out falsely detected QRS-complexes (artifacts and arrhythmias) using the commercial *Rozinn* software.

## 3. LINEAR MEASURES OF HRV

The clinical importance of HRV was first noted in 1965 by Hon and Lee [3]. Since then, the statistical properties of the interbeat interval sequences have attracted the attention of a wide scientific community. An increased risk of post-infarction mortality was associated with the reduced HRV by Wolf et al. [4] in 1977.

The problem received wider attention in the early 1980s, when Akselrod et al. [5] introduced the spectral methods for the HRV analysis. The spectral characteristics are generally referred to as "frequency-domain characteristics" and are opposed to the "time-domain methods", which are derived directly from the $t_{NN}$-sequence. In the late 1980s, the clinical importance of HRV became generally recognized. Several studies confirmed that HRV was a strong and independent predictor of mortality following an acute myocardial infarction [6−8]. As a result, a breakthrough has been achieved: the "linear" measures of HRV became important tools of clinical practice.

A nonexhaustive list of the parameters currently used in medical practice is as follows: the mean NN-interval, the difference between night and day heart rate, the longest and shortest NN-intervals, the standard deviation of the NN-interval (SDNN, typically calculated over a 24-hour period), the standard deviation of locally (usually 5 min) averaged NN-intervals (SDANN), the mean of the 5-minute

standard deviation of the NN-interval (averaged over 24 h; SDNN index), the square root of the mean squared differences of successive NN-intervals (RMSSD), the percentage of interval differences of successive NN-intervals greater than 50 ms (pNN50), the spectral power of high- and low-frequency fluctuations in NN-sequences.

## 4. RECONSTRUCTED PHASE-SPACE

It is widely accepted that the heart rhythm generation in the complex of the sinus node and atrio-ventricular node can be well described by nonlinear dynamical models, where the SA node and AV node form a system of nonlinear coupled oscillators [9−10]. The model has been proven to be viable and predicts several experimentally observed phenomena, such as Wenckebach and Mobitz type II arrhythmias and bistable behaviour [10]. This deterministic nonlinear model predicts that the phase trajectories of an healthy heart lie on an attractor of the coupled system of oscillators. Consequently, one should be able to observe well-defined patterns on the Poincarè sections of the phase-space. Note that in the case of physiological data, there is no information, what might be the canonical variables. Therefore, the phase trajectory is reconstructed in time-delay coordinates $U(t)$, $U(t + \tau)$, ..., $U[t + (D − 1)\tau]$ [or $t_{NN}(n)$, $t(n + 1)$, ..., $t(n + D − 1)$]. Here $D$ is the so-called embedding dimensionality, i.e. the dimensionality of the reconstructed phase-space. It is expected that the real phase trajectory is mapped to the reconstructed trajectory by a smooth transform.

Exactly such a reasoning has led to the idea that the dynamical characteristics from the theory of nonlinear dynamics could be used for the diagnostic purposes. The early studies by Babloyantz et al. [11] gave rise to extensive studies in the 1990s [12−15]. The experimental observations seemingly confirmed the theoretical expectations. Particularly, the correlation dimension of the continuous ECG recording (i.e. the recorded voltage as a function of time) has been reported to be between 3.6 and 5.2. The conclusion has been that the dynamics of the heart of a healthy person is less regular than that of a person with severe cardiac pathologies. Correspondingly, the correlation dimension has often been thought to be a measure for the healthiness of the heart. The other tools of the analysis of nonlinear dynamical systems (such as Lyapunov exponents; Kolmogorov, Shannon, pattern, and approximate entropies; etc.) have been exploited to an equal extent.

The correlation dimension of a data sequence is typically calculated according to the Grassberger–Procaccia algorithm [16]. In a reconstructed phase-space of dimensionality $D$, the correlation sum $C = \frac{2}{N(N-1)} \sum_{i,j} \theta(r − |r_i − r_j|)$ is calculated as a function of the radius $r$; it is expected to behave as a power-law $C \propto r^{\nu(D)}$. Here $r_i$ denotes the $D$-dimensional radius-vector of the $i$th data-point, and $\theta(r)$ stands for the Heaviside function. The correlation dimension $d_c$ is found as the limit of $\nu$ at large values of $D$ (in fact, it is expected that for $D > d_c$, the exponent $\nu$ is independent of $D$, and in that case $\nu = d_c$).

However, there are various arguments leading us to the conclusion that the formally calculated correlation dimension of a heart rhythm does not correspond to the dimensionality of an intrinsic attractor; similarly, the formally calculated Lyapunov exponents, entropies, etc. do not describe the respective aspects of underlying nonlinear dynamics. First, it has been pointed out that physiological time-series are typically nonstationary and noisy, and therefore, the correlation dimension cannot be calculated reliably [17−19]; this fact is nowadays widely accepted. In the case of the human heart, the "noise" comes from the autonomous nervous system in the form of inputs regulating the heart rate (cf. [20−22]): from the viewpoint of the underlying nonlinear deterministic system, these effectively nondeterministic signals perform the role of high-level noise. It should also be noted that some inputs of the autonomous nervous system may lead to quasi-periodic signals – an easy source of false detection of low-dimensional chaos and apparent patterns in simple time delay maps (see Figs. 3, 4). Thus, respiration gives rise to the signal of a typical period of 4 s; the effect is most pronounced when the patient is at rest, and is stronger for young persons. Second, it has been emphasized that a reasonable fitting of a correlation sum to a power law does not necessarily mean that the obtained exponent is the correlation dimension of the underlying dynamical system; instead, a thorough nonautomatable verification procedure has to be done [23]. Third, the length of the data sequences is often inadequate for reliable calculation of high values of the correlation dimension $d_c \gtrsim 6$, cf. [15,23].
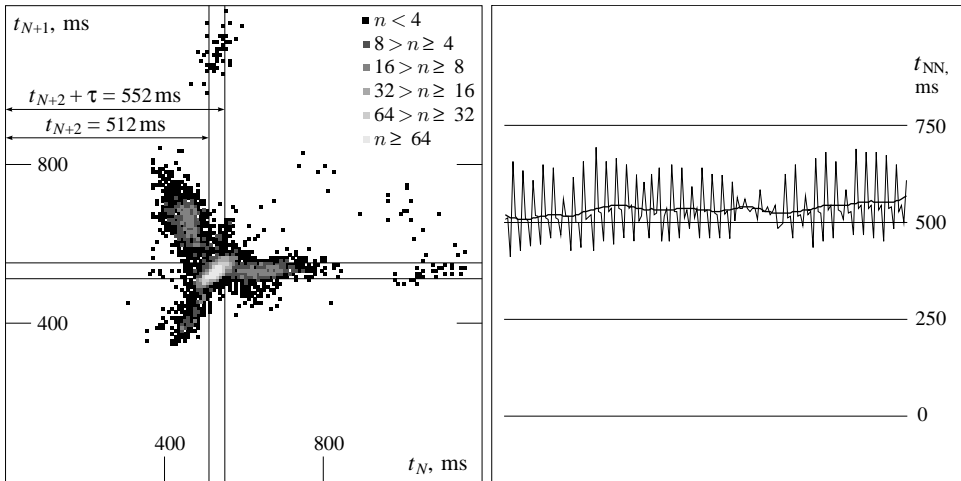


**Fig. 3.** A cross-section of the 3-dimensional reconstructed phase-space for a patient with pronounced 4:1 mode-locking (see also Section 7); around the central cloud of points, three major satellite-clouds can be seen; these satellite-clouds correspond to the sequence of interbeat intervals, shown on the right-hand plot. The observed oscillations with period 4 can be attributed to the modulation of the heart rate by respiration.
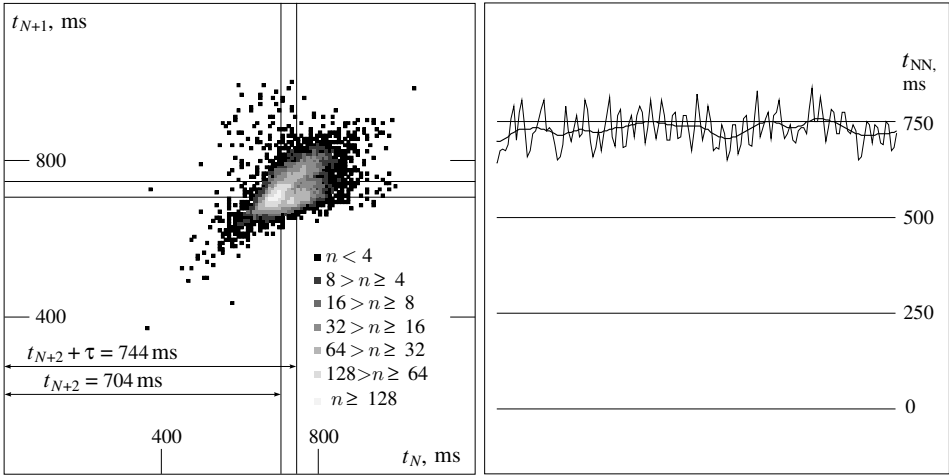
**Fig. 4.** The same as in Fig. 3. Mode-locking (4:1 and 5:1) is weaker, but the heart rate modulation by the respiration is significant. One can distinguish two branches of the central cloud, which are caused by the respiratory modulation.

The above discussed research results can be summarized as follows: (1) The correlation sums of the human heart rate follow typically a scaling law. (2) In most cases, the scaling exponents are not the correlation dimensions. This leads us to a natural question: what is the physical meaning of these formally calculated exponents? Our answer to this question is based on simple observations, valid for healthy patients: (a) the long-time variability of the interbeat intervals is typically much higher than the variability on the time-scale of few heartbeats; (b) for the periods when the mean heart rate is high (when the subject is performing physical exercise) HRV is low; (c) the heart rate is controlled by effectively random nondeterministic inputs arriving from the autonomous nervous system. As a consequence, in time delay coordinates, an HRV time-series generates a baseball bat-shaped cloud of points. Although the theoretical value of the correlation dimension of such a cloud is infinite, the finite resolution of the recording apparatus, finite length of the time-series, and the linear structure of the cloud result in a smaller value. This is evident for a very narrow "bat", which is efficiently one-dimensional.

Our conjecture passes also a quantitative test: the correlation sum of surrogate data-sets constructed using Gaussian random data-series and mimicking the features (a)–(c) (see Fig. 5) scales almost identically to that of clinical HRV data (see Fig. 6 and [24]).
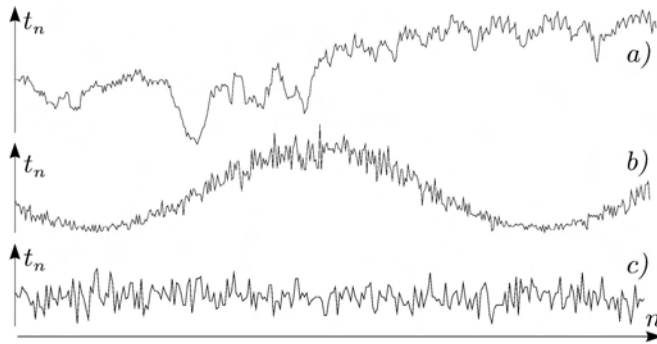
**Fig. 5.** Time-series for real HRV data (a), surrogate data (b), and Gaussian noise (c); the beat interval $t_n$ is plotted versus the beat number $n$.
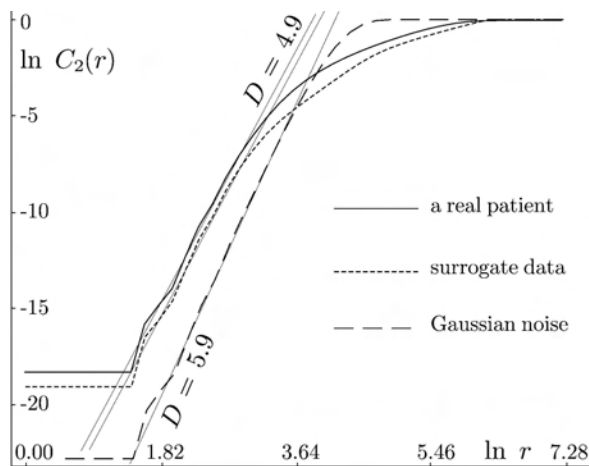


**Fig. 6.** The correlation sum $C_2(r)$ (as a function of the radius $r$) of surrogate data scales almost identically to the real clinical data.

To conclude, the measures based on the reconstructed phase-space fail to describe a deterministic chaos inside the heart, because the deterministic dynamics is suppressed by essentially intermittent signals arriving from the autonomous nervous system and regulating the heart rhythm. However, some fine-tuned measures (e.g. various entropies; cf. [25]) can be useful in describing the level of short-time variability of the heart rhythm, and complement the linear quantity pNN50 (which also measures the high-frequency component of HRV).

## 5. SCALE-INDEPENDENT MEASURES

Recent studies have shown that scale-invariant characteristics can be successfully applied to the HRV analysis [26−29]. However, this conclusion has been disputed, and certain scale-dependent measures (particularly, the amplitude of the wavelet spectra at a specific time-scale) have been claimed to provide better results [30]. The scale-independent methods have been believed to be more universal, subject-independent, and to reflect directly the dynamics of the underlying system, unlike the scale-dependent methods which may reflect characteristics specific to the subject and/or to the method of analysis [29]. The opposing argument has been that certain heart disorders affect HRV at a specific scale or range of scales; owing to this circumstance, at the properly chosen time-scale, scale-dependent measures may provide a useful information [30].

The simplest relevant scale-independent measure is the Hurst exponent $H$, which has been introduced to describe statistically self-affine random functions $f(r)$ of one or more variables [31]. Such a function is referred to as a *fractional Brownian function* and satisfies the scaling law

$$\langle [f(r_1) - f(r_2)]^2 \rangle \propto |r_1 - r_2|^{2H}.$$

Note that $H = \frac{1}{2}$ is a special case of ordinary Brownian function – the increments of the function are delta-correlated, and $f(r)$ can be thought to be the displacement of a Brownian particle as a function of time $r$. Therefore, in the case of $H < \frac{1}{2}$, there is a negative *long-range correlation* between the increments of the function. Analogously, $H > \frac{1}{2}$ corresponds to a positive correlation. Note that the early scale-invariant studies of HRV were based on power spectra [32,33], an aspect closely related to the scaling exponent $H$.

Many phenomena in nature exhibit this kind of scale-invariance and lead to fractional Brownian time-series [31]. The same is true for HRV: after filtering out short-scale components with $\tau < 30$ s (corresponding to the respiratory rhythm, to the blood-pressure oscillations, and to the pathological Cheyne–Stokes respiration), the fluctuation function $F(n)$, defined as

$$F(\nu) = \langle |t_n - t_{n+\nu}| \rangle \tag{1}$$

revealed a good scaling behaviour $F(\nu) \propto \nu^H$ [26]. While for healthy patients, the increments of the heart rhythm were found to be significantly anticorrelated resulting in $H < \frac{1}{2}$, the heart rhythm of the patients with dilated cardiomyopathy was essentially Brownian with $H \approx \frac{1}{2}$ [26]. In the case of our patient groups, there was no significant correlation between the diagnosis and the Hurst exponent, and there were also ca 7% healthy subjects with $H = 0.5 \pm 0.05$ (cf. Fig. 7 and Table 2).

Finally, various techniques, such as detrended fluctuation analysis [27], detrended time-series analysis [34], and wavelet amplitude analysis [35] have been proposed to fine-tune the Hurst-exponent-based approach.
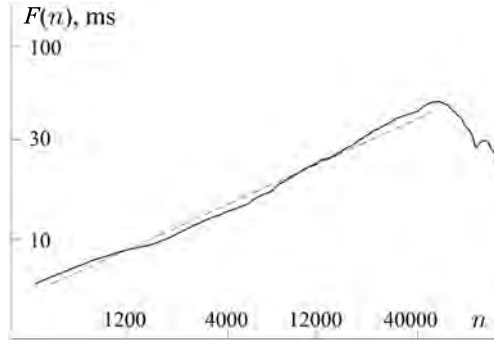
**Fig. 7.** The fluctuation function $F(\nu)$ is plotted versus the time lag $\nu$. The almost straight line indicates a good scaling behaviour $F(\nu) \propto \nu^H$ (here with $H = 0.50$).

**Table 2.** For the patient groups of Table 1, the diagnosis and the Hurst exponent $H$ values were effectively uncorrelated

|  | Healthy | IHD | SND | VES | PCI | RR | FSK |
|---|---|---|---|---|---|---|---|
| Mean value of $H$ | 0.30 | 0.28 | 0.32 | 0.35 | 0.29 | 0.29 | 0.28 |
| Std. dev. of $H$ | 0.10 | 0.09 | 0.11 | 0.12 | 0.12 | 0.08 | 0.06 |

Complex nonstationary time-series cannot be described by a single scaling exponent $H$. Indeed, simple scaling behaviour is expected if there is a Gaussian distribution of increments. However, even in the case of Gaussian functions, the scaling exponent is not necessarily constant over the whole range of scales. Instead, it can be a slow (e.g. logarithmic) function of the scale, so that other descriptions (such as stretched exponentials) may be required. Physiological time-series are typically non-Gaussian. For such functions, scale-invariance can be very complicated. A nonexhaustive way to describe such a behaviour is to calculate the multifractal spectrum of Hurst exponents [36]. Therefore, it is not surprising that the human heart rate signal was found to obey a multi-affine structure [28,29].

Qualitatively, a multifractal time-series behaves as follows. Each point of the time-series is characterized by its own Hurst exponent $h$ (referred to as the Lipschitz–Hölder exponent); this exponent describes the local scaling of fluctuations. Then, the distribution of points of fixed values of $h$ is self-similar and is described by a fractal dimension $f(h)$. Technically, the spectrum $f(h)$ can be calculated by the means of wavelet transform (cf. [29]). This scheme includes the calculation of the scaling exponents $\tau(q)$ (referred to as the mass exponents), which describe, how the $q$th moment of the wavelet transform amplitude scales with the wavelet width. The scaling exponents $\tau(2)$ and $\tau(5)$ have been found to have

a significant prognostic value (for the post-infarction prognosis) [29]. The wavelet transform amplitudes, calculated for a specific wavelet width ($\approx 5$ min) have been claimed to be of even higher prognostic value [30]. However, independent studies have shown that the scale-invariant measures seem to be superior tools [37]. It should also be noted that the wavelet transform amplitude at a fixed time-scale is closely related to the linear measure SDANN. Substituting the robust standard deviation by a wavelet transform amplitude is a technical fine-tuning which cannot be expected to result in a qualitatively new information.

The multifractal structure of the heart rate signal has several consequences. Thus, the $q$th-order structure function (a concept borrowed from the theory of the fully-developed turbulence) of the heart rate interval has a scaling behaviour, with the scaling exponent $\zeta(q)$ being a function of $q$ [38]. Note that this spectrum of exponents is very closely related to the above-mentioned $\tau(q)$ spectrum (both describing the same physical phenomenon, differences being of a technical kind). However, the wavelet-transform-based technique makes a more complete utilization of the underlying data and therefore, the $\tau(q)$ spectrum can be expected to yield somewhat superior prognostic and/or diagnostic results.

Another aspect related to the multifractal nature of the heart rhythm is the multi-scale entropy (MSE) [39]. While the single-scale entropies (approximate entropy, Shannon entropy) are related to the short-time dynamics of the heart rhythm and to the probability distribution function of points in the reconstructed phase-space, the MSE extends these concepts to longer time-scales. The MSE is not directly reducible to the multifractal spectra $f(h)$ [or $\tau(q)$]; however, both techniques address the question of how wide is the range of dynamics for the mean heart rate (averaged over a time $T$), depending on the time-scale $T$. The clinical usefulness of the MSE is still unclear (apart from the fact that it has been claimed to distinguish between healthy subjects and patients with congestive heart failure [39]).

## 6. INTERMITTENCY OF HRV

A multifractal spectrum addresses only one aspect of the non-Gaussianity of the time-series increments by revealing the possible range of scaling laws for the long-range [at time-scale of many ($\gg 1$) heartbeat intervals] dynamics of the mean heart rhythm. While the origin of the multifractal scaling is in the intertwining of periods of different variability levels (cf. [12] and Fig. 8), the multifractal spectra fail to reflect all the features of the intertwining phenomena. In particular, this applies to the long-term correlations in the dynamics of short-time variability (which, in effect, does fluctuate in a complex manner). A quantitative scale-invariant analysis of this aspect is based on the distribution law of the low-variability periods [40,41], which will be discussed below. Another aspect of such an intertwining is the clustering of the periods of a similar mean heart rate: the heart rate signal can be divided into segments of a different mean heart rate, with distinct boundaries

**Fig. 8.** For healthy patients, the high- and low-variability periods of the heart rhythm are intertwined.

between these segments; there is a power-law segment-length distribution of the segments [42].

In order to analyse quantitatively the intertwining of high- and low-variability periods, we have studied the distribution of low-variability periods and showed that typically, it follows a multiscaling Zipf's law. Originally, Zipf's law has been formulated by G. K. Zipf for the frequency of words in natural languages [43]. For a given language (e.g. English), the frequency (the number of occurrences divided by the total number of words) of each word is calculated on the basis of a large set of texts. The ranks are determined by arranging the words according to their frequency $f$: the most frequent word obtains rank $r = 1$, the second frequent – $r = 2$, etc. It turns out that for a wide range of ranks (starting with $r = 1$), there is a power law $p(r) \propto r^{-\alpha}$, where $\alpha \approx 1$. This law is universal; it holds for all the natural languages and for a wide variety of texts [43]. Furthermore, similar scaling laws describe the rank-distribution of many other classes of objects as well. Thus, when cities are arranged according to their population $s$, the population of a city $s \propto r^{-\alpha}$, with $\alpha \approx 1$ [43]. Another example is the income-rank relationship for companies; here we have again $\alpha \approx 1$ [43]. In the most general form, the law can be formulated as $p \propto (r + r_0)^{-\alpha}$, and $\alpha$ is not necessarily close to unity [36]. This more general form of the law can be applied to the distribution of scientists according to their citation index, to the distribution of internet sites according to the number of visitors, etc.

Zipf's law is characteristic of such dynamical systems at statistical equilibrium, which satisfy the following conditions: (a) the system consists of elements of different size; (b) the element size has upper and lower bounds; (c) there is no intermediate intrinsic size for the elements. The human heart rate, when divided into the low-variability periods, satisfies all these requirements. The duration $\tau$ of these periods varies in a wide range of scales, from few to several hundreds of heartbeats. Thus, one can expect that the rank-length distribution $r(\tau)$ follows Zipf's law,

$$r \propto \tau^{-\gamma}. \tag{2}$$

First we have to define the local HRV as the deviation of the heart rate from the local average,

37

$$\delta(n) = [t_{\mathrm{NN}}(n) - \langle t_{\mathrm{NN}}(n)\rangle]/\langle t_{\mathrm{NN}}(n)\rangle\,;$$

the local average is calculated using a narrow ($\approx$ 5-second-wide) Gaussian weight-function. Then, the low-variability regions are defined as consecutive sequences of intervals with $|\delta(n)| < \delta_0$; the length $\tau$ of such a region is measured as the number of beats in the sequence. Further, all the low-variability regions are numbered (to identify them later), and arranged according to their length; regions of equal length are ordered randomly. In such a way, the longest observed region obtains rank $r = 1$, second longest – $r = 2$, etc. Typically, the length-rank relationship reveals multiscaling properties, i.e. within a certain range of scales, the scaling law (2) is observed, the scaling exponent $\gamma$ being a (nonconstant) function of the threshold level, $\gamma = \gamma(\delta_0)$ (see Fig. 9).

It is not surprising that the scaling behaviour is not perfect. Indeed, the heart rhythm is a nonstationary signal affected by the nonreproducible daily activities of the subjects. The nonstationary pattern of these activities, together with their time-scales, is directly reflected in the rank-length law. This distribution law can also have a fingerprint of the characteristic time-scale (10 to 20 s) of the blood pressure oscillations (which modulate the level of HRV, cf. [44]). It should be emphasized that the problem of the nonreproducible daily activities affects also the
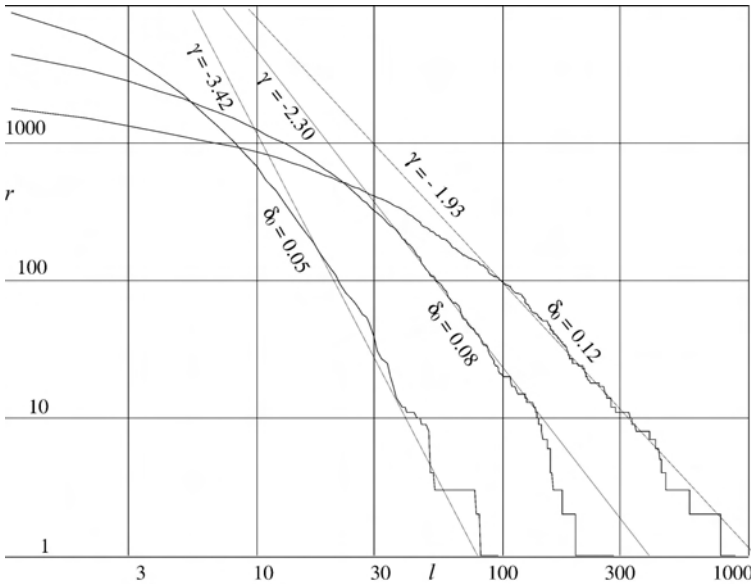


**Fig. 9.** Multiscaling behaviour: the rank $r$ of low-variability intervals is plotted against the length $l$ of the intervals (measured in the number of heartbeats). The scaling exponent $\gamma$ depends on the threshold value $\delta_0$.

reliability of the other scale-invariant measures and is probably the main obstacle preventing the clinical application of the seemingly extremely efficient diagnostic and prognostic techniques. Finally, there is a generic reason why Zipf's law is nonperfect at small rank numbers: while Zipf's law is a statistical law, each rank-length curve is based only on a single measurement. In particular, there is only one longest low-variability period (likewise, only one most-frequent word), the length of which is just as long as it happens to be; there is no averaging whatsoever. For large ranks, the relative statistical uncertainty can be estimated as $1/\sqrt{r}$.

The distribution function of the low-variability periods as a whole contains a significant amount of diagnostically valuable information, which is not covered by any other (linear or nonlinear) measure of HRV. The most part of this information seems to be reflected (according to the Student test analysis using the test groups of Table 1) by the parameters $\tau_{\mathrm{end}}$ (the scale at which the scaling law breaks; for a precise definition, see [41]), $r_{\mathrm{max}}$ (the maximal observed rank), and $r_{100}$ (the rank of the interval with $\tau = 100$; the diagnostical performance of this parameter is similar to that of $r_{\mathrm{max}}$). These measures allow a clear distinction between the healthy subjects and the IHD, VES, and PCI groups [41]; the $p$-values are presented in Table 3 (for a reference, the data of the two best-performing linear measures are also provided).

Table 3. $p$-values of the Student test. Data in the topmost triangular region (with label $A$) are calculated using the parameter $\ln \tau_{\mathrm{end}}$ (the logarithmic measure is used to achieve a nearly-Gaussian data distribution). Triangular region $B$ corresponds to the parameter $\ln r_{\mathrm{max}}$, region $C$ – to the linear measure pnn50, and region $D$ – to the linear measure SDNN. Since multiple tests were carried out, modified Bonferroni correction [45] has to be applied. Grey background highlights the tests with the adjusted significance $p' < 10\%$. The control parameter value $\delta_0 = 0.05$ has been used

| $p$, % | Healthy | IHD | SND | VES | PCI | RR |
|---|---|---|---|---|---|---|
| Healthy $B$ / $A$ | | 0.06 | 17.21 | 0.02 | 0.07 | 1.59 |
| IHD | 0.36 | | 2.85 | 96.79 | 97.62 | 21.93 |
| SND | 2.99 | 59.10 | | 2.10 | 3.04 | 25.77 |
| VES | 0.08 | 91.60 | 63.79 | | 94.18 | 17.59 |
| PCI | 25.27 | 21.61 | 46.37 | 22.89 | | 22.50 |
| RR | 0.14 | 73.57 | 77.69 | 80.49 | 28.90 | |
| Healthy $D$ / $C$ | | 7.01 | 10.01 | 0.01 | 0.98 | 4.34 |
| IHD | 3.89 | | 2.70 | 45.88 | 62.20 | 74.98 |
| SND | 0.64 | 0.10 | | 1.44 | 3.40 | 3.23 |
| VES | 8.83 | 64.71 | 0.15 | | 3.46 | 16.26 |
| PCI | 14.93 | 0.99 | 3.31 | 1.98 | | 12.63 |
| RR | 21.58 | 1.07 | 1.94 | 2.38 | 70.25 | |

## 7. MODE-LOCKING BETWEEN THE HEART RHYTHM AND RESPIRATION

As mentioned above, respiration affects (modulates) the heart rhythm. This effect is mediated by the blood pressure, and the effect known as baroreflex (heart rhythm depends on the blood pressure). The heart is most responsive with respect to the signals of the autonomous nervous system when the heart rate is slow, i.e. when the patient is at rest. In that case, HRV is driven by weaker signals, like the signals induced by respiration, which (due to their quasi-periodic nature) may lead to a mode-locking. In the case of mode-locking, the heart rate is automatically slightly adjusted so that the respiration and heart beat periods relate to each other as (small) integers. As a result, the decorrelation time between the heart rhythm and respiration can be very long. This is the effect which is in most cases the cause of the patterns (isolated clouds of points) observable in the reconstructed phase space (see Fig. 3).

The mode-locking has been studied using bivariate data (simultaneous ECG and respiration data) and the technique called cardiorespiratory synchrogram [44]. Also, a univariate data analysis method using the angle-of-returntime map has been elaborated [46]. In that case, the data-set is used to reconstruct the phase of forcing (breathing) and the phase of oscillator (heart). These phases are plotted versus each other; in the case of mode-locking, disjoint clouds of points will appear.

Recently, we have developed an independent, intuitive and easy to use method of mode-locking detection from univariate data (RR-interval sequence), which is based on analysis of the fluctuation function $F(\nu)$, defined by Eq. (1) [24]. The fluctuation function of the patients with mode-locking revealed the presence of an oscillatory component, see Fig. 10b. By dividing the entire 24-hour HRV record into one-hour intervals, and calculating the amplitude of the oscillatory component (via a wavelet transform) of the fluctuation function for each interval, we were able to locate the periods responsible for the satellite clouds in the reconstructed phase-space. These were always the periods before falling asleep, around 10 or 11 pm, characterized by a low heart rate and a high respiration-driven short-time variability. The phase between the heart rate and respiration is locked during tens of seconds, confirming the observations of Schäfer et al. [44]. Thus, in a certain sense, the heart and respiratory complex act as a system of coupled oscillators. Finally we note that a specific feature of the patients with strong mode-locking was the presence of well-defined "satellite clouds" in time-delay map (see Fig. 3). Therefore, the time-delay map can be also used to detect mode-locking; however, this method is nonquantitative, less sensitive than the fluctuation-function-based technique, and does not give a hint which mode-locking modes are observed. The presence of a natural quantitative measure (the wavelet transform amplitudes) is also the main advantage of our approach over the alternative method.

As compared with the alternative techniques, our method of mode-locking detection is very simple and does not require synchronous respiration rhythm recording (unlike the thorough method [44]), and can be conveniently used to find
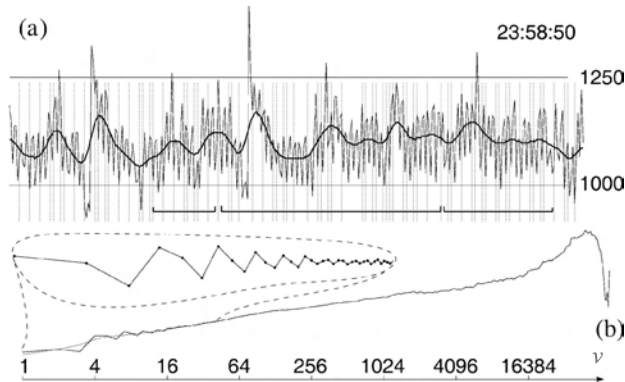
**Fig. 10.** Patient with 3:1 mode-locking between the heart rate and respiration: (a) heartbeat intervals (in milliseconds) plotted versus the beat number. The heart rate has a pronounced oscillatory component; vertical lines mark the period of three heartbeats, horizontal lines indicate the sequences with coherent phase. (b) Fluctuation function (arbitrary units) is plotted versus the time lag $\nu$ (in heartbeats); the oscillating component is magnified.

relatively short ($\gtrsim 10\,\mathrm{min}$) locking periods from a 24-hour recording. Besides, it provides a natural measure to quantify the degree of mode-locking (unlike the method of using the angle-of-returntime map [46]).

## 8. CONCLUSIONS

Below is an attempt to classify the measures of heart rate variability.

1. "Classical" linear methods – based on standard statistical measures and on the Fourier analysis. These are the only methods widely used in clinical practice.

2. "New" linear methods: wavelet spectra.

3. Nonlinear methods:

(a) scale-invariant methods:

i. single-scaling analysis (calculation of the Hurst exponent $H$);

ii. multi-scaling analysis – calculation of the exponent spectra [Lipschitz– Hölder spectrum $f(h)$, mass exponents $\tau(q)$, or structure function exponent spectrum $\zeta(q)$]; these seem to be the most promising measures, at least for prognostic purposes;

iii. calculation of the multiscale entropy;

iv. analysis of the HRV-data segments with a similar mean heart rate;

v. analysis of the distribution law of low-variability periods (performs well in diagnostic tests, there are no prognostic tests yet);

(b) scale-dependent methods:

i. performing a phase-space analysis (entropy-based measures, correlation dimension, Lyapunov exponents, etc.);

ii. heart rhythm and respiration mode-locking analysis.

The human heart rate fluctuates in a complex and nonstationary manner. Elaborating efficient and adequate tools for the analysis of such signals has been a great challenge for the researchers during last decades. The above long list of nonlinear techniques proves that the research has been successful and various important features of such time-series have been revealed. Nevertheless, there is no consensus of which methods are the most efficient ones from the point of view of clinical applications. On the one hand, this is caused by the high nonstationarity and irreproducibility of these time-series: the complex measures of HRV depend not only on the healthiness of the heart, but also on the daily habits of the subject [47] and on the random events of the recording day. On the other hand, dialogue between physicists and doctors seems to be inefficient: physicists publish research results based on small test groups; doctors are waiting for follow-up studies using extended and homogeneous test groups. However, the situation is expected to start improving, owing to the new projects bringing together medical doctors and physicists (cf. http://www.physionet.org).

## REFERENCES

1. Liebovitch, L. S., Todorov, A. T., Zochowski, M., Scheurle, D., Colgin, L., Wood, M. A., Ellenbogen, K. A., Herre, J. M. and Bernstein, R. C. Nonlinear properties of cardiac rhythm abnormalities. *Phys. Rev. E*, 1999, **59**, 3312–3319.
2. Lass, J. *Biosignal Interpretation: Study of Cardiac Arrhythmias and Electromagnetic Field Effects on Human Nervous System*. PhD theses, TTU Press, 2002.
3. Hon, E. H. and Lee, S. T. Electronic evaluations of the fetal heart rate patterns preceding fetal death, further observations. *Am. J. Obstet. Gynec.*, 1965, **87**, 814–826.
4. Wolf, M. M., Varigos, G. A., Hunt, D. and Sloman, J. G. Sinus arrhythmia in acute myocardial infarction. *Med. J. Australia*, 1978, **2**, 52–53.
5. Akselrod, S., Gordon, D., Ubel, F. A., Shannon, D. C., Barger, A. C. and Cohen, R. J. Power spectrum analysis of heart rate fluctuation: a quantitative probe of beat to beat cardiovascular control. *Science*, 1981, **213**, 220–222.
6. Kleiger, R. E., Miller, J. P., Bigger, J. T., Moss, A. J. and the Multi-center Post-Infarction Research Group. Decreased heart rate variability and its association with increased mortality after acute myocardial infarction. *Am. J. Cardiol.*, 1987, **59**, 256–262.
7. Malik, M., Farrell, T., Cripps, T. and Camm, A. J. Heart rate variability in relation to prognosis after myocardial infarction: selection of optimal processing techniques. *Eur. Heart J.*, 1989, **10**, 1060–1074.
8. Bigger, J. T., Fleiss, J. L., Steinman, R. C., Rolnitzky, L. M., Kleiger, R. E. and Rottman, J. N. Frequency domain measures of heart period variability and mortality after myocardial infarction. *Circulation*, 1992, **85**, 164–171.
9. West, B. J., Goldberger, A. L., Rooner, G. and Bhargava, V. Nonlinear dynamics of the heartbeat. 1. The av junction: passive conduct on active oscillator. *Physica D*, 1985, **17**, 198–206.

10. Engelbrecht, J. and Kongas, O. Driven oscillators in modelling of heart dynamics. *Appl. Anal.*, 1995, **57**, 119–144.
11. Babloyantz, A. and Destexhe, A. Is the normal heart a periodic oscillator? *Biol. Cybern.*, 1988, **58**, 203–211.
12. Poon, C. S. and Merrill, C. K. Decrease of cardiac chaos in congestive heart failure. *Nature*, 1997, **389**, 492–495.
13. Voss, A., Kurths, J., Kleiner, H. J., Witt, A., Wessel, N., Saparin, P., Osterziel, K. J., Schurath, R. and Dietz, R. The application of methods of non-linear dynamics for the improved and predictive recognition of patients threatened by sudden cardiac death. *Cardiovasc. Res.*, 1996, **31**, 419–433.
14. Pincus, S. Approximate entropy (ApEn) as a complexity measure. *Chaos*, 1995, **5**, 110–117.
15. Govindan, R. B., Narayanan, K. and Gopinathan, M. S. On the evidence of deterministic chaos in ECG: surrogate and predictability analysis. *Chaos*, 1998, **8**, 495–502.
16. Grassberger, P. and Procaccia, J. Measuring the strangeness of a strange attractor. *Physica D*, 1983, **9**, 189–208.
17. Kantz, H. and Schreiber, T. Dimension estimates and physiological data. *Chaos*, 1995, **5**, 143–154.
18. Kanters, J. K., Holstein-Rathlou, N. H. and Agner, E. Lack of evidence for low-dimensional chaos in heart rate variability. *J. Cardiovasc. Electrophys.*, 1994, **5**, 591–601.
19. Bezerianos, A., Bountis, T., Papaioannou, G. and Polydoropoulus, P. Nonlinear time series analysis of electrocardiograms. *Chaos*, 1995, **5**, 95–101.
20. Berne, R. M. and Levy, N. M. *Cardiovascular Physiology*. Eighth edition. Mosby, New York, 2001.
21. Kaplan, D. L. and Talajic, M. Dynamics of heart rate. *Chaos*, 1991, **1**, 251–256.
22. Rosenblum, M. and Kurths, J. A model of neural control of the heart rate. *Physica A*, 1995, **215**, 439–450.
23. Kantz, H. and Schreiber, T. *Nonlinear Time Series Analysis*. Cambridge University Press, 1997.
24. Säkki, M., Kalda, J., Vainu, M. and Laan, M. What does measure the scaling exponent of the correlation sum in the case of human heart rate? *Chaos*, 2004, **14**, 138–144.
25. Zebrowski, J. J., Poplawska, W., Baranowski, R. and Buchner, T. Symbolic dynamics and complexity in a physiological time series. *Chaos, Solitons, Fractals*, 2000, **11**, 1061–1075.
26. Peng, C. K., Mietus, J., Hausdorff, J. M., Havlin, S., Stanley, H. E. and Goldberger, A. L. Long-range anticorrelations and non-Gaussian behavior of the heartbeat. *Phys. Rev. Lett.*, 1993, **70**, 1343–1347.
27. Peng, C. K., Havlin, S., Stanley, H. E. and Goldberger, A. L. Quantification of scaling exponents and crossover phenomena in nonstationary heartbeat time series. *Chaos*, 1995, **5**, 82–87.
28. Ivanov, P. Ch., Rosenblum, M. G., Amaral, L. A. N., Struzik, Z., Havlin, S., Goldberger, A. L. and Stanley, H. E. Multifractality in human heartbeat dynamics. *Nature*, 1999, **399**, 461–465.
29. Amaral, L. A. N., Goldberger, A. L., Ivanov, P. Ch. and Stanley, H. E. Scale-independent measures and pathologic cardiac dynamics. *Phys. Rev. Lett.*, 1998, **81**, 2388–2391.
30. Thurner, S., Feurstein, M. C. and Teich, M. C. Multiresolution wavelet analysis of heartbeat intervals discriminates healthy patients from those with cardiac pathology. *Phys. Rev. Lett.*, 1998, **80**, 1544–1547.
31. Mandelbrot, B. B. and Van Ness, J. V. Fractional Brownian motion, fractional noises and applications. *SIAM Rev.*, 1968, **10**, 422–434.

32. Kobayashi, M. and Musha, T. $1/f$ fluctuation of heart beat period. *IEEE Trans. Biomed. Eng.*, 1982, **29**, 456–457.
33. Yamamoto, Y. and Hughson, R. L. Coarse-graining spectral analysis: new method for studying heart rate variability. *J. Appl. Physiol.*, 1991, **71**, 1143–1150.
34. Ashkenazy, Y., Lewkowicz, M., Levitan, J., Havlin, S., Saermark, K., Moelgaard, H. and Bloch Thomsen, P. E. Discrimination of the healthy and sick cardiac autonomic nervous system by a new wavelet analysis of heartbeat intervals. *Fractals*, 1999, **7**, 85–91.
35. Ashkenazy, Y., Lewkowicz, M., Levitan, J., Moelgaard, H., Bloch Thomsen, P. E. and Saermark, K. Discrimination of the healthy and sick cardiac autonomic nervous system by a new wavelet analysis of heartbeat intervals. *Fractals*, 1998, **6**, 197–203.
36. Mandelbrot, B. B. *The Fractal Geometry of Nature*. Freeman, San Francisco, 1983.
37. Saermark, K., Moellery, M., Hintzey, U., Moelgaardz, H., Bloch Thomsenx, P. E., Huikuri, H., Makikiallio, T., Levitan, J. and Lewkowicz, M. Comparison of recent methods of analyzing heart rate variability. *Fractals*, 2000, **8**, 315–322.
38. Lin, D. C. and Hughson, R. L. Modeling heart rate variability in healthy humans: a turbulence analogy. *Phys. Rev. Lett.*, 2001, **86**, 1650–1653.
39. Costa, M., Goldberger, A. L. and Peng, C.-K. Multiscale entropy analysis of complex physiologic time series. *Phys. Rev. Lett.*, 2002, **89**, 068102 (4 pages).
40. Kalda, J., Vainu, M. and Säkki, M. The methods of nonlinear dynamics in the analysis of heart rate variability for children. *Med. Biol. Eng. Comp.*, 1999, **37**, 69–72.
41. Kalda, J., Säkki, M., Vainu, M. and Laan, M. Zipf's law in human heartbeat dynamics. *e-print* http://arxiv.org/abs/physics/0110075, 2001 (4 pages).
42. Bernaola-Galván, P., Ivanov, P. Ch., Amaral, L. A. N. and Stanley, H. E. Scale invariance in the nonstationarity of human heart rate. *Phys. Rev. Lett.*, 2001, **87**, 168105 (4 pages).
43. Zipf, G. K. *Human Behavior and the Principle of Least Effort*. Addison-Wesley, Cambridge, 1949.
44. Schäfer, C., Rosenblum, M. G., Kurths, J. and Abel, H. H. Heartbeat synchronized with ventilation. *Nature*, 1998, **392**, 239–240.
45. Jaccard, J. and Wan, C. K. *LISREL Approaches to Interaction Effects in Multiple Regression*. Sage Publications, Thousand Oaks, CA, 1996.
46. Janson, N. B., Balanov, A. G., Anishchenko, V. S. and McClintock, P. V. E. Phase synchronization between several interacting processes from univariate data. *Phys. Rev. Lett.*, 2001, **86**, 1749–1752.
47. Struzik, Z. R. Revealing local variability properties of human heartbeat intervals with the local effective Hölder exponent. *Fractals*, 2001, **9**, 77–93.

# Mittelineaarne ja mastaabi-invariantne südamerütmi muutlikkuse analüüs

Jaan Kalda, Maksim Säkki, Meelis Vainu ja Mari Laan

Inimese südamerütm fluktueerub keerulisel ja mittestatsionaarsel moel. Efektiivsete ja seda tüüpi ajajadade jaoks adekvaatsete analüüsimeetodite väljatöötamine on viimaste aastakümnete jooksul olnud teadlastele tõsiseks väljakutseks. Käesolevas ülevaates käsitletakse selles valdkonnas saavutatud põhitulemusi. Pearõhk pannakse küsimustele, millised on südamerütmi ajajada olulisimad eriomased jooned ja millised on diagnostiliste ja prognostiliste rakenduste seisukohast kõige perspektiivikamad mittelineaarsed rütmimuutlikkuse mõõdud.

# THE DISTRIBUTION OF LOW-VARIABILITY PERIODS IN HUMAN HEARTBEAT DYNAMICS.

M. SÄKKI, J. KALDA, M. VAINU, M. LAAN
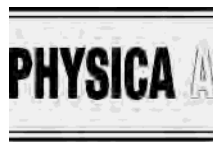
# The distribution of low-variability periods in human heartbeat dynamics

M. Säkki[a,*], J. Kalda[a], M. Vainu[b], M. Laan[c]

[a] Institute of Cybernetics, Tallinn Technical University, Tallinn, Estonia
[b] Tallinn Diagnostical Center, Tallinn, Estonia
[c] Tallinn Children's Hospital, Tallinn, Estonia

## Abstract

We study the long-term dynamics of the short-time variability level of human heart rate, an aspect which is not addressed by the traditional methods of non-linear time-series analysis. The length-distribution of low-variability periods in human heartbeat dynamics typically follows a multi-scaling power law. The values of the scaling exponents are personal characteristics and depend on the daily habits of the subjects. Though, the distribution function of the low-variability periods as a whole discriminates efficiently between several heart pathologies.
© 2004 Elsevier B.V. All rights reserved.

*PACS:* 87.10.+e; 05.45.Tp; 87.80.Tq

*Keywords:* Biological and medical physics; Time-series analysis; Biological signal processing and instrumentation

## 1. Introduction

Human heart rate fluctuates in a complex and non-stationary manner. This phenomenon can be related to the intermittent nature of human life, the events of which are reflected in the heart rate dynamics via competing (non-linearly interacting) neuroautonomic signals (parasympathetic signals decrease and sympathetic stimulations increase the heart rate). Heart pathologies may decrease the responsiveness of the heart and lead to an overall reduction of the heart rate variability (HRV). Understanding the diagnostic and prognostic significance of the various measures of HRV has a great importance

---

* Corresponding author. Fax: +372-6204251.
*E-mail address:* max@cens.ioc.ee (M. Säkki).

for the cardiological practice, because HRV measurements are low-cost and harmless for the patients, unlike the invasive methods of diagnostics.

As a result of intensive studies following the pioneering paper [1], various linear measures of HRV became widely used by practical medicine as important non-invasive diagnostic and prognostic tools. Meanwhile, recent studies have revealed the importance of non-linear and scale-invariant characteristics, and resulted in many methods of very high prognostic performance on test groups [2–7]. The scale-independent methods have been believed to be less subject-independent than the scale-specific measures [2]. It has been recognized that the heart rhythm reflects the activities of the subject (sleeping, watching TV, walking, etc.) [8,9]. The most adequate model of HRV dynamics has been believed to be multi-affine fractional Brownian motion (fBm) [2,3].

While the approach based on fBm addresses long-time dynamics of the heart rhythm, it neglects the short-scale dynamics on time scales less than one minute (these frequencies are typically filtered out [6]). The *short-time variability* has been described only by some linear measures, e.g. $p_{NN50}$ (the probability that two adjacent normal heart beat intervals differ more than 50 ms). Meanwhile, the level of short-time variability varies also in a complex manner (the high- and low-variability periods are deeply intertwined [8]) and therefore, cannot be appropriately described by linear measures. Switching between low and high levels of short-term variability is a physiologically important aspect, because typically, low levels are caused by the heart being in a stressed state. The scale-invariant aspects of such switching can be addressed by studying the length-distribution of the low-variability periods [10]. Here, we provide a brief description of this method and show that typically, the distribution of low-variability periods in the activity of a normal heart follows a power law. We also discuss fitting the distribution function by stretched exponentials and derive some diagnostically significant measures.

## 2. Experimental data

Our analysis is based on ambulatory Holter-monitoring data (recorded at Tallinn Diagnostic Centre) of 218 patients with various diagnoses, the main groups are shown in Table 1. The ECG-s were recorded at the sampling rate of 180 Hz during 24 h, under

Table 1
Test groups of patients

|  | Healthy | IHD | SND | VES | PCI | RR | FSK |
|---|---|---|---|---|---|---|---|
| Number of patients | 103 | 8 | 11 | 16 | 7 | 11 | 6 |
| Mean age | 45.5 | 65.4 | 50.0 | 55.9 | 47.3 | 55.5 | 11.7 |
| Standard deviation of age | 20.5 | 11.4 | 19.3 | 14.3 | 11.6 | 14.4 | 4.6 |

Abbreviations are as follows: IHD—Ischemic Heart Disease (Stenocardia); SND—Sinus Node Disease; VES—Ventricular Extrasystole; PCI—Post Cardiac Infarction; RR—Blood Pressure Disease; FSK—Functional Disease of Sinus Node.

normal daily activities of the patients. The commercial software (Rozinn) was used to calculate the sequence of the *normal-to-normal* (NN) intervals $t_{NN}$ (in milliseconds), which are defined as the intervals between two subsequent normal heartbeats (normal QRS complexes).

## 3. Intermittency of HRV and distribution of low-variability periods

It has been pointed out that the NN-sequences of healthy subjects consist of inter-twined high- and low-variability periods [8]. This conclusion can be easily verified by a simple visual observation of the sequences of NN-intervals, see Fig. 1. The duration $\tau$ of the low-variability periods varies in a wide range of scales, from few to several hundreds of heart beats. In order to analyse quantitatively this aspect of HRV, we have studied the distribution of low-variability periods. To begin with, we define the local variability for each ($i$th) interbeat interval as the deviation of the heart rate from the local average,

$$\delta(i) = \frac{|t_{NN}(i) - \langle t_{NN}(i) \rangle|}{\langle t_{NN}(i) \rangle} \ , \tag{1}$$

where $t_{NN}$ is the interval between two adjacent non-arrhythmic beats. The angular braces denote the local average, which is calculated using a narrow (5 beats wide) Gaussian weight function. Further, we introduce a threshold value $\delta_0$; $i$th interbeat interval is said to have a low variability, if the condition

$$\delta(i) \leqslant \delta_0 \tag{2}$$

is satisfied. A *low-variability period* is defined as a set of consecutive low-variability intervals; its length $\tau$ is measured in the number of heartbeats. Finally, all the low-variability periods are arranged according to their lengths and associated with ranks (the longest period obtains rank $r = 1$). The rank of a period is plotted versus its length in a logarithmic graph, see Fig. 2. For a very low threshold parameter $\delta_0$, all the low-variability periods are very short, because it is difficult to satisfy the stringent condition (2). Also, in that case, the inertial range of scales is too short for a meaningful
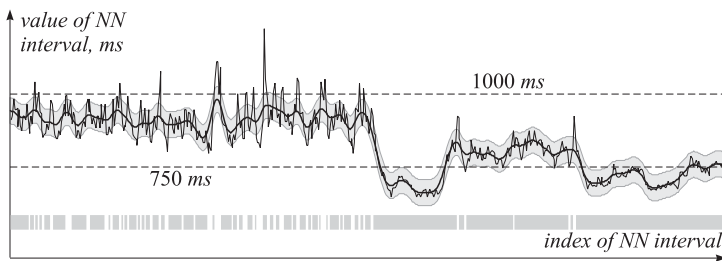


Fig. 1. Periods of low variability for 600 interbeat intervals (approx. 9 min of ECG recording) are shown below as gray thick lines ($\delta_0 = 0.03$). The longest period is measured to be 127 beats long, the shortest—1 beat.
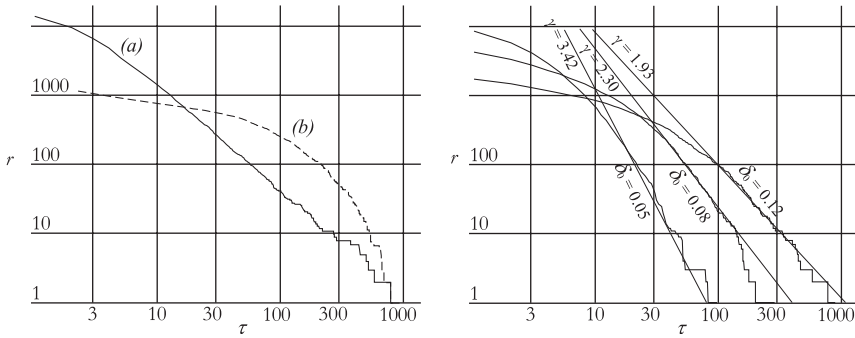
Fig. 2. *Left*: rank-length curves for a patient with a good power law (a) and for a patient with no power law (b). In both cases, the threshold parameter $\delta_0 = 0.05$. *Right*: multi-scaling distribution of the low-variability periods: the rank $r$ of a period is plotted versus its duration $\tau$ (measured in heartbeats) for different values of the threshold parameter $\delta_0$.

rank-length law. On the other hand, for a very high value of $\delta_0$, there is a single low-variability period occupying the entire HRV-recording. Between these two extreme cases, there is such a range of the values of $\delta_0$, which leads to a non-trivial rank-length law. Typically, the length-rank relationship reveals multiscaling properties, i.e. within a certain range of scales, the scaling law

$$r(\tau) \propto \tau^{-\gamma} \tag{3}$$

is observed, the scaling exponent $\gamma$ being a (non-constant) function of the threshold level, $\gamma = \gamma(\delta_0)$.

It is not surprising that the scaling behaviour is not perfect. Indeed, the heart rhythm is a non-stationary signal affected by the non-reproducible daily activities of the subjects. The non-stationary pattern of these activities, together with their time-scales, is directly reflected in the rank-length law. This distribution law can also have a fingerprint of the characteristic time-scale (10–20 s) of the blood pressure oscillations, which modulate the level of HRV, cf. [12]. It should be emphasized that the problem of the non-reproducible daily activities affects also the reliability of the other scale-invariant measures and is probably the main obstacle preventing the clinical application of the seemingly extremely efficient diagnostic and prognostic techniques.

It turned out that for a typical patient, the best approximation of the function $r(\tau)$ with a power law is achieved for $\delta_0 \approx 0.05$ (see Fig. 2a); in what follows, all further calculations were done for $\delta_0 = 0.05$. For some patients, the length-rank distribution is still far from a power law (Fig. 2b), and is better fitted by a stretched exponential $A e^{-a\tau^\alpha}$. However, power law turned out to be more typical. For our test groups, there was no significant correlation between the type of the law (power law, stretched exponential, or something intermediate), and the diagnosis. The parameters based on the stretched exponential $(a, \alpha)$ had a significantly lower diagnostic value than those discussed below.

First, we analysed the correlation between the diagnosis of a patient and the scaling exponent $\gamma$. This parameter has been calculated (see [10] for details) for the curves of

Table 2
*p*-values of the Student test

| p (%) | Healthy | IHD | SND | VES | PCI | RR | FSK | Healthy | IHD | SND | VES | PCI | RR | FSK |
|---|---|---|---|---|---|---|---|---|---|---|---|---|---|---|
| Healthy | B　　A | 0.06 | 17.21 | 0.02 | 0.07 | 1.59 | 1.55 | D　　C | 1.27 | 43.12 | 0.01 | 6.27 | 87.40 | 73.99 |
| IHD | 0.36 | | 2.85 | 96.79 | 97.62 | 21.93 | 20.05 | 4.82 | | 4.87 | 90.04 | 27.13 | 6.11 | 5.83 |
| SND | 2.99 | 59.10 | | 2.10 | 3.04 | 25.77 | 25.57 | 47.91 | 6.37 | | 3.81 | 12.31 | 55.50 | 63.46 |
| VES | 0.08 | 91.60 | 63.79 | | 94.18 | 17.59 | 16.20 | 0.34 | 81.67 | 6.02 | | 11.04 | 3.69 | 4.43 |
| PCI | 25.27 | 21.61 | 46.37 | 22.89 | | 22.50 | 20.62 | 38.38 | 18.24 | 27.25 | 12.40 | | 20.45 | 17.37 |
| RR | 0.14 | 73.57 | 77.69 | 80.49 | 28.90 | | 98.20 | 85.74 | 6.80 | 59.23 | 4.01 | 42.81 | | 88.81 |
| FSK | 46.48 | 5.20 | 8.72 | 5.52 | 20.06 | 6.45 | | 65.87 | 9.45 | 81.38 | 9.53 | 38.30 | 77.74 | |

Data in the triangular region A are calculated using the parameter $\ln \tau_{\text{end}}$. Triangular region B corresponds to the parameter $\ln r_{\text{max}}$, region C—to $\ln r_{100}$, and region D—to $\ln \tau_{40}$. Since multiple tests were carried out, modified Bonferroni correction [11] has been applied. In total, there are 84 *p*-values; therefore, the adjusted significance of the $n$th smallest *p*-value is obtained as $p' = 84 p/n$. Gray background highlights the tests with $p < 10\%$.

all the patients using a fixed threshold $\delta_0 = 0.05$; Student test was applied to every pair of groups. Typically, the significance was low; the best distinguishable groups were RR and FSK (with $p \approx 5.7\%$). One can argue that the slopes of linear parts are mostly personal characteristics depending on the daily habits of the subjects, and are weakly correlated with diagnosis.

Further we tested, how is the failure of the power law correlated with the diagnosis. The width of the scaling range $\Delta$ was used as a measure of how well the curve is corresponding to a power law. The Student test results for the parameter $\Delta$ turned out to be similar to what has been observed for the parameter $\gamma$: the correlation between the failure of the power law and diagnosis was weak. Thus, a rank-length curve resembling the one depicted by a dashed line in Fig. 2, does not hint to heart pathology. It should be also noted that the dashed curve in Fig. 2 can be considered as a *generalized form of scale-invariance* with scale-dependent differential scaling exponent.

Finally, we analysed the diagnostic significance of start- ($\ln \tau_{\text{start}}$) and end-points ($\ln \tau_{\text{end}}$) of the scaling range (see Ref. [10] for details). Note that the scaling range edge-points can be expected to correspond to certain physiologically relevant time-scales. The parameter $\ln \tau_{\text{end}}$ provided, indeed, a remarkable resolution between the groups of patients, see Table 2. According to the Student test, the healthy patients, were distinct from five heart pathology groups with probability $p < 1.6\%$. The diagnostical information contained in $r(\tau)$-law turned out to be not limited by $\ln \tau_{\text{end}}$: the overall number of low-variability periods $r_{\text{max}}$ (which is small, if there are lot of long low-variability periods) and the coordinates of specific points of the $r(\tau)$-curve (such as the length $\tau_R$ of the period with a fixed rank $R$, e.g. $\tau_{40}$, and the rank $r_T$ of a period with a fixed length $T$) were also of high diagnostic performance, see Table 2.

## 4. Conclusion

In conclusion, new aspect of non-linear time-series has been discovered, the scale-invariance of low-variability periods. We have shown that the distribution of low variability periods in the activity of human heart rate typically follows a *multi-scaling*

*power law*. The presence or failure of a power law, as well as the values of the scaling exponents, are personal characteristics depending on the daily habits of the subjects. Meanwhile, the distribution function of the low-variability periods as a whole contains a significant amount of diagnostically valuable information These quantities characterize the complex structure of human HRV signal, where the short-time variability level fluctuates intermittently, an aspect which is not addressed by the other methods of heart rate variability analysis (such as fractional Brownian motion based multifractal analysis). The support of Estonian SF Grant No. 5036 is acknowledged.

## References

[1] E.H. Hon, S.T. Lee, Am. J. Obstet. Gynec. 87 (1965) 814.
[2] L.A.N. Amaral, et al., Phys. Rev. Lett. 81 (1998) 2388.
[3] P.Ch. Ivanov, et al., Nature 399 (1999) 461.
[4] S. Thurner, M.C. Feurstein, M.C. Teich, Phys. Rev. Lett. 70 (1998) 1544.
[5] K. Saermark, et al., Fractals 8 (2000) 315.
[6] C.K. Peng, et al., Phys. Rev. Lett. 70 (1993) 1343.
[7] C.K. Peng, et al., Chaos 5 (1) (1995) 82.
[8] C.S. Poon, C.K. Merrill, Nature 389 (1997) 492.
[9] Z.R. Struzik, Fractals 9 (2001) 77.
[10] J. Kalda, M. Säkki, M. Vainu, M. Laan, preprint physics/0110075 (2001).
[11] J. Jaccard, C.K. Wan, LISREL Approaches to Interaction Effects in Multiple Regression, Sage Publications, Thousand Oaks, CA, 1996.
[12] C. Schäfer, M.G. Rosenblum, J. Kurths, H.H. Abel, Nature 392 (1998) 239.

# Non-linear analysis of the electroencephalogram for detecting effects of low-level electromagnetic fields.

M. Bachmann, J. Kalda, J. Lass,
V. Tuulik, M. Säkki, H. Hinrikus

# Non-linear analysis of the electro-encephalogram for detecting effects of low-level electromagnetic fields

M. Bachmann[1]    J. Kalda[2]    J. Lass[1]    V. Tuulik[1]
M. Säkki[2]    H. Hinrikus[1]

[1]Biomedical Engineering Centre, Tallinn University of Technology, Estonia
[2]Institute of Cybernetics, Tallinn University of Technology, Estonia

**Abstract**—*The study compared traditional spectral analysis and a new scale-invariant method, the analysis of the length distribution of low-variability periods (LDLVPs), to distinguish between electro-encephalogram (EEG) signals with and without a weak stressor, a low-level modulated microwave field. During the experiment, 23 healthy volunteers were exposed to a microwave (450 MHz) of 7 Hz frequency on-off modulation. The field power density at the scalp was 0.16 mW cm$^{-2}$. The experimental protocol consisted of ten cycles of repetitive microwave exposure. Signals from frontal EEG channels FP1 and FP2 were analysed. Smooth power spectrum and length distribution curves of low-variability periods, as well as probability distribution close to normal, confirmed that stationarity of the EEG signal during recordings was achieved. The quantitative measure of LDLVPs provided a significant detection of the effect of the stressor for the six subjects exposed to the microwave field but for none of the sham recordings. The spectral analysis revealed a significant result for one subject only. A significant effect of the exposure to the EEG signal was detected in 25% of subjects, with microwave exposure increasing EEG variability. The effect was not detectable by power spectral measures.*

**Keywords**—*Scaling analysis, Spectral analysis, Distribution, Stationarity, EMF effects, Microwave*

## 1 Introduction

MODERN TECHNOLOGY generates electromagnetic fields (EMFs) much stronger than the fields created by natural sources. Electromagnetic fields of various devices can affect humans, especially their central nervous system, the most sensitive organ with respect to such external stimuli. However, except for extreme non-healthy environments, the effect of EMFs is too weak to result in easily detectable changes in the intrinsically very non-stationary bio-electrical activity of the human brain.

Quantitative analysis of changes in the electro-encephalogram (EEG) dynamics is complicated owing to the irregular nature of the signal. Traditionally, EEG is treated as a realisation of a linear stochastic process, and numerous applications in the clinical field are based on this idea. In general, these mainly involve different methods based on the spectral analysis of EEG.

The four terms, delta, theta, alpha and beta, have corresponded to the medical standard of classifying EEG frequency bands for several decades (NIEDERMEYER and LOPES DA SILVA,

1993). Different methods and parameters, such as the weighted spectral intensity of the EEG beta, alpha, theta and delta rhythms, bispectral index, burst-suppression ratio and others, have been successfully realised in EEG monitors, with applications in clinical work. During recent years, the methods based on non-linear dynamics have become popular in EEG analysis. These studies require the assumption of the stochastic nature of EEG signals. Indeed, in the case of Gaussian stochastic signals, non-linear measures cannot reveal any new information (compared with linear measures).

Achievements in EEG analysis have made it possible to distinguish between states of the brain disturbed owing to a strong stressor. Various methods can be used to evaluate the depth of anaesthesia (WIDMAN *et al.*, 2000), to detect physiological disorders in the brain in epilepsy (ELGER and LENHERZ, 1997; MCSHARRY *et al.*, 2003; ROSSO *et al.*, 2004; LOPES DA SILVA *et al.*, 2003; VAN DRONGELEN *et al.*, 2003), to distinguish between sleep stages (considered as different psychophysiological states) (HUUPPONEN *et al.*, 2003; PEREDA *et al.*, 1998; SINHA, 2004, SHEN *et al.*, 2003) etc. In many cases, the analysis and prediction of epileptic seizures by non-linear methods have proved useful. For example, LOPES DA SILVA *et al.* (2003) proposed that the neuronal networks involved in epilepsy possess multistable dynamics that can be characterised in phase-space with different attractors. It has also been demonstrated that entropy measures and correlation dimensions are useful for anticipating seizures

(VAN DRONGELEN et al., 2003; ELGER and LENHERZ, 1997). Sleep analysis has been believed to be one of the best prospective uses of non-linear EEG analysis (SHEN et al., 2003; PEREDA et al., 1998).

The influence of a weak stressor, such as a mental task or low-level non-ionising radiation, on EEG activity is usually very small, and linear statistical analysis is unable to provide a reliable, statistically significant distinction between the EEG signals with and without the stressor (KRAUSE et al., 2000; LASS et al., 2002, WOOD et al., 2003). Therefore the question of whether a feasible effect, if any, of low-level radiation on the brain's bio-electric activity exists is still open.

Non-linear methods of EEG analysis can be expected to be more sensitive with respect to small changes in the signals. Indeed, bio-electric signals are generated by simultaneous activity of multiple sources modulated by different physiological factors, which are intermittent by their nature. Therefore EEG can also be expected to be non-Gaussian and intermittent. Such intermittency can severely lower the stationarity of linear measures; various non-linear measures have been devised to cope with intermittency and non-stationarity in the best possible way.

In this study, we propose a new method for EEG analysis: scaling analysis of the length distribution of low-variability periods (LDLVPs). Measures based on the scaling of LDLVPs have proved sensitive tools for the non-linear interpretation of heart rate variability (KALDA et al., 2001; SÄKKI et al., 2004a). The LDLVP analysis provides a simple route to detecting the multifractal characteristics of a time series and yields somewhat better temporal resolution than traditional multifractal analysis. Thus it can be expected that this method is sensitive with respect to small, 'hidden' changes in such a complicated physiological signal as the EEG. We chose spectral analysis, a widely used method in quantitative EEG analysis, for purposes of comparison.

The aim of this study was to compare the sensibility of non-linear analysis of LDLVPs and linear spectral analysis to detect EEG signals with and without the influence of a low-level modulated microwave field. The hypothesis was that microwave exposure increases the variability of the EEG signal and causes a decrease in the length of low-variability periods as well as changes in the power spectrum.

# 2 Method and equipment

## 2.1 Subjects

An experimental study was carried out on a group of volunteers. The group consisted of 23 young persons (aged 21–24): 12 male and 11 female. Their physical and mental condition (tiredness, sleepiness) before the experiment was evaluated by a questionnaire and a clinical interview. All the subjects selected were healthy, without any medical or psychiatric disorders; tired or sleepy people were excluded. After the recordings, they described how they felt during the experiment. The subjects reported neither alertness nor any strain experienced during the recordings.

The measurements were performed in a dark laboratory, but no other special conditions were provided. The subjects lay in a relaxed position, with eyes closed and ears blocked during the experiments.

All the subjects were exposed and sham-exposed. Only one experimental EEG recording was performed for a subject during a day. The measurements were double blinded. During each test session, the exposed and sham-exposed subjects were randomly assigned. The subjects were not informed of their exposure; however, they were aware of the possibility of being exposed. Subjective factors were also excluded from

the computer-performed data analysis: the same algorithms were applied for all the recordings (both for exposed and sham-exposed subjects).

The experiments were conducted with the understanding and written consent of each subject.

## 2.2 Microwave exposure

We used modulated microwave radiation at a non-thermal level of field power density, identical to our previous studies (LASS et al., 2002; PARTS et al., 2003). Microwave exposure conditions were the same for all subjects.

The 450 MHz microwave radiation was generated by a signal generator*. The RF signal was 100% amplitude modulated by a pulse modulator[†] at 7 Hz frequency (duty cycle 50%). The generator signal was amplified by a power amplifier[‡]. Located in the laboratory, the generator and amplifier were carefully shielded. The 1 W EMF output power was guided by a coaxial lead to a 13 cm quarter-rhythm antenna**, located 10 cm from the subject's skin on the left side of the head.

The calculation of the specific absorption rate (SAR) inside the brain was based on the known field power density on skin. The Central Physical Laboratory of the Estonian Health Protection Inspection measured the spatial distribution of the microwave power density with a field strength meter.[††] The calibration curves of the field power density dependence on the distance from the radiating antenna were obtained from these measurements taken in the actual conditions of the experiment. During the experiments, the stability of the microwave level was monitored by another field strength meter.[‡‡]

Estimated from the measured calibration curves, the field power density at the skin was 0.16 mW cm$^{-2}$. The SAR, calculated by the formula SAR $= \sigma E^2/2\rho$ for brain conductivity at 450 MHz, $\sigma = 1.18$ S m$^{-1}$ and density $\rho = 1000$ kg m$^{-3}$, was 0.35 W kg$^{-1}$. The level of power density, as well as the calculated SAR, was so low that thermal effects were extremely unlikely.

## 2.3 Recording protocols and equipment

The study consisted of two experimental protocols, identical for all subjects. The first protocol was recorded as described below.

First, the reference EEG was recorded over 60 s.

Secondly, modulated microwave radiation was applied. The duration of the exposure was 60 s, and the compensatory pause after the exposure was 60 s. Continuous EEG recordings were made during and 60 s after exposure. The procedure of the cycle was repeated ten times. The microwave exposure was switched on every first 60 s of the cycle. During ten cycles of microwave exposure, the modulation frequency always remained at 7 Hz.

The recording protocol for one subject lasted for 21 min, during which the EEG was continuously recorded.

The second protocol for the sham-exposure included the same steps, except that the microwave generator was switched off.

EEG measurement equipment*** was used for the EEG recordings. The EEG was recorded by means of nine electrodes, placed on the subject's head according to the international 10–20 electrode position classification system. The following channels

---

*Model SML02, Rhode & Swartz, Germany
[†]Model SML-B3, Rhode & Swartz, Germany
[‡]Model MSD-2597601, Dage Corporation, USA
**NMT450 RA3206, Augon Mobile Communication AB, Sweden
[††]Fieldmeter C.A 43 Chauvin Arnoux, France
[‡‡]Digi Field C, IC Engineering, USA
***Easy II EEG, Cadwell, USA

were chosen: frontal: FP1, FP2; temporal: T3, T4; parietal: P3, P4; occipital: O1, O2; and the reference electrode Cz. The EEG recordings were stored on a computer at a sampling frequency of 400 Hz. The recorded EEG signals were examined by an experienced neurologist. Artifacts were detected by visual inspection. The recordings containing multiple artifacts were removed, and the whole recording was repeated.

The pre-processing of the signals was performed in the LabVIEW programming and signal-processing environment. The EEG spectrum of 0.5–48 Hz was selected for the analysis. The modulating frequency belonged to the same region (7 Hz); therefore it was removed by a narrow-band (0.2 Hz) filter. The results of the preceding validation of the set-up confirmed the absence of other low-frequency modulation components, caused by parasitic interference between EEG and radio-frequency equipment.

### 2.4 Selection of signals

Our previous results demonstrated that the effect of microwave radiation is more noticeable in frontal EEG channels (HINRIKUS et al., 2004). Therefore recordings from channels FP1 and FP2 were selected for further analysis.

Initially, all the EEG recordings were divided into two subsignals. The recordings performed with the first recording protocol were divided as follows:

- the first subsignal contained all 1 min periods without microwave exposure (all the odd minutes from the initial EEG recording)
- the second subsignal contained all minutes with microwave exposure (all even minutes of the initial EEG recording).

The recordings performed with the second recording protocol were divided similarly:

- the first sham subsignal contained all the odd minutes
- the second sham subsignal contained all the even minutes of the initial recording.

### 2.5 Scaling analysis of the EEG signal based on the LDLVP method

When selecting a method for the EEG analysis, we should take into account the features of the EEG signal. Linearity and stochasticity are, in fact, very restricting assumptions that are, typically, not satisfied for natural time-series (such as ECG, rainfall time-series, financial time-series etc.). This was realised over a decade ago (KANTZ and SCHREIBER, 1997). Accordingly, a wide variety of non-linear and scale-invariant tools of analysis have been elaborated, as a rule, taking into account the heart rate variability data (BABLOYANTZ and DESTEXHE, 1988; PENG et al., 1993; IVANOV et al., 1999; COSTA et al., 2002); for a review, see KALDA et al. (2004).

Some authors have reported that EEG rhythms reflect the existence of a chaotic dynamics of sources, at least for a specific range of parameters of thalamo-cortical neurons (RÖSCHKE et al., 1997; THEILER and RAPP, 1996; WANG, 1994). Other authors have not obtained evidence that would allow for the conclusion that EEG rhythms, in general, reflect the existence of chaotic dynamics. EEG rhythms are most likely to arise in neuronal networks that work as complex filters of random sources (LOPES DA SILVA et al., 1974; 1997).

Although the problem of the presence of deterministic chaos caused by the formation of EEG signals certainly deserves comprehensive studies, the measures to be adopted on the

---

*Cadwell Easy II

bases of (reconstructed) phase-space dynamics are still premature. Indeed, even assuming that deterministic dynamics participates in the bio-electrical activity of the brain, meaningful calculation of measure, such as the correlation dimension and Lyapunov exponents, requires noiseless long signals (KANTZ and SCHREIBER, 1997), a requirement directly contradicting the above-mentioned assumption of stochasticity.

This conclusion is in agreement with observations concerning heart rate variability: the heart rhythm of patients with severe heart failure may show fingerprints of deterministic dynamics (BABLOYANTZ and DESTEXHE, 1988). However, for a more or less, healthy heart, this dynamics is suppressed by intermittent, non-deterministic inputs (SÄKKI et al., 2004b). Thus, taking into account that EEG signals are much more complicated than ECG signals, we can presume that, on time-scales longer than a few periods of the gamma rhythm, EEG signals also behave in an efficiently non-deterministic and intermittent manner.

Unlike the measurements based on the analysis of time-delay space, the LDLVP method does not assume any deterministic dynamics and is suited to characterise the (supposedly) intermittent pattern of EEG fluctuations. This method has common roots with multifractal analysis (IVANOV et al., 1999). However, multifractal analysis assumes the presence of scale-invariance throughout the analysed time-scales. For that reason, multifractal analysis is not used for heart rate variability in the shortest time-scales (where the fingerprints of respiration and blood pressure oscillations are evident). For the same reason, multifractal analysis is not suited for EEG analysis at time-scales comparable with the periods of the known physiological frequency bands.

The LDLVP analysis consists of several steps.

First, we define the local variability as the deviation of the current value of the signal from the local average

$$\delta V(t) = V(t) - T^{-1} \int_{-T/2}^{T/2} V(t + \tau) \, d\tau \tag{1}$$

where $V(t)$ is the recorded voltage, and the time-window width $T$ is a free (adjustable) parameter. The particular choice of this parameter is guided by the following considerations. First, it should not be smaller than the dominant time-scale of high-frequency variations. Secondly, it should not be too large, because, otherwise, the scaling range of LDLVP would be too narrow (because $T$ also plays the role of the lower cutoff scale of LDLVP). To achieve the widest possible scaling range, we opted for the smallest sensible value $T = 60$ ms (which is of the order of the reciprocal of the EEG alpha-rhythm frequency). Here, it should be noted that the microwave radiation (modulated at 7 Hz frequency) has been found to have the most pronounced effect on the EEG energy spectrum at the frequencies of the alpha rhythm (HINRIKUS et al., 2004).

Secondly, low-variability periods are defined as continuous intervals with

$$\delta V(t) < \delta_0 \tag{2}$$

Finally, the number of low-variability periods $N$ exceeding length $T_0$ is plotted against length $T_0$.

The character of this length distribution depends qualitatively on the threshold parameter $\delta_0$: if $\delta_0$ is very small, all the low-variability periods are very short; if $\delta_0$ is very large, there is a single low-variability period occupying the whole recording. For intermediate values of $\delta_0$, the non-trivial scale-invariant distribution law is observed (KALDA et al., 2001; SÄKKI et al., 2004a). In this study, the value of

$\delta_0$ was adjusted for each recording individually, reaching a minimum value so that, for both subsignals, the length of the longest low-variability period was at least 3750 ms.

The hypothesis of this work was that microwave exposure increases EEG variability. Owing to higher variability, there are fewer long low-variability periods. Therefore it is expected that microwave exposure lowers the curve in the right-hand part of the graph (i.e. at large values of $T_0$). According to this assumption, the weighted area

$$S_W = \sum_{N=1}^{128} \ln\left(\frac{N}{\max(N-1, 1/4)}\right) \ln(T_0) N^{1/2} \qquad (3)$$

under the curve of the function $T_0 = T_0(N)$ was selected as the non-linear quantitative measure.

In the denominator of this formula, $N - 1$ is substituted by max $(N - 1, 1/4)$ for a simple reason: to take into account the longest low-variability period (with $N = 1$) without divergence of the expression. The weighting factor $N^{1/2}$ was introduced to enhance the stationarity of the measure. In other words, the least stationary part of the $T_0(N)$-curve is the region $N \approx 1$, because the relative statistical uncertainty of $N$ at a given $T_0$ is inversely proportional to the square root of the number of underlying data points $N^{-1/2}$. The overall variance is minimised when each term of the sum has a weight equal to the reciprocal of its uncertainty.

### 2.6 Linear quantitative measure

The power spectral density (PSD) was estimated by means of Welch's averaged periodogram method. The subsignals were divided into overlapping sections (50%), with a length of 2048 points, and windowed by a Hanning window.

Afterwards, the power on the theta-alpha-beta band (4–40 Hz) $W_{mn}$ was computed for each subject (indexed by $n \in [1, 23]$) and subsignal (indexed by $m = 1, 2$) as the area under the spectrum for the corresponding frequency band (integral of the band).

To locate the possible influences of microwave exposure, the powers computed from the first subsignals were subtracted from the powers computed from the second subsignals. The channel FP1 or FP2 with a smaller power difference was chosen for further analysis.

The same procedure was repeated with sham subsignals, resulting in spectral powers $\tilde{W}_{mn}$.

### 2.7 Statistical analysis

For sham recordings, the subsignals were completely equivalent. The mathematical expectation of the difference in their spectral powers was zero, $\langle \tilde{W}_0 - \tilde{W}_1 \rangle = 0$. Next, an estimate of the variance could be obtained as the mean of squared differences

$$\sigma^2 = \frac{1}{23} \sum_{n=1}^{23} (\tilde{W}_{0n} - \tilde{W}_{1n})^2 \qquad (4)$$

According to the 'zero hypothesis', the EEG recordings of subjects under microwave exposure cannot be distinguished from sham signals. Thus, the zero hypothesis implies that $\langle W_0 - W_1 \rangle = 0$ and $\langle (W_0 - W_1)^2 \rangle = \langle (\tilde{W}_0 - \tilde{W}_1)^2 \rangle$. Consequently, if the zero hypothesis is true, the quantity $x = (W_{0n} - W_{1n})^2 \sigma^{-2}$ is an $f$-distributed random quantity, the cumulative distribution of which is routinely designated as $F_{1,23}(x)$; the indices 1 and 23 stand for the numbers of degrees of freedom.

Accordingly, the ratio of the computed power difference to the standard deviation of the differences can be used as a quantitative measure, showing how well the zero hypothesis is satisfied; respective $p$-values are obtained by means of the cumulative $f$-distribution

$$p = F_{1,23}\lfloor (W_{0n} - W_{1n})^2 \sigma^{-2} \rfloor \qquad (5)$$

The same technique has been applied to the non-linear quantitative measure (derived from LDLVP), resulting in another series of $p$-values.

## 3 Results

As an example, the calculated PSD distribution of the first and second subsignals for exposed and sham recordings for one subject is shown in Fig. 1. For the same subsignals, the number of low-variability periods $N$ exceeding length $T_0$ is plotted against length $T_0$ in Fig. 2.
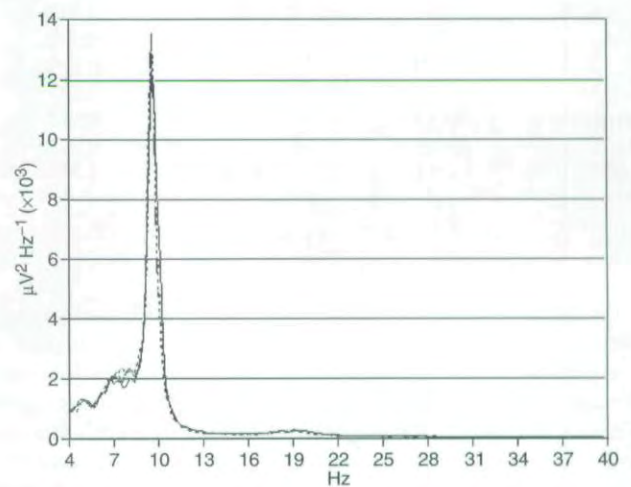


**Fig. 1** *Power spectral density for typical subject: (—) second subsignal of exposed recording (intervals with microwave); (–·–·) first subsignal of exposed recording (intervals without microwave); (– – –) first and second subsignals for sham recordings*
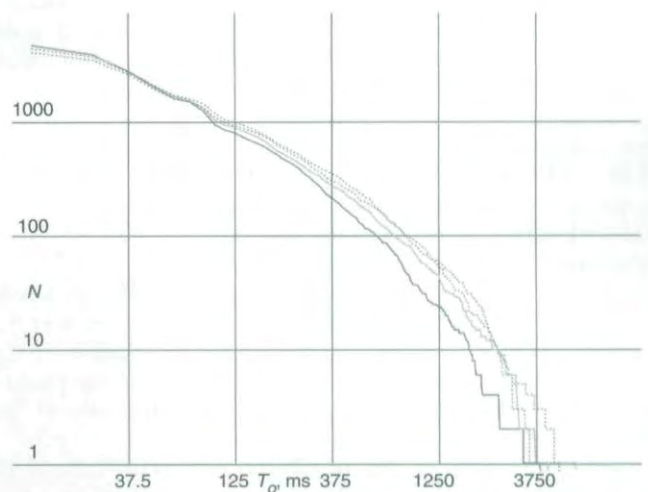


**Fig. 2** *Number of low-variability periods N exceeding length $T_0$ for typical subject: (—) second subsignal of exposed recording (intervals with microwave); (–·–·) first subsignal of exposed recording (intervals without microwave); (– – –) first and second subsignals for sham recordings*

*Table 1   PSD and LDLVP quantitative measures for microwave-exposed and sham recordings for each subject*

| Microwave exposure | | | | Sham | | | |
| PSD | | LDLVP | | PSD | | LDLVP | |
| $\sqrt{x}$ | $p$ | $\sqrt{x}$ | $p$ | $\sqrt{x}$ | $p$ | $\sqrt{x}$ | $p$ |
|---|---|---|---|---|---|---|---|
| **3.73** | **0.001** | **− 8.24** | **$2.58 \times 10^{-8}$** | 2.04 | 0.053 | − 1.97 | 0.061 |
| 0.44 | 0.663 | **− 7.84** | **$6.05 \times 10^{-8}$** | 0.33 | 0.742 | − 1.59 | 0.125 |
| 0.08 | 0.939 | **− 7.18** | **$2.58 \times 10^{-7}$** | 1.67 | 0.109 | − 1.59 | 0.125 |
| −0.30 | 0.768 | **− 4.32** | **$2.55 \times 10^{-4}$** | −0.40 | 0.694 | − 1.45 | 0.160 |
| 1.03 | 0.313 | **− 4.28** | **$2.81 \times 10^{-4}$** | 0.24 | 0.815 | − 1.25 | 0.223 |
| 0.89 | 0.385 | − 2.73 | 0.012 | −0.11 | 0.915 | − 0.70 | 0.493 |
| 0.02 | 0.981 | − 1.65 | 0.112 | **3.18** | **0.004** | − 0.62 | 0.543 |
| 0.04 | 0.969 | − 1.59 | 0.125 | −0.35 | 0.732 | − 0.40 | 0.694 |
| −0.06 | 0.950 | − 1.57 | 0.130 | −0.08 | 0.935 | − 0.39 | 0.704 |
| 2.53 | 0.019 | − 1.51 | 0.144 | −0.91 | 0.374 | − 0.36 | 0.723 |
| 0.36 | 0.719 | − 0.90 | 0.380 | −0.18 | 0.860 | − 0.32 | 0.753 |
| −0.27 | 0.788 | − 0.62 | 0.543 | −0.05 | 0.961 | − 0.12 | 0.906 |
| 0.65 | 0.521 | − 0.24 | 0.813 | −0.52 | 0.610 | 0.00 | 1.000 |
| −0.05 | 0.960 | 0.00 | 1.000 | 0.70 | 0.492 | 0.06 | 0.953 |
| −0.20 | 0.840 | 0.14 | 0.890 | −0.01 | 0.995 | 0.46 | 0.651 |
| 0.02 | 0.987 | 0.24 | 0.813 | −0.20 | 0.841 | 0.46 | 0.651 |
| 0.04 | 0.967 | 0.62 | 0.543 | −1.58 | 0.128 | 0.56 | 0.583 |
| 0.94 | 0.359 | 0.92 | 0.370 | 0.12 | 0.903 | 0.62 | 0.543 |
| 0.97 | 0.340 | 1.30 | 0.208 | −0.31 | 0.758 | 0.74 | 0.469 |
| −0.29 | 0.774 | 1.21 | 0.237 | −0.10 | 0.918 | 0.94 | 0.359 |
| −0.48 | 0.635 | 1.39 | 0.177 | −0.49 | 0.630 | 1.14 | 0.267 |
| −0.13 | 0.896 | 1.87 | 0.074 | −0.48 | 0.635 | 1.43 | 0.165 |
| −2.75 | 0.011 | **4.58** | **$1.34 \times 10^{-4}$** | 0.02 | 0.987 | 1.81 | 0.083 |

Visual inspection of the PSD distribution of EEG subsignals, with and without microwave exposure, in Fig. 1 indicated no considerable difference between the subsignals. The difference became evident in Fig. 2: three curves of EEG subsignals (without microwave exposure) were close to each other, but the lowering of one of the curves (subsignal with microwave exposure) was obvious in the right-hand part of the graph (i.e. at large values of $T_0$).

The PSD and LDLVP quantitative measures of the first and second subsignals for microwave-exposed and sham recordings, calculated for each subject, are presented in Table 1. The ratio of the computed power difference to the standard deviation of the differences $\sqrt{x}$ of more than three, and $p$ values not larger than 0.001 were considered as significant deviations from the zero hypothesis and are marked bold. Note that these results remain significant even after application of the modified Bonferroni correction, according to which the smallest $p$-value is to be multiplied by the number of data points 23, the second smallest is to be multiplied by $23/2 = 11.5$ etc.

As can be seen, the PSD measures for exposed, as well as for sham recordings, resulted in the ratio of the computed power difference to the standard deviation of the differences (calculated on the basis of sham signals) exceeding a value of 3 only for one subject. LDLVP measures resulted in the ratio of the computed power difference to the standard deviation of the differences being higher than 3 for six subjects in the case of microwave exposure and for no subjects in the case of sham recordings.

Histograms of the number of subjects against the ratio of the computed spectral power difference to the standard deviation of the differences are shown in Fig. 3, both for recordings with microwave exposure and sham recordings. Histograms of the number of subjects against the ratio of the computed LDLVP weighted area difference to the standard deviation of these differences are shown in Fig. 4.
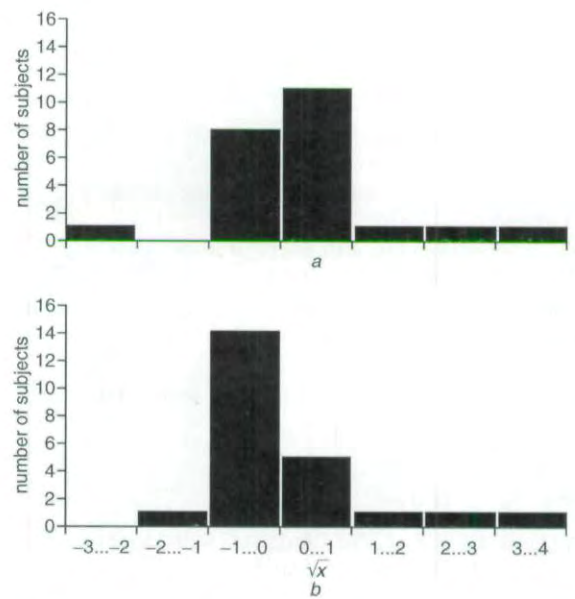


**Fig. 3** *Distribution of subjects according to ratio of computed spectral power difference to standard deviation of differences $\sqrt{x}$ for (a) recordings with microwave exposure and (b) sham recordings*

## 4 Discussion

### 4.1 Quality of EEG recordings

The EEG signals observed are highly variable and non-stationary during short-term recordings. Non-stationarity can be either fundamental (regardless of the observation period, no stationarity can be observed) or conditional (signals become stationary during sufficiently long-term recordings). Dominating sources of non-stationarity for EEG signals are
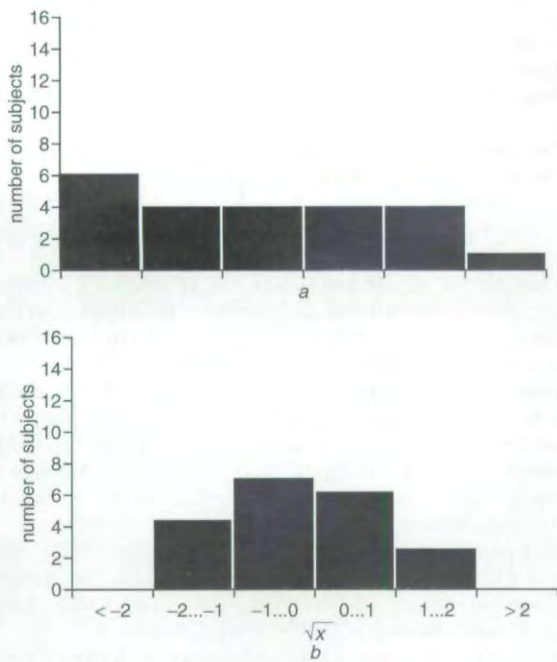
**Fig. 4** *Distribution of subjects according to ratio of computed LDLVP weighted area difference to standard deviation of differences $\sqrt{x}$ for (a) recordings with microwave exposure and (b) sham recordings*

external stimuli, which themselves arrive intermittently. To achieve stationarity of the EEG signal during the recording period (in the absence of the studied stressor, the low-level modulated microwave field), all external stimuli were minimised (eyes closed, ears blocked, etc.) during the experiments. The fact that, in the cases of sham exposure, the probability distribution in the histograms for differences (Figs 3 and 4) is close to normal supports the idea that EEG signals are stationary if external stimuli (microwave exposure) do not affect them.

The results of EEG recordings presented in Figs 1 and 2 demonstrated a smooth power spectrum and smooth length distribution curves of low-variability periods. Stationarity is not achievable for EEG analysis at time scales comparable with the periods of the known physiological frequency bands. Smooth curves confirm that the selected length of the recording was sufficient, and stationarity of the EEG signal during the recordings was achieved.

The probability distribution of differences in the case of sham exposure is symmetrical and close to normal (Figs 3*b* and 4*b*). This fact supports the idea of the random nature of EEG rhythms (the presence of one subject with $p \approx 0.004$ may, but not necessarily, refer to slight non-Gaussianity: after the Bonferroni correction, this value translates into $23 \times 0.004 \approx 0.09$). This finding is in good agreement with the conclusion in the theoretical work by LOPES DA SILVA *et al.* (1974; 1997), reporting that EEG rhythms, in general, are stochastic rather than reflect the existence of chaotic dynamics. This fact also shows that the recording was of sufficient length, and recording conditions guaranteed the stationarity of EEG signals.

### 4.2 Distinction of stressor effect

The character of the probability distribution is substantially different in the case of microwave-exposed EEG recordings: the histogram in Fig. 4*a* corresponds to a constant rather than to a normal distribution. This trend of change in the probability distribution is not noticeable in Fig. 3*a*. A comparison of the

histograms shows that the LDLVP enables us to determine the effect of microwave exposure, whereas the PSD does not.

The probability distribution in Fig. 4 demonstrates changes in the nature of the EEG rhythm compared with the sham recordings: the evidence of the microwave effect as an external stimulus leads to different distributions of the proposed measures. The existence of different dynamics in the case of a specific stressor may not be surprising in view of the model studies by WANG (1994), who demonstrated the existence of chaotic dynamics only for a specific range of parameters of neurons.

Differences in the subsignals with and without microwave exposure are also confirmed by Fig. 2, where the distribution of the number of low-variability periods $N$, exceeding length $T_0$, is plotted against length $T_0$. The effect of the lowering of one curve (subsignals with microwave exposure), compared with three other curves (subsignals without exposure), is obvious in the area of large $T_0$ values. It means that microwave exposure increases short-term variability: high-variability episodes are met more often, so that long, low-variability periods are broken into smaller parts.

Visual inspection of the PSD distribution of EEG subsignals with and without microwave exposure indicated no considerable difference between subsignals (Fig. 1), thus indicating no influence of microwave exposure.

Differences in the ability of the PSD and LDLVP methods to detect the effect of microwave exposure are most evident when we compare the quantitative measures calculated according to these methods (see Table 1).

As can be seen, the PSD measures provide only one result in both groups (exposed and sham), exceeding the limit of significant deviation from the zero hypothesis. Those results can be explained by statistical variability.

However, LDLVP measures resulted in significant results for six subjects in the case of microwave exposure and for none of the subjects in the case of sham recordings (Table 1). For five subjects under exposure, the computed LDLVP weighted area decreased and it increased for only one subject. Such a decrease in the number of low-variability periods allows us to conclude that, typically, microwave exposure causes an increase in EEG variability.

Previously, several linear and non-linear methods were applied by our group to detect possible changes in EEG signals, using the same exposure conditions and an experimental protocol similar to that of this study, except for the use of photic stimulation (HINRIKUS *et al.*, 2004; PARTS *et al.*, 2003). In particular, linear statistical analysis has been applied to relative changes in EEG rhythms energy of the cycles with and without low-level modulated microwave exposure. These results demonstrated changes in the EEG theta and alpha rhythm activity, induced by microwave exposure, in different EEG channels that were observable during different cycles of exposure. However, these findings were not statistically significant (HINRIKUS *et al.*, 2004).

In addition, bispectral analysis has been applied to evaluate the effects of photic and microwave exposure on human EEG. The analysis demonstrated clear differences between EEG signals with and without photic exposure. However, the effect of microwave exposure was not detected (PARTS *et al.*, 2003).

Another research group used Higuchi's fractal dimension analysis on the same signals (LIPPING *et al.*, 2003). Their results showed that photic stimulation caused a significant increase in the fractal dimension of the EEG signal; however, no consistent correlation was noticed between microwave stimulation and the fractal dimension of the EEG. Other research groups have obtained similar results; for a review see D'ANDREA *et al.* (2003).

These efforts demonstrate that the EEG changes induced by low-level microwave exposure cannot be detected by the methods above. However, the analysis by the LDLVP method used for the detection of the EMF effect demonstrated good sensitivity. A large variability in individual subject sensitivity with respect to the EMF exposure has been observed. Compared with our earlier results (LASS *et al.*, 2002; HINRIKUS *et al.*, 2004), significant EMF effects detected for a quarter of subjects suggest an advance in the studies.

## 5 Conclusions

Non-linear scaling analysis of the length distribution of low-variability periods is a sensitive method for distinguishing EEG signals with and without a weak stressor and is superior to spectral analysis.

The probability distribution of the studied measures of the EEG signal, which was close to normal, and the smooth power spectrum and smooth length distribution curves of the low-variability periods showed that the recording length was sufficient, and the recording conditions were under adequately rigorous control to guarantee EEG signal stationarity.

Sensitivity to microwave exposure varied a great deal for different subjects: a significant effect of exposure to the EEG signal was detected for about 25% of subjects. Prevalently, microwave exposure increased EEG variability.

## References

BABLOYANTZ, A. and DESTEXHE, A. (1988): 'Is the normal heart a periodic oscillator?', *Biol. Cybern.*, **58**, pp. 203–211

COSTA, M., GOLDBERGER, A. L., and PENG, C. -K. (2002): 'Multiscale entropy analysis of complex physiologic time series', *Phys. Rev. Lett.*, **89**, 068102 (http://link.aps.org/abstract/PRL/v89/e068102, accessed August 2004)

D'ANDREA, J. A., CHOU, C. K., JOHNSTON, S. A., and ADAIR, E. R. (2003): 'Microwave effects on nervous system', *Bioelectromagnetics*, **S6**, pp. 107–147

ELGER, C. E. and LENHERZ, K. (1997): 'Seizure prediction by non-linear time series analysis of brain electrical activity', *Eur. J. Neurosci.*, **10**, pp. 786–789

HINRIKUS, H., PARTS, M., LASS, J., and TUULIK, V. (2004): 'Changes in human EEG caused by low-level modulated microwave exposure', *Bioelectromagnetics*, **25**, pp 431–440

HUUPPONEN, E., HIMANEN, S. L., HASAN, J., and VARRI, A. (2003): 'Automatic analysis of electro-encephalogram sleep spindle frequency throughout the night', *Med. Biol. Eng. Comput.*, **41**, pp. 727–732

IVANOV, P. Ch., ROSENBLUM, M. G., AMARAL, L. A. N., STRUZIK, Z., HAVLIN, S., GOLDBERGER, A. L., and STANLEY, H. E. (1999): 'Multifractality in human heartbeat dynamics', *Nature*, **399**, pp. 461–465

KALDA, J., SÄKKI, M., VAINU, M., and LAAN, M. (2001): 'Zipf's law in human heartbeat dynamics'. http://arxiv.org/abs/physics/0110075

KALDA, J., SÄKKI, M., VAINU, M., and LAAN, M. (2004): 'Nonlinear and scale-invariant analysis of heart rate variability', *Proc. Est. Acad. Sci. Phys.-Math*, **53**, pp. 26–44

KANTZ, H., and SCHREIBER, T. (1997): 'Nonlinear time series analysis' (Cambridge University Press, Cambridge, 1997)

KRAUSE, C. M., SILLANMÄKI, L., KOIVISTO, M., HÄGGQVIST, A., SAARELA, C., REVONSUO, A., LAINE, M., and HÄMÄLÄINEN, H. (2000): 'Effects of electromagnetic fields emitted by cellular phones on the electroencephalogram during a visual working memory task', *Int. J. Radiat. Biol.*, **76**, pp. 1659–1667

LASS, J., TUULIK, V., FERENETS, R., RIISALO, R., and HINRIKUS, H. (2002): 'Effects of 7 Hz-modulated 450 MHz electromagnetic radiation on human performance in visual memory tasks', *Int. J. Radiat. Biol.*, **78**, pp. 937–944

LIPPING, T., OLEJARCZYK, E., and PARTS, M. (2003): 'Fractal dimension analysis of the effects of photic and microwave stimulation on the brain function'. *Proc. World Cong. Med. Phys. & Biomed. Eng.*, Sydney, Australia, (CD-ROM) ISBN 1877040142, paper 3695

LOPES DA SILVA, F. H., HOEKS, A., SMITH, H., and ZETTENBERG, L. H. (1974): 'Model of brain rhythmic activity: the alpha-rhythm of the thalamus', *Kybernetik*, **15**, pp. 27–37

LOPES DA SILVA, F. H., PIJN, J. P., VELIS, D., and NIJSSEN, P. C. G. (1997): 'Alpha rhythms: noise, dynamics and models', *Int. J. Neurophys.*, **26**, pp. 237–249

LOPES DA SILVA, F., BLANES, W., KALITZIN, S. N., PARRA, J., SUFFCZYNSKI, P., and VELIS, D.N. (2003): 'Epilepsies as dynamical diseases of brain systems: basic models of the transition between normal and epileptic activity', *Epilepsia*, **44**, pp. 72–83

MCSHARRY, P. E., SMITH, L. A., and TARASSENKO, L. (2003): 'Comparison of predictability of epileptic seizures by linear and non-linear methods', *IEEE Trans. Biomed. Eng.*, **50**, pp. 628–633

NIEDERMEYER, E., and LOPES DA SILVA, F. (1993): 'Electroencephalography, basic principles, clinical applications and related fields' (William & Wilkins, Baltimore, 1993)

PARTS, M., LIPPING, T., LASS, J., and HINRIKUS, H. (2003): 'Bispectrum for the detection of the effect of photic and microwave exposure on human EEG'. *Proc. 25th IEEE EMBS Ann. Int. Conf.*, Cancun, Mexico, CD-ROM, pp. 2327–2330

PENG, C. K., MIETUS, J., HAUSDORFF, J. M., HAVLIN, S., STANLEY, H. E., and GOLDBERGER, A. L. (1993): 'Long-range anticorrelations and non-Gaussian behavior of the heartbeat', *Phys. Rev. Lett.*, **70**, pp. 1343–1347

PEREDA, E., GAMUNDI, A., RIAL, R., and GONZALEZ, J. (1998): 'Non-linear behaviour of human EEG: fractal exponent versus correlation dimension in awake and sleep stages', *Neurosci. Lett.*, **250**, pp. 91–94

RÖSCHKE, J., FELL, J., and MANN, K. (1997): 'Non-linear dynamics of alpha and theta rhythm: correlation dimensions and Lyapunov exponents from healthy subject's spontaneous EEG', *Int. J. Psychophysiol.*, **26**, pp. 251–261

ROSSO, O. A., FIGLIOLA, A., CRESO, J., and SERRANO, E. (2004): 'Analysis of wavelet-filtered tonic-clonic electroencephalogram recordings', *Med. Biol. Eng. Comput.*, **42**, pp. 516–523

SÄKKI, M., KALDA, J., VAINU, M., and LAAN, M. (2004a): 'The distribution of low-variability periods in human heartbeat dynamics', *Physica A*, **338**, pp. 255–260

SÄKKI, M., KALDA, J., VAINU, M., and LAAN, M. (2004b): 'What does measure the scaling exponent of the correlation sum in the case of human heart rate?', *Chaos*, **14**, pp. 138–144

SHEN, Y., OLBRICH, E., ACHERMANN, P., and MEIER, P. F. (2003): 'Dimensional complexity and spectral properties of the human sleep EEG', *Clin. Neurophysiol.*, **114**, pp. 199–209

SINHA, R. K. (2004): 'Electro-encephalogram disturbances in different sleep-wake states following exposure to high environmental heat', *Med. Biol. Eng. Comput.*, **42**, pp. 282–287

THEILER, J., and RAPP, P. E. (1996): 'Re-examination of the evidence for low-dimensional, non-linear structure in the human electroencephalogram', *Electroenceph. Clin. Neurophysiol.*, **98**, pp. 213–222

VAN DRONGELEN, W., NAYAK, S., FRIM, D. M., KOHRMAN, M. H., TOWLE, V. L., LEE, H. C., MCGEE, A. B., CHICO, M. S., and HECOX, K. E. (2003): 'Seizure anticipation in pediatric epilepsy: use of Kolmogorov entropy', *Pediatr. Neurol.*, **29**, pp. 207–213

WANG, X.-J. (1994): 'Multiple dynamic modes of thalamic relay neurons: rhythmic bursting and intermittent phase-locking', *Neuroscience*, **59**, pp. 21–31

WIDMAN, G., SCHREIBER, T., REHBERG, B., HOEFT, A., and ELGER, C. E. (2000): 'Quantification of depth of anesthesia by nonlinear time series analysis of brain electrical activity', *Phys. Rev. E*, **62**, pp. 8380–8386

WOOD, A. W., HAMBLIN, D. L., and CROFT, R. J. (2003): 'The use of a 'phantom scalp' to assess the possible direct pickup of mobile phone handset emissions by electroencephalogram electrode leads', *Med. Biol. Eng. Comput.*, **41**, pp. 470–472

## Authors' biographies

MAIE BACHMANN graduated from the Tallinn University of Technology in 2001. She received an MSc in biomedical engineering in 2003. Her research interest is EEG signal processing.

JAAN KALDA obtained his degree in physics from the Moscow Institute of Physics and Technology in 1989, and PhD from the same university in 1990 with a dissertation on collective transport phenomena in plasmas. His research interests are intermittent time-series and turbulent diffusion.

JAANUS LASS is a senior research fellow at Biomedical Engineering Centre. He obtained his PhD in Natural Sciences from Tallinn University of Technology in 2002.

VIIU TUULIK received an MD from the University of Tartu in 1963, and a DM in neurology in 1994. Her research interest is neurophysiology.

MAKSIM SÄKKI graduated from the Tallinn University of Technology in 1999 (Technical Physics) and received an MSc on the fractality in human heart rate dynamics (2001). His research interests include biological time-series and fractality.

HIIE HINRIKUS is professor of radio physics at the Tallinn University of Technology. She obtained a PhD degree 1967, and a DSc from the Institute of Radio and Electronic Engineering, Academy of Sciences USSR in 1967 and 1989 respectively. Her research interests are biomedical engineering and biological effects of microwaves.

# EFFECT OF 450 MHz MICROWAVE MODULATED WITH 217 Hz ON HUMAN EEG IN REST.

M. BACHMANN, M. SÄKKI, J. KALDA,
J. LASS, V. TUULIK, H. HINRIKUS

# Effect of 450 MHz microwave modulated with 217 Hz on human EEG in rest

Maie Bachmann[1], Maksim Säkki[2], Jaan Kalda[2], Jaanus Lass[1], Viiu Tuulik[1], and Hiie Hinrikus[1]

[1]Biomedical Engineering Centre, Tallinn University of Technology

Address:  5 Ehitajate Rd, 19086 Tallinn, Estonia

[2]Institute of Cybernetics at Tallinn University of Technology

Address: 21 Academy Rd, 12618 Tallinn, Estonia


Correspondence to:

Maie Bachmann

Biomedical Engineering Centre, Tallinn University of Technology

5 Ehitajate Rd, 19086 Tallinn, Estonia

Tel: 372 6202200

Fax: 372 6202201

e-mail:maie@cb.ttu.ee

**Summary.** This study focuses on discrimination of changes, produced by low-level microwave exposure in intensity and time variability of the human EEG at rest. The power spectral density (PSD) method and nonlinear scaling analysis of the length distribution of low variability periods (LDLVP) were selected for analysis of the EEG signal. During the study, 19 healthy volunteers were exposed to a microwave (450 MHz) of 217 Hz frequency on-off modulation. The field power density at the scalp was 0.16 mW/cm$^2$. The experimental protocol consisted of ten cycles of repetitive microwave exposure. Signals from frontal, temporal, parietal and occipital EEG channels on EEG theta, alpha and beta rhythms were analysed. Exposure to microwave causes average increase of EEG activity. LDLVP analysis discriminated significant effect in time variability for 2 subjects (11%). PSD method detected significant changes in intensity for 4 subjects (21%). The effect of low-level microwave exposure is stronger on EEG beta rhythm in temporal and parietal regions of the human brain.

**1 Introduction**

Starting with the new era of portable telecommunication solutions, artificial electromagnetic fields present stronger radiation than the fields created by natural sources. For most of the time, people may not be aware of such radiation, so they solely rely on safety standards.

Modulated microwave radiation at non-thermal level of field power density can affect human central nervous system in a sensible way (D'ANDREA *et al*., 2003; SALFORD *et al*., 2003). Except in unhealthy artificial conditions, the effect of electromagnetic field is weak and difficult-to-detect. With carefully planned measurement technique and recording protocol, the measurement of the bioelectrical activity of the brain has been proven to be one of the most successful ones and selected as our primary data source. The measurement and data analysis must take into account the normal fluctuations of EEG signal and presence of other complicate detectable factors. Thus, quantitative measures should be carried out to estimate the overall effect.

During recent years, non-thermal effect of low-level electromagnetic field on human nervous system has become a subject of discussions. The reports of possible non-thermal effects are often contradictory. Several investigators have reported that low-level exposure produces alterations in the EEG signal and brain behavior (BAWIN *et al*., 1973; VOROBYOV *et al*., 1997; MANN *et al.,* 1996; WAGNER *et al*., 1998; HUBER *et al*., 2000; LASS *et al*., 2002; HINRIKUS *et al*., 2004). The conclusion reported by the other researchers is that the exposure to electromagnetic field does not alter the resting EEG (HIETANEN *et al.,* 2000; KRAUSE *et al*., 2000; KRAUSE *et al*., 2000). Mechanisms behind the effects are still unclear and the question about the existence of any feasible effect of a low-level radiation on brain bioelectric activity has been left open.

In our previous studies the relative changes in the EEG rhythms energy, mainly in theta and alpha bands, were investigated and effect, produced by microwave exposure, reported (HINRIKUS *et al*., 2004). Modulation of microwave at 7 Hz frequency, which belongs to the band of physiological frequencies of the brain, was applied. However, those results did not present statistically important changes. Likewise, the power spectrum analysis could not differentiate sham recordings from recordings under the influence of microwave stimulation at 7 Hz on-off modulation. However, nonlinear scaling analysis of the length distribution of low variability periods (LDLVP) detected significant effect of exposure to the EEG signal for about 25% of subjects (BACHMANN *et al*., 2005). Increase in EEG variability, caused by microwave exposure, was reported.

The analyzed frequencies are lower, than modulation and pulse frequencies in technical systems. Therefore, here we study the physiological effect of the modulation frequency 217 Hz. To this end, we compare the EEG signals

recorded at the presence of a modulated low-level microwave field, with sham signals. 217 Hz is the GSM signal's pulse frequency and the population is most widely exposed to microwave modulated at that frequency. The mechanisms of low-level microwave interaction with biological tissues are not clear. Therefore, it is not possible to predict the character of changes in brain bioelectrical activity, caused by microwave exposure. The effect could be related to stimulation or depression of the brain activity, which leads to changes in intensity of the EEG signal. The effect could be related to changes on neurons spiking frequency or processes in synapses, which leads to changes in time variability of the EEG signal. Experimental effects that depend on low frequency modulation of microwave radiation can also be related to more complicated nonlinear responses in biological tissue and living cells (BALZANO *et al*., 2003). Therefore, two different methods for analysis of the EEG signals were used in this study: the first for discrimination of changes in intensity, and the second for discrimination of changes in time variability of the EEG signals.

The intensity of the EEG signal is most completely described by power spectrum of the EEG signal. The power spectral density method, a widely used method in quantitative EEG, was selected for intensity analysis of the EEG signals. The powers of EEG theta, alpha and beta rhythms bands were analyzed.

The LDLVP analysis provides a simple route to detecting the multifractal characteristics of a time-series and yields somewhat better temporal resolution than the traditional multifractal analysis. Thus, it can be expected that this method is sensitive with respect to small "hidden" changes in such a complicated physiological signal as EEG. The LDLVP method was selected for time variability analysis of the EEG signals.

The hypothesis, evaluated in this study, is that modulated at 217 Hz microwave exposure increases variability of the EEG signal and causes changes in the power spectrum of the human EEG.

## 2 Method and equipment

### 2.1 Subjects

An experimental study was carried out on a group of volunteers. The group consisted of 19 healthy, young people (aged 21-24): 8 male and 11 female. Their physical and mental condition (tiredness, sleepiness) before the experiment was evaluated by a questionnaire and a clinical interview. After the recordings, they described how they felt during the experiment. The subjects reported neither alertness nor any strain experienced during the recordings.

The experiments were conducted with the understanding and written consent of each subject. The study was conducted in accordance with the Declaration of Helsinki and has formally approved by the local Medical Research Ethics Committee.

The measurements were performed in a dark laboratory, but no other special conditions were provided. The subjects lay in a relaxed position, with eyes closed and ears blocked during the experiments.

All the subjects were exposed and sham exposed. Only one experimental EEG recording was performed for a subject during a day. The measurements were double blinded. During each test session, the exposed and sham-exposed subjects were randomly assigned. The subjects were not informed of their exposure; however, they were aware of the possibility of being exposed. Subjective factors were also excluded from the computer-performed data analysis: the same algorithms were applied for all the recordings (both for exposed and sham-exposed subjects).

**2.2 Microwave Exposure**

The modulated microwave radiation at non-thermal level of field power density, identical to our previous studies, except modulation frequency (LASS et al., 2002), was used. Microwave exposure conditions were the same for all subjects. The 450 MHz microwave radiation was 100% amplitude modulated at 217Hz frequency (duty cycle 50%). The 1W EMF output power was guided by a coaxial lead to the 13cm quarter-rhythm antenna, located 10 cm from the subject's skin on the left side of the head.

Estimated field power density at the skin was 0.16 mW/cm2. The level of power density was so low that thermal effects were extremely unlikely.

**2.3     Recording protocols and equipment**

The study consisted of two experimental protocols, identical for all subjects. The first protocol was recorded as described below.

First, the reference EEG was recorded over 60 s. Secondly, modulated microwave radiation was applied. The duration of the exposure was 60 s, and the compensatory pause after the exposure was 60 s. Continuous EEG recordings were made during and 60 s after exposure. The procedure of the cycle was repeated ten times. The microwave exposure was switched on every first 60 s of the cycle. During ten cycles of microwave exposure, the modulation frequency always remained at 217 Hz.

The recording protocol for one subject lasted for 21 min, during which the EEG was continuously recorded.

The second protocol for the sham-exposure included the same steps, except that the microwave generator was switched off.

The Cadwell Easy II EEG measurement equipment was used for the EEG recordings. The EEG was recorded by means of 19 electrodes, placed on the subject's head according to the international 10-20-electrode position classification system, with Cz as reference. The recorded EEG signals were examined by an experienced neurologist. Artifacts were detected by visual inspection. The recordings containing multiple artifacts were removed, and the whole recording was repeated.

For the analysis, EEG spectrum 0.5 - 40 Hz was selected, as the results of the preceding validation of the set-up confirmed the absence of modulation components, caused by parasitic interference between EEG and radio frequency equipment.

**2.4 Selection of signals**

Recordings from the following channels were selected for further power analysis: frontal: FP1, FP2; temporal: T3, T4; parietal: P3, P4; occipital: O1, O2. For scaling analysis, only channels FP1 and FP2 were used, as formerly shown, the results from different EEG channels did not differ (BACHMANN *et al.* 2005).

Initially, all the EEG recordings were divided into two sub-signals. The recordings performed with the first recording protocol were divided as follows: the first subsignal contained all 1 min periods without microwave exposure (all the odd minutes from the initial EEG recording); the second subsignal contained all minutes with microwave exposure (all even minutes of the initial EEG recording).

The recordings performed with the second recording protocol (sham) were divided similarly: the first sham subsignal contained all the odd minutes; the second sham subsignal contained all the even minutes of the initial recording.

**2.5 Scaling analysis of the EEG signal based on the LDLVP method**

The LDLVP method has been used and described in details in our previous studies (KALDA *et al.*, 2001; SÄKKI *et al.*, 2004; BACHMANN *et al.*, 2005). The analysis consists of several steps.

First, we define the local variability as the deviation of the current value of the signal from the local average. The time-window width T, for the local average, is a free (adjustable) parameter. For EEG signals, a reasonable value is provided by $T = 60$ ms, cf (BACHMANN *et al.*, 2005).

Secondly, low-variability periods are defined as continuous intervals where local variability is smaller than $\delta_0$.

The value of $\delta_0$ was adjusted for each recording individually, reaching a minimum value so that, for both subsignals, the length of the longest low-variability period was at least 3750 ms.

Finally, the number of low-variability periods $N$ exceeding length $T_0$ is plotted against length $T_0$.

The weighted area of the function $T_0 = T_0(N)$ was selected as the non-linear quantitative measure.

**2.6 Power spectral density analysis**

The power spectral density (PSD) was estimated by means of Welch's averaged periodogram method. The subsignals were divided into overlapping sections (50%), with a length of 2048 points, and windowed by a Hanning window.

Afterwards, the power $W_{mnf}$ was computed for each subject (indexed by $n \in [1,19]$), subsignal (indexed by m=1,2) and frequency band (f = θ for theta band [4-8Hz], f = α for alpha band [8-13 Hz] and f = β for beta band [13-40 Hz] ), as the area under the spectrum for the corresponding frequency band (integral of the band).

To locate the possible influences of microwave exposure, difference of two sub-signals was selected as the PSD measure for further analysis.

The same procedure was repeated with sham subsignals, resulting in spectral powers $\tilde{W}_{mnf}$ .

**2.7 Statistical analysis**

For sham recordings, subsignals were completely equivalent. According to the "zero hypothesis", the EEG recordings of subjects under microwave exposure cannot be distinguished from sham signals. Consequently, if the zero hypothesis is true, the ratio of the computed power difference to the standard deviation of the differences is an *f*-distributed random quantity and it can be used as a quantitative measure, showing how well the zero hypothesis is satisfied; respective *p*-values are obtained by means of the cumulative *f*-distribution.

The same technique has been applied to the non-linear quantitative measure (derived from LDLVP), resulting in another series of *p*-values.

**3      Results**

The results of LDLVP analysis for a subject are presented in Fig. 1. The number of low-variability periods N exceeding the length $T_0$ is plotted versus the length $T_0$ for the first and second sub-signal for exposed recording. As can be seen, microwave exposure lowers the curve at the right-hand part of the graph (large values of $T_0$). Such a change in curve indicates that microwave exposure increases variability of the EEG signal: owing to higher variability there are fewer long low variability periods.

Fig. 2 presents the average values of calculated relative changes in PSD measures for different frequency bands, for exposed and sham recordings. While in sham recordings the power in theta frequency band increases, the power decreases for alpha and beta frequencies. Average values of the measure for microwave-exposed recordings are always positive, therefore, the power of all frequency bands is increasing during microwave stimulation.

Statistical analysis of the PSD and LDLVP quantitative measures for microwave-exposed and sham recordings, were calculated for each subject. The ratio of the computed power difference to the standard deviation of differences of more than three, and *p* values not larger than 0.001 were considered as significant deviations from the zero hypothesis.

The analysis based on the PSD measures resulted in the ratio of the computed power difference to the standard deviation of differences (calculated on the basis of sham signals) being higher than three for 12 cases in the case of microwave exposure. For sham recordings, 2 cases were significant. The analysis based on the LDLVP measures for exposed recordings resulted in the ratio of the computed power difference to the standard deviation of differences exceeding the value of three for 2 subjects and for no subjects in case of the sham recordings.

All of the results, except for two cases in frontal region (PSD measures), remain significant even after application of the modified Bonferroni correction. The number of subjects having significant results after Bonferroni correction for microwave exposed and sham recordings are presented in Table 1. As for PSD measures, there was no significant result for theta and alpha frequency band, only beta band is presented.

## 4. Discussion

LDLVP measures resulted in significant results for two subjects in the case of microwave exposure and for none of the subjects in the case of sham recordings (Table 1). Accordingly, significant effect of exposure to the EEG signal was detected for about 11 % of subjects. However, for one subject under the exposure, the computed LDLVP weighted area decreased and for other, it increased. For both subjects, the departure from the sham behavior is statistically reliable. This is somewhat different from what has been observed for the modulation frequency 7 Hz, when the sign of the departure was always negative (corresponding to increased variability) (BACHMANN *et al.*, 2005). This observation gives us a hint that the physiological effect of the microwave stimulation depends on the modulation frequency (at least there is a difference between the 7 Hz and 217 Hz frequencies).

The PSD measures exceeded the limit of significant deviation from zero hypothesis only in beta frequency band (Table 1). In temporal region, the PSD measures provided the most results: 3-4 cases out of 19, ~16 – 21 %. The influence was somewhat smaller in parietal region: 1-2 cases out of 19, ~ 5 – 11 %. The frontal region did not present significant changes after Bonferroni correction, while occipital region did not present any significant change.

As for sham recordings, the PSD measure resulted in significant results for one subject in channel T3 and in T4. However, those were very close to the limit of significance - *0.05* - and therefore, can be arguably explained with the statistical variability.

Looking at the average values calculated for sham recordings (Fig 2), one can see that the results are in a good agreement with the findings of MALTEZ *et al*., 2004. They showed that alpha and beta power decreased towards the end of recording session during resting conditions, while delta and theta power showed a systematic increase. Except for delta power, which was not under investigation, our results showed the same trend.

However, average values for microwave-exposed recordings reveal an increase of power for all frequency bands. For theta frequency band the level is almost the same as for sham recordings, referring probably to the normal time course and variability of power. At the same time, the average values for alpha and beta band are opposite from sham, implying to the influence of microwave stimulation by increase of power.

The analysis by the LDLVP and PSD methods detected the effect of exposure for about 11% and 21 % of subjects respectively. For instance, the rate of multiple chemical sensitivity (MCS) occurrence is estimated to be between 2 and 10 % in the general population (CULLEN, 1987). MCS is characterized by recurrent symptoms involving multiple organ systems and occurring in response to demonstrable exposures to multiple chemically unrelated compounds at doses far below those established to cause harmful effects. Taking this into consideration, low-level microwave exposure influences even higher part of population than multiple chemically unrelated compounds.

**Conclusion**

1.  Modulated at 217 Hz low-level 450 MHz microwave exposure produced statistically significant changes in time variability and intensity of the EEG signal for 10 -20% of healthy subjects.

2.  The effect of low-level 450 MHz microwave exposure is stronger on EEG beta rhythm in temporal and parietal regions of the human brain.

3.  Exposure to modulated at 217 Hz low-level 450 MHz microwave causes average increase in EEG activity.

The mechanism of these changes is not clear and the effect needs further investigation.

**Acknowledgements**

**References**

M. Bachmann, J. Kalda, J. Lass, V. Tuulik, M. Säkki, H. Hinrikus, "Non-linear analysis of the electroencephalogram for detecting effects of low-level electromagnetic fields," Med Biol Eng Comput 2005; 43: 142-149

Q. Balzano, A. Sheppard, "RF nonlinear interaction in living cells-I: nonequilibrium thermodynamic theory," Bioelectromagnetics 2003; 24:473-482

S.M. Bawin, R.J. Gavalas-Medici, WR. Adey, "Effects of modulated very high frequency fields on specific brain rhythms in cats," Brain Res 1973; 58: 365-84

M.R. Cullen, "Workers with multiple chemical sensitivities," Occupational medicine: state of the art reviews. Philadelphia: Hanley & Belfus, Inc. 1987; 2: 655-661

J.A. D'Andrea, C.K. Chou, S.A. Johnston, E.R. Adair, "Microwave effects on nervous system," Bioelectromagnetics 2003; S6: 107-147.

M. Hietanen, T. Kovala, A.M. Hamalainen, "Human brain activity during exposure to radiofrequency fields emitted by cellular phones," Scand J Work Environ Health 2000; 26: 87-92

H. Hinrikus, M. Parts, L. Lass, and V. Tuulik, "Changes in human EEG caused by low-level modulated microwave exposure," Bioelectromagnetics 2004; 25(6): 431-440

R. Huber, T. Graf, K.A. Cote, L. Wittmann, E. Gallmann, D. Matter, J. Schuderer, N. Kuster, A.A. Borbely, P. Achermann, "Exposure to pulsed high-frequency electromagnetic field during waking affects human sleep EEG," Neuroreport 2000; 11: 3321-3325

Kalda, J., Säkki, M., Vainu, M., and Laan, M. (2001): 'Zipf's law in human heartbeat dynamics', available: http://arxiv.org/abs/physics/0110075

C.M. Krause, L. Sillanmäki, M. Koivisto, A. Häggqvist, C. Saarela, A. Revonsuo, M. Laine, H. Hämäläinen, "Effects of electromagnetic field emitted by cellular phones on the EEG during a memory task," Neuroreport 2000; 11: 761-764.

C.M. Krause, L. Sillanmäki, M. Koivisto, A. Häggqvist, C. Saarela, A. Revonsuo, M. Laine, H. Hämäläinen, "Effects of electromagnetic fields emitted by cellular phones on the electroencephalogram during a visual working memory task," Int J Radiat Biol 2000; 76:1659-1667

J. Lass, V. Tuulik, R. Ferenets, R. Riisalo, and H. Hinrikus, "Effects of 7Hz-modulated 450 MHz electromagnetic radiation on human performance in visual memory tasks," Int. J. Radiat. Biol. 2002; 78:937-944

J. Maltez, L. Hyllienmark, V.V. Nikulin, T. Brismar, "Time course and variability of power in different frequency bands of EEG during resting conditions", J Clin Neurophysiol 2004; 34:195-202

K. Mann, J. Roschke, "Effects of pulsed high-frequency electromagnetic fields on human sleep," Neuropsychobiology 1996; 33:41-47

L.G. Salford, A.E. Brun, J.L. Eberhardt, L. Malmgren, B.R. Persson, "Nerve cell damage in mammalian brain after exposure to microwaves from GSM mobile phones," Environ Health Perspect 2003; 111(7):881-883.

M. Säkki, J. Kalda, M. Vainu, M. Laan, "The distribution of low-variability periods in human heartbeat dynamics," Physica A 2004; 338:255-260.

V.V. Vorobyov, A.A. Galchenko, N.I. Kukushkin, I.G. Akoev, "Effects of weak microwave fields amplitude modulated at ELF on EEG of symmetric brain areas in rats," Bioelectromagnetics 1997; 18: 293-298

P. Wagner, J. Roschke, K. Mann, W. Hiller, C. Frank, "Human sleep under the influence of pulsed radiofrequency electromagnetic fields: a polysomnographic study using standardized conditions," Bioelectromagnetics 1998; 19: 199-202.

Table 1. Number of subjects with significant results after Bonferroni correction in the case of microwave exposed and sham recordings.

| Method | LDLVP | PSD | | | | | | | |
|---|---|---|---|---|---|---|---|---|---|
| Frequency band | full EEG | beta | | | | | | | |
| Channel | FP1/FP2 | FP1 | FP2 | T3 | T4 | P3 | P4 | O1 | O2 |
| Exposed | 2 | 0 | 0 | 3 | 4 | 2 | 1 | 0 | 0 |
| Sham | 0 | 0 | 0 | 1 | 1 | 0 | 0 | 0 | 0 |

Fig. 1. The number of low-variability periods N exceeding the length $T_0$ for a significant subject: line 1 - second sub-signal of exposed recording (intervals with microwave); line 2 - first sub-signal of exposed recording (intervals without microwave).
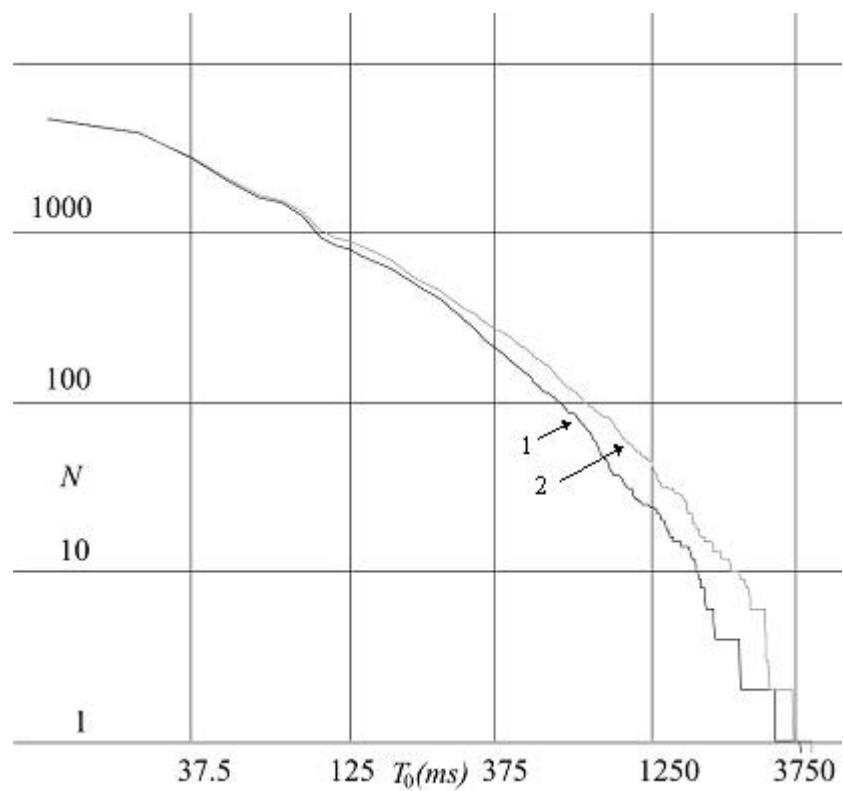
Fig. 2. Calculated relative changes in intensity between exposed and non-exposed segments of the EEG signals on main EEG rhythms. Vertical bars denote 0.95 confidence intervals.
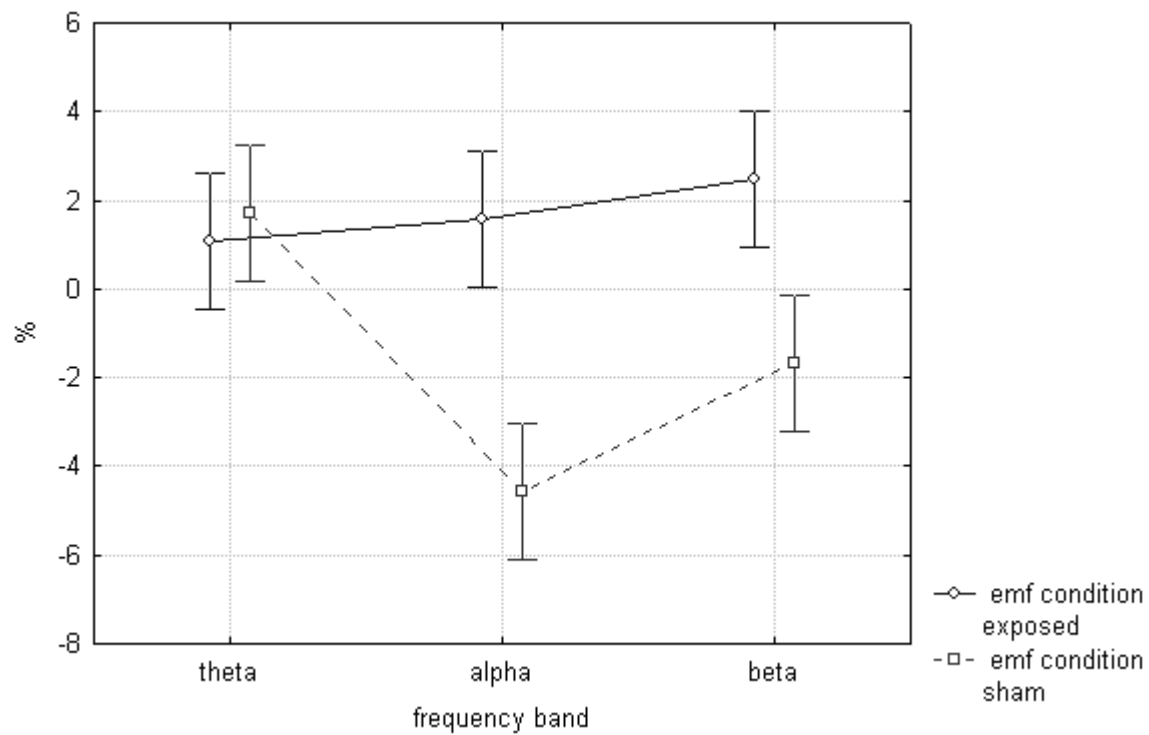
# Appendix 1: Standard measures of HRV in clinical use

A non-exhaustive list of the standard (based on linear statistical measures and on the Fourier analysis) parameters of heart rate variability, which are currently used in medical practice (implemented in most commercial diagnostic equipment). NN [normal-to-normal] interval – interval between 2 adjacent non-arrithmic heartbeats.

**Time-domain measures**:

- the mean NN interval

- the difference between night and day heart rate

- the longest and shortest NN intervals

- SDNN $\equiv$ the standard deviation of the NN interval (typically calculated over 24-hour period)

- SDSD $\equiv$ the standard deviation of differences between adjacent NN intervals

- SDANN $\equiv$ the standard deviation of locally (usually 5 min) averaged NN intervals

- SDNN index $\equiv$ the mean of the 5-minute standard deviation of the NN interval (averaged over 24h)

- RMSSD $\equiv$ the square root of the mean squared differences of successive NN intervals

- pNN50 $\equiv$ the percentage of interval differences of successive NN intervals greater than 50 ms

**Frequency-domain measures**:

- VLF $\equiv$ the spectral power of fluctuations in NN-sequences in very low frequency range ($\lesssim 0.04$ Hz)

- LF $\equiv$ the spectral power of fluctuations in NN-sequences in low frequency range (0.04 - 0.15 Hz)

- HF $\equiv$ the spectral power of fluctuations in NN-sequences in high frequency range (0.15 - 0.4 Hz)

# Appendix 2: Nonlinear measures of HRV

A list of selected "nonlinear" measures used for describing of HRV. The classifying does not pretend to be explicit because some methods can be related to several sections, i.e. calculating multiscale entropy (MSE) is entropy-based approach, however it is closely related to multiscaling anaysis.

**Reconstructed phase space analysis**:

- $D_2 \equiv$ scaling exponent of correlation sum (correlation dimension)

- $\lambda \equiv$ Lyapunov exponent

- heart rhythm and respiration mode-locking analysis

**Entropy-based measures**:

- $K_2 \equiv$ lower bound of the Kolmogorov-Sinai entropy, Grassberger and Procaccia, 1983, cf. [55]

- $K_{ER} \equiv$ estimator of the Kolmogorov-Sinai entropy, Eckmann and Ruelle, 1985, cf. [56]

- $ApEn \equiv$ approximate entropy, a "regularity statistic" that quantifies the unpredictability of fluctuations in a time series, Pincus, 1991, cf. [57]

- Zhang's Complexity $\equiv$ the sum of scale-dependent Shannon entropies over all possible scales, Zhang, 1991, cf. [67]

- $S_p \equiv$ pattern entropy (modified Shannon entropy), Zebrowski *et al.*, 1994, cf. [69]

- $SampEn \equiv$ sample entropy, Richman and Moorman, 2000, cf. [63]

- MSE $\equiv$ multiscale entropy, Costa *et al.*, 2002, cf. [65]

**Single- and multi-scaling analysis**:

- $H \equiv$ global Hurst exponent (single-scaling analysis), Hurst, cf. [102]

- $f(h) \equiv$ Lipschitz-Hölder spectra; $\tau(q) \equiv$ mass exponent spectra; $\zeta(q) \equiv$ structure function exponent spectra (multi-scaling analysis)

- DFA $\equiv$ detrended fluctuation analysis, quantifying long-range correlations for non-stationary time series, Peng *et al.*, 1995, cf. [82].

- multiresolution wavelet analysis, Ivanov *et al.*, cf. [85]

- analysis of the distribution law of low-variability periods (Pareto-Zipf's law-like distribution)

- analysis of heart rate data segments with a similar mean values [101]

# Appendix 3: Bonferroni correction

The *Bonferroni correction* (multiple-comparison correction) addresses the problem with standard $p$-values when several (dependent or independent) statistical tests are being performed simultaneously.

Suppose that a single test was employed to test a null hypothesis, using significance level $\alpha = 0.05$ and if the null hypothesis was actually true. The probability $p$ of reaching the right conclusion (i.e., not significant) in that case is $p = 1 - \alpha = 0.95$. By running more tests on a given data set, there is an increasing probability of getting a significant result simply by chance: if $n$ hypotheses were tested on the same dataset and if all of them were true, the probability of being right on all occasions (simply the product of the individual probabilities if tests are independent) would decrease substantially to $p^n = 0.95^n$, i.e, the probability of getting a significant result *erroneously* would increase to $1 - p^n = 1 - 0.95^n$. In order to guarantee that the *overall* significance test is still at the same level ($\alpha$), one has to lower the significance level of the *individual* test ($\alpha'$). These two significance levels are related to each other as $(1 - \alpha')^n = 1 - \alpha$, which implies that $\alpha' = 1 - (1 - \alpha)^{1/n}$. For small values of significance level $\alpha \ll 1$ this result reduces to $\alpha' = \alpha/n$. For example, to make sure that the probability of falsely attaching significance to any test (from $n$) is $0.05$, one can use a *corrected* significance value of $0.05/n$. If the corrected value is still less than $0.05$, only then the null hypothesis is rejected. Such a reasoning to correct $p$-values for multiple significance testing on the same data set was first proposed by Italian statistician C.E. Bonferroni in 1936 [120].

The idea of $p$-values correction leads to several still disputable conclusions. First, if one carries out multiple tests on a single data set, the interpretation of a relationship between two variables actually depends on how many other tests were performed. Second, if Bonferroni correction were to be made obligatory and universal in statistical tests, some studies would make results more significant simply by *not including* many other tests they would have done with non-significant results, and thus not applying correction to same extent as they should. Finally, tests published in previous papers on the same dataset (in medicine the same groups of patients) or tests done subsequently would need to be corrected taking into account the number of previous tests. These problems possess disagreements among statisticians over universal use of the Bonferroni correction [121, 122, 123]. Also note that the Bonferroni correction is too conservative if the hypothesis tests are mutually correlated, this leads to underestimation of the resulting significance. Therefore, Bonferroni correction in its pure form should be used only for fully independent tests. Otherwise, one should use modified Bonferroni correction [124]. In medicine, the Bonferroni correction usually used in two cases: *a)* a group of individuals subjected to a number of *independent* tests of associations between *different* biological parameters; *b)* the same test being repeated in many subgroups (grouped by age, sex, diagnosis, etc.)

# Curriculum Vitae

## 1. Personal data

| | |
|---|---|
| Name and surname | Maksim Säkki |
| Date and place of birth | 02.05.1977, Narva |
| Citizenship | Estonian |
| Marital status | married |

## 2. Contact data

| | |
|---|---|
| Address | Akadeemia tee 21, 12618 Tallinn, Estonia |
| Phone | +372 620 4251 |
| E-mail | max@cens.ioc.ee |

## 3. Education

Master of Science in Natural Sciences, 2001, Tallinn University of Technology, *On the fractality of the human heart rate dynamics*.
Bachelor of Science in Natural Sciences, 1999, Tartu University, *The methods of nonlinear dynamics in the analysis of heart rate variability for children.*

## 4. Languages

| | |
|---|---|
| Estonian | Fluent |
| Russian | Fluent |
| English | Satisfactory |

## 5. Professional employment

| | |
|---|---|
| 09/2003 – . . . | TUT Institute of Cybernetics, researcher |
| 10/1996 – 09/2003 | TUT Institute of Cybernetics, engineer |

## 6. Scientific work (publications, conferences participated)

For list of publications, cf. page 6.
3rd European Interdisciplinary School on Nonlinear Dynamics for System and Signal Analysis *Euroattractor*, Warsaw, 2002
4th International Conference on Modern Problems in Theoretical Physics, Kyiv, 2002.
2nd International Conference on Frontier Science. *A Nonlinear World: the Real World*, Pavia, 2003

## 7. Main research areas

Low-dimensional chaos, scale-invariance of biosignals (heart rate, EEG).

# Elulookirjeldus

## 1. Isikuandmed

| | |
|---|---|
| Ees- ja perekonnanimi | Maksim Säkki |
| Sünniaeg ja -koht | 02.05.1977, Narva |
| Kodakondsus | Eesti |
| Perekonnaseis | abielus |

## 2. Kontaktandmed

| | |
|---|---|
| Aadress | Akadeemia tee 21, 12618 Tallinn, Eesti |
| Telefon | 620 4251 |
| E-post | max@cens.ioc.ee |

## 3. Hariduskäik

Loodusteaduste magister, 2001, Tallinna Tehnikaülikool, *Fraktaalsusest inimese südame rütmi dünaamikas*.

Loodusteaduste bakalaureus, 1999, Tartu Ülikool, *Mittelineaarse dünaamika meetodid laste südame rütmi variaabelsuse uurimisel*.

## 4. Keelteoskus

| | |
|---|---|
| Eesti keel | Kõrgtase |
| Vene keel | Kõrgtase |
| Inglise keel | Kesktase |

## 5. Teenistuskäik

| | |
|---|---|
| 09/2003 – … | TTÜ Küberneetika Instituut, teadur |
| 10/1996 – 09/2003 | TTÜ Küberneetika Instituut, insener |

## 6. Teadustegevus (publikatsioonid, osalemine konverentsidel)

Publikatsioonide nimekirja vt. lk. 6.

3rd European Interdisciplinary School on Nonlinear Dynamics for System and Signal Analysis *Euroattractor*, Varssavi, 2002

4th International Conference on Modern Problems in Theoretical Physics, Kiiev, 2002.

2nd International Conference on Frontier Science. *A Nonlinear World: the Real World*, Pavia, 2003

## 7. Teadustöö põhisuunad ja teised uurimisobjektid

Kaoseteooria, biosignaalide mastaabiinvariantsus.